AFML-TR-74-282

A STRESS INTENSITY FACTOR CALIBRATION FOR CORNER FLAWS AT AN OPEN HOLE

METALS BEHAVIOR BRANCH
METALS AND CERAMICS DIVISION

MAY 1975

TECHNICAL REPORT AFML-TR-74-282

AIR FORCE MATERIALS LABORATORY
Air Force Systems Command
Wright-Patterson Air Force Base, Ohio

NOTICE

When Government drawings, specifications, or other data are used for any purpose other than in connection with a definitely related Government procurement operation, the United States Government thereby incurs no responsibility nor any obligation whatsoever; and the fact that the government may have formulated, furnished, or in any way supplied the said drawings, specifications, or other data, is not to be regarded by implication or otherwise as in any manner licensing the holder or any other person or corporation, or conveying any rights or permission to manufacture, use, or sell any patented invention that may in any way be related thereto.

This report has been reviewed by the Information Office (IO) and is releasable to to the National Technical Information Service (NTIS). At Ntis, it will be available to the general public, including foreign nations.

This technical report has been reviewed and is approved for publication.

A. F. Grandt, Jr.

A.F. GRANDT, JR., Capt, USAF
Project Engineer

FOR THE COMMANDER

Vincent J. Russo

VINCENT J. RUSSO
Chief, Metals Behavior Branch
Metals & Ceramics Division

Copies of this report should not be returned unless return is required by security considerations, contractual obligations, or notice on a specific document.

UNCLASSIFIED

SECURITY CLASSIFICATION OF THIS PAGE *(When Data Entered)*

REPORT DOCUMENTATION PAGE		READ INSTRUCTIONS BEFORE COMPLETING FORM
1. REPORT NUMBER AFML-TR-74-282	2. GOVT ACCESSION NO.	3. RECIPIENT'S CATALOG NUMBER
4. TITLE *(and Subtitle)* A STRESS INTENSITY FACTOR CALIBRATION FOR CORNER FLAWS AT AN OPEN HOLE		5. TYPE OF REPORT & PERIOD COVERED AFIT Thesis 6. PERFORMING ORG. REPORT NUMBER
7. AUTHOR(s) Johnny R. Snow Capt., USAF		8. CONTRACT OR GRANT NUMBER(s)
9. PERFORMING ORGANIZATION NAME AND ADDRESS Air Force Institute of Technology (AFIT-EN) Wright-Patterson AFB, Ohio 45433		10. PROGRAM ELEMENT, PROJECT, TASK AREA & WORK UNIT NUMBERS
11. CONTROLLING OFFICE NAME AND ADDRESS Air Force Materials Laboratory (AFML-LLN) Wright-Patterson AFB, Ohio		12. REPORT DATE May 1975 13. NUMBER OF PAGES 79
14. MONITORING AGENCY NAME & ADDRESS*(if different from Controlling Office)* Jerry C. Hix, Captain, USAF Director of Information, AFIT Wright-Patterson AFB, Ohio		15. SECURITY CLASS. *(of this report)* Unclassified 15a. DECLASSIFICATION/DOWNGRADING SCHEDULE
16. DISTRIBUTION STATEMENT *(of this Report)* Approved for public release; distribution unlimited		
17. DISTRIBUTION STATEMENT *(of the abstract entered in Block 20, if different from Report)*		
18. SUPPLEMENTARY NOTES Approved for public release; IAW AFR 190-17		
19. KEY WORDS *(Continue on reverse side if necessary and identify by block number)* Crack Growth Rates Stress Intensity Factors Fatigue		
20. ABSTRACT *(Continue on reverse side if necessary and identify by block number)* This study was an experimental stress intensity factor calibration of a part-thru, corner flaw at an open hole. The fatigue crack growth test was used to investigate corner flaws at holes in polymethylmethacrylate plates loaded in uniform, cyclic tension. Using baseline data and Paris' relationship, a calibration of stress intensity factor for the constant thickness, constant hole diameter specimens was made. It was found that a frequency of 1 or 2 cps could be used for fatigue crack growth in PMMA. Nondimen-		

DD FORM 1 JAN 73 1473 EDITION OF 1 NOV 65 IS OBSOLETE

AIR FORCE - 3-9-75 - 400

UNCLASSIFIED

SECURITY CLASSIFICATION OF THIS PAGE *(When Data Entered)*

(Block 20)
sional stress intensity factors were plotted for crack shape values, ratios of crack length at the hole to crack length at the surface, of 1.2 to 1.6. In general, this study demonstrated lower stress intensity at the hole and higher stress intensity at the surface for larger crack sizes when compared to other researchers. It was concluded that fatigue crack growth rate testing with PMMA is a useful method of obtaining stress intensity factor calibrations for complex, three-dimensional problems where no exact solutions exist.

PREFACE

This report was prepared by Captain Johnny R. Snow for presentation to the faculty of the School of Engineering of the Air Force Institute of Technology in partial fulfillment of the requirements of the degree of Master of Science. The work was conducted at the Air Force Materials Laboratory under Project 7351, "Research on Metals and Ceramics Leading to Superior Materials for Advanced Air Force System Applications," Task Number 735106, "Fundamentals of Failure Mechanisms," with Captain A.F. Grandt, Jr. (AFFML/LLN) acting as project sponsor. This report covers work conducted from December 1973 to December 1974.

The author extends his gratitude to many people for their help in completing this Study. The work was suggested and supervised by Capt A.F. Grandt, Jr., to whom special thanks is given. Valuable technical assistance with the testing equipment was furnished by Mr. M.B. Strope. The author especially appreciatesthe encouragement and guidance provided during the course of this study by his thesis advisor, Major Louis Montulli.

Table of Contents

List of Figures

List of Tables

A STRESS INTENSITY FACTOR CALIBRATION FOR CORNER FLAWS AT AN OPEN HOLE

I. Introduction

The principles of fracture mechanics have been used with a high degree of success to analyze fatigue and structural damage encountered during the operational life of many structures. In applying its principles to aircraft structures, the user of fracture mechanics must address the problem of cracks emanating from bolt and rivet holes. A comprehensive report (Ref 5) on aircraft structural failures was completed in 1971 and cited bolt and rivet holes as the origin for 33% of critical failures, by far the largest single location. Realizing that some of today's aircraft have over a million bolts and rivets, the aircraft designer must understand the significance of flaws emanating from fastener holes. In addition, the Air Force has recently adopted a new design philosophy for certain fracture critical parts which incorporates tolerance criteria based on the existence of assumed initial cracks.

Using fracture mechanics to analyze and to design for flawed fastener holes requires that the stress intensity factor be known for the flaw geometry of interest. The stress intensity factor is the fundamental parameter of fracture mechanics that enables the calculation of the critical flaw size for a given structure and loading as well as the estimation of

the service life of parts having subcritical flaws. To date, the three-dimensional nature of flaws at fastener holes has prevented a complete fracture mechanics solution for these common structural defects.

The purpose of this study was to make stress intensity factor determinations for the single geometry of a part-thru, corner flaw emanating from a hole in a specimen loaded in uniform, cyclic tension. In addition, this would further establish the fatigue crack growth test as a useful technique for obtaining stress intensity factors for difficult, three-dimensional problems where analytical solutions are non-existent. The geometry of the part-thru corner crack and pertinent parameters are shown in Fig. 1. Stress intensity factor calibrations for only the end points of the flaw, that is, points A and C, were found. In addition, specimen thickness, T, and hole radius, r, remained constant from test to test. This resulted in corner cracks with a range in a/c (See Fig. 1) of a little more than 1.0 to about 1.6. The most common shape was approximately 1.4. In sections to follow, the procedures and results of the fatigue crack growth test are described and examined. First, a brief summary of background information and previous studies is presented.

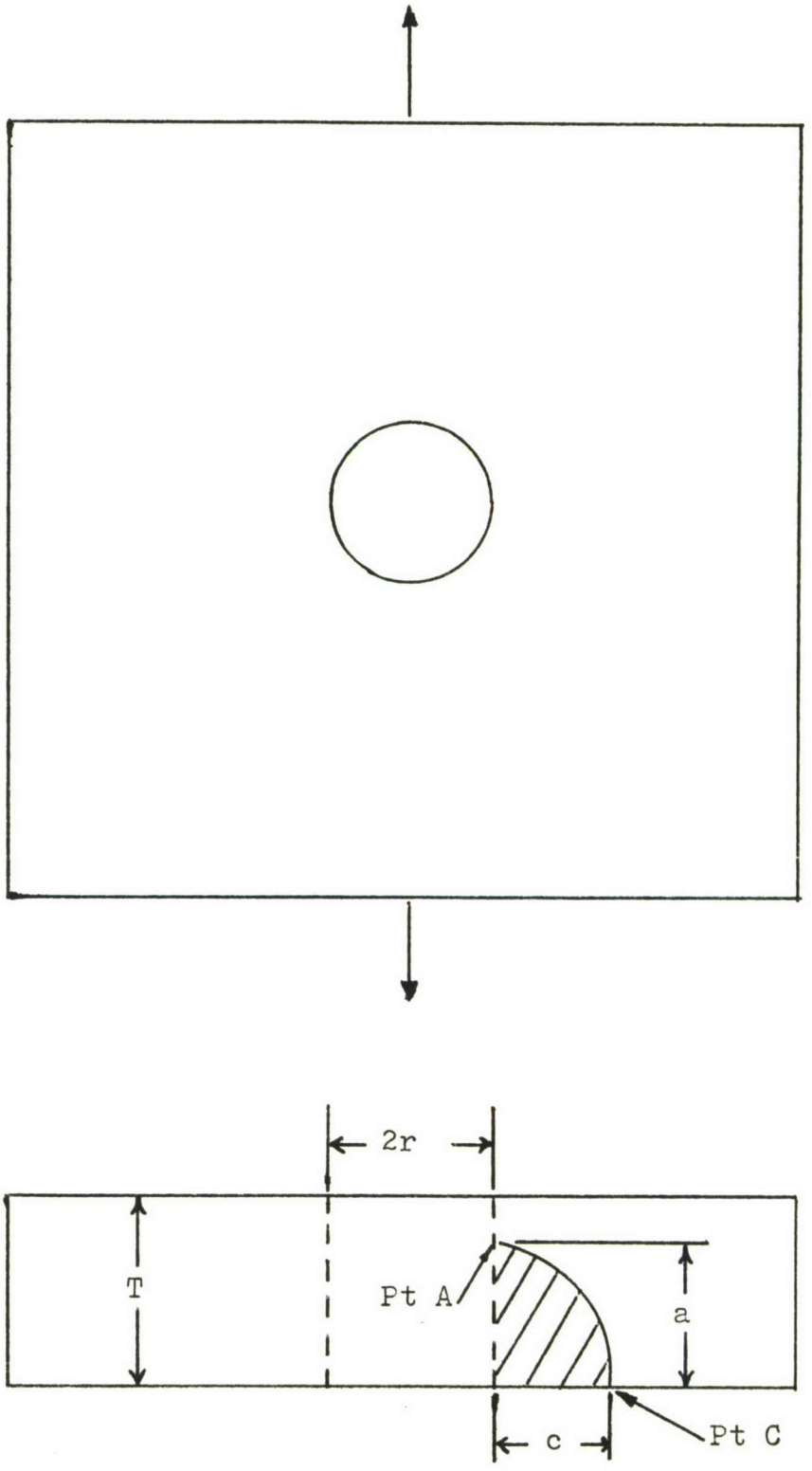

Fig. 1. Geometry of a Part-Thru Corner Crack

II. Review of Information

Background

By applying the theories of elasticity to a flawed specimen loaded perpendicular to the crack surfaces, one can show that the stresses local to the crack tip can be characterized by a single parameter, K, called the stress intensity factor. K, in general, assumes the form

$$K = \sigma \sqrt{\pi a}\ MF \qquad (1)$$

where σ is the far field stress, a is crack length, and MF is a magnification factor that incorporates specimen and crack geometry. K can be thought of physically as a parameter that describes the redistribution of stress due to the introduction of a crack. K normally has the units of psi-$\sqrt{\text{in}}$, which means that MF is dimensionless. In fact, it is often desirable to calibrate (Ref 20) K in terms of crack length, which can be done by solving Eq. 1 for MF, resulting in what is sometimes called a dimensionless stress intensity factor. Calibrations for K which are given in dimensionless form (i.e. in terms of MF) can be used to obtain K values for specimens of different dimensions and varying magnitudes of remote loading.

The determination of K is important to fatigue crack growth analyses. There is a threshold value of K, say K_{th}, below which a flawed specimen can be cycled without measurable crack extension. At the other extreme is K_c, called fracture toughness, a value of K at which a flaw will propagate unstably.

Therefore, fatigue crack growth must occur in the range K_{th} to K_c.

If a specimen contains a flaw (due to metallurgical history, fabrication, improper fitting, etc.) the size of the flaw may be too small for incipient fracture under certain loading conditions. However, the flaw may be large enough to grow from subcritical to critical size under cyclic loading. If the cyclic loading is constant amplitude the crack growth can be predicted by Paris' power law (Ref 17)

$$da/dn = C(\Delta K)^m \qquad (2)$$

where da/dn is crack growth rate, C and m are experimentally determined constants, and ΔK is the stress intensity range between which the specimen is cycled. Paris' relationship is the foundation of the fatigue crack growth test. C and m are material properties, like K_c, which are independent of geometry. Like K_c, the constants C and m may vary with testing variables such as temperature, humidity, and environment. Varying thickness from specimen to specimen also could influence C and m, just as K_c may vary from a plane stress K_c for thin specimens to a plane strain K_c, called K_{Ic}, for thick specimens.

Previous Studies

Part-thru cracks at holes present an extremely difficult three-dimensional elasticity problem, and no exact solutions exist to date. Analytical and numerical approaches are few and

primarily limited to estimates and models of the problem. Cruse and Besuner (Refs 2,4) have combined a boundary-integral equation method for elastic stress analysis with an influence function method for modeling key surface crack growth parameters to yield a technique for calculating K and subsequent fatigue life of surface cracks in areas of concentrated stresses. Kobayashi (Ref 12) has extended an alternating method for ellipitical flaw analysis to solve the corner flaw problem in a quarter-infinite solid. Finite element methods are being applied in fracture mechanics areas with considerable success. Cracked elements have been created specifically for fracture mechanics use, but a three-dimensional capability has not been shown. Known surface flaw solutions have been modified to yield estimates for the corner flaw problem by Liu (Ref 13), Hsu and Liu (Ref 11), and Hall, Engstrom, and Shah (Ref 8). In another experimental method, McGowan and Smith (Ref 15) used stress freezing photoelasticity and a numerical method to obtain K's for the corner flaw problem. The fatigue crack growth method of calibrating K has been used most recently by Grandt and Hinnerichs to study the effect of coldworking holes (Ref 6). They also presented some preliminary results for surface flawed holes using PMMA, a transparent polymer. Their work and techniques formed a base of information from which this study grew.

III. Experimental Program

The Method

With $da/dn = C(\Delta K)^m$ as the foundation, the fatigue crack growth analysis can be broken into three steps:

1. Determine C and m experimentally by measuring da/dn for known K geometries. (Baseline tests)

2. Measure da/dn experimentally for the flaw geometry of interest.

3. Using the basic Paris relation, solve for ΔK.

For step one, several geometries are available, to include the Bowie problem (Ref 3) of a thru crack emanating from a hole, compact tension specimens, and 3 or 4 point bend specimens. Test procedures and standards for baseline tests are given in ASTM-STP-410 (Ref 19). The rationale for steps two and three is that if the K parameter embodies flaw geometry, the ΔK range that is plotted versus da/dn in baseline tests applies not only to the flaw geometries used in the baseline tests but also to any other flaw geometry of interest. This method has the advantages of being simple, inexpensive (renders several data points per specimen), and permits the calibration of complex flaw geometries. Its prime disadvantage is that it requires data to be differentiated; therefore, care must be taken to make crack measurements accurately and to differentiate properly.

Materials

To enable direct observation of crack growth, polymethyl-

methacrylate (PMMA), a transparent polymer, was selected as the test material. It has the advantage of being relatively isotropic and is also quite brittle, thus confining crack tip plasticity to a very small zone. PMMA shows fatigue growth that is macroscopically similar to that occurring in metals (Refs 14,15), and it has been substantiated that the variation in range of stress intensity factor, ΔK, controls cyclic crack growth over at least a limited range.

The nine 8" x 14" specimens used in these tests were made from a 0.72 inch bulk plate of PMMA. After the holes were bored and carefully reamed, each plate was annealed at 100°-104°C for 24 hours and then slowly cooled for 24 hours to room temperature. PMMA is sensitive to time, temperature, and environment changes. Also, thick components may soften from heat generated by higher frequency cyclic loading. Testing temperature (normally 70-75°F) and testing conditions were not controlled but did remain quite constant. Cyclic frequencies were 1 or 2 cps (cycles per second); Arad, Mukherjee, and Hertzberg (Refs 1,10,16) found that no significant heating takes place at less than 5 cps. Pitoniak (Ref 18) conducted several tests using PMMA at a frequency of 3 cps with good success. An MTS (10,000 lb capacity) electrohydraulic fatigue testing machine was used for Test 1. For all other tests an MTS machine with 20,000 lb capacity was used.

Procedures

A total of nine tests were completed: seven tests on the

corner flaw geometry and two baseline tests to determine any frequency effect of 1 versus 2 cps. Using the data from the baseline tests and also data from a previous work (Ref 6) the constants C and m for PMMA were found. Fatigue crack growth rate measurements for the corner flaw geometry were then used to calculate the range in stress intensity factor from Eq 2.

Previous baseline tests were conducted at a frequency of 1 cps by Grandt and Hinnerichs using compact tension, 3 and 4-point bend specimens. In an effort to shorten testing time, two baseline tests of 1 versus 2 cps were conducted to determine the effect of using the higher frequency. The same specimens with a thru crack emanating from a 0.75 inch hole were used for the baseline tests, making them Bowie type problems.

A sketch of a typical specimen after being epoxy bonded and bolted to grips for mounting in the testing machine is shown in Fig. 2. A small crack was initiated by one of two methods. The first was to make a small notch with a file and then sharpen the crack with a razor blade. The second, and more effective method, was to make a starter notch with a jeweller's saw and sharpen the crack with a small scalpel blade. The initial test was conducted on the 10,000 lb MTS machine, which allowed the use of universal joints with eyebolts at each end of the specimen. Subsequent tests were conducted on the 20,000 lb machine, and space limitations allowed the use of only eyebolts at each end of the specimen. This setup required extreme care in aligning the specimen to avoid the in-

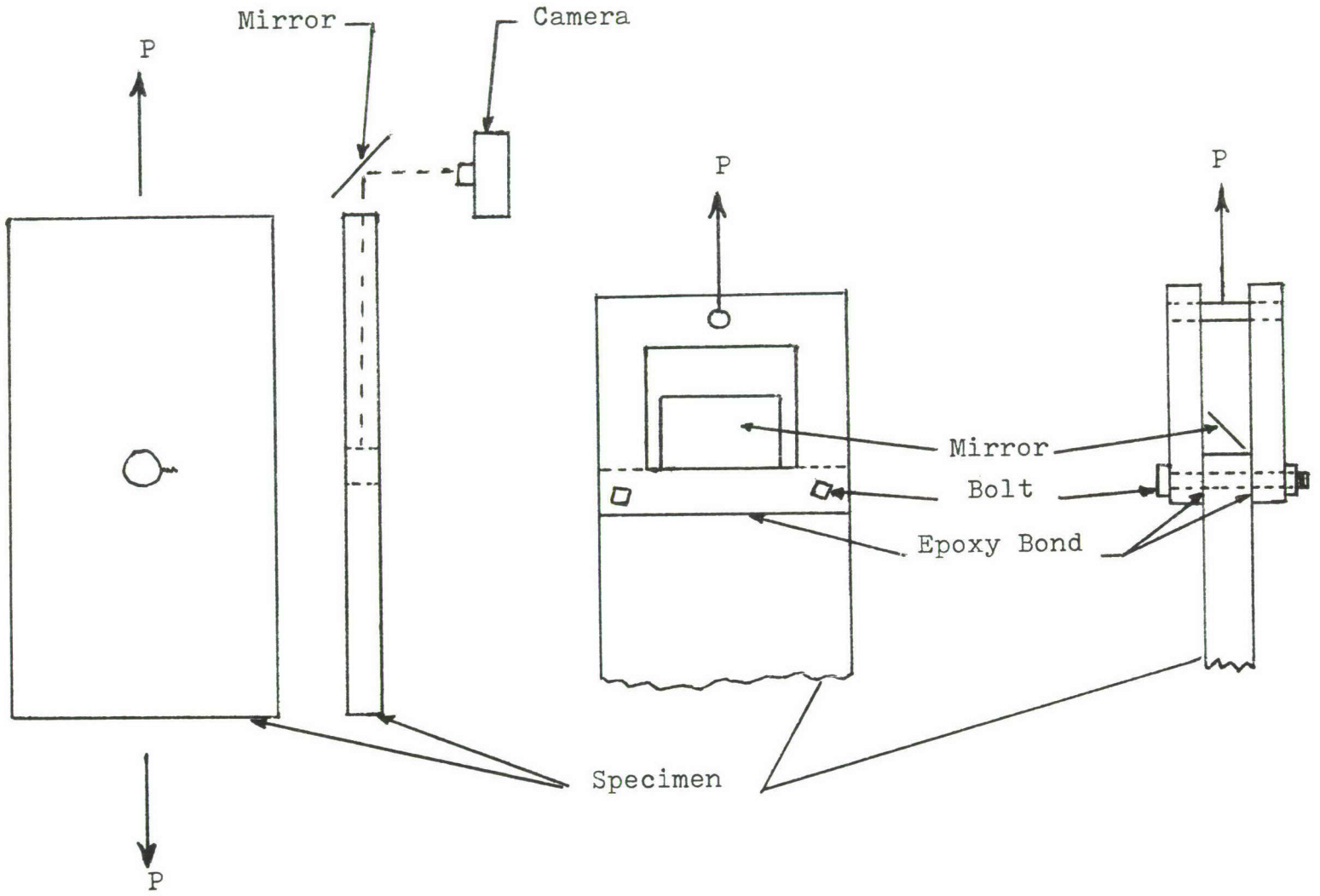

Fig. 2. Schematic of Experimental Apparatus
(From Ref 6)

troduction of any bending loads. After Tests 2 and 3, it was found that one universal joint could be included at one end of the loading setup, making alignment of loading much easier. A small polariscope was used on a few tests to check symmetry of actual loading around the hole. While symmetric loading was noted, no indication of bending could be observed.

The specimen was then cycled at stresses of up to 780 psi until a fatigue crack started to form. The load was then reduced to yield an operating stress of 590 psi for the corner flaw until a uniform crack front was formed. Cyclic loading was sinusoidal, ranging from 100 lbs to 3500 lbs for a ΔP of 3400 lbs, with maximum deviations of ±20 lbs. This range of loading results in an R-ratio ($R = \sigma_{min}/\sigma_{max}$) of about 0.029. Hence, R-ratio effects were assumed negligible and were not included in calculations. K_{min} for the cyclic loading corresponds to the minimum load of 100 lbs, which is assumed to be zero when compared with the maximum load of 3500 lbs. Consequently, ΔK becomes equal to K. ΔP of 3400 lbs versus P_{max} of 3500 lbs was used for all calculations.

Crack growth was recorded by means of a 35 mm camera with bellows. Using the mirror setup as shown in Fig. 2, pictures were made directly through the end perpendicular to the crack using TRI-X (ASA 400) black-and-white film. Lighting of the crack, especially in early growth stages, was particularly difficult. A high-intensity lamp aligned parallel and as close to the camera as possible was found to provide the best illumination.

Measurements of crack lengths on the 35 mm negatives were made using film readers that magnified the image approximately ten times. Photographs were taken at varying cyclic intervals that allowed measurable crack growth of as small as 0.005 inch. A scaling factor for the measurements was formed using the hole diameter as a reference length. Some typical crack photographs are shown in Figures 3 and 4. Reflections of the crack and both surfaces of the plate were very troublesome when measuring small cracks, and this reflection can also be seen in the photos.

The Bowie baseline tests were conducted using the same procedures as above with few exceptions. The initial, thru crack was made with a jeweller's saw, and then the specimen was cycled until a complete, thru-the-thickness, fatigue crack had formed. Photographs were then made under a sinusoidal, cyclic loading of 100 to 2300 lbs. Again, the R-ratio was approximately 0.044, and its effect was thus neglected.

A process that was used by Grandt in a previous work (Ref 7) was used to differentiate present crack growth versus cycles data. Five successive pairs (a,n) of data points were considered in a set. A least-squares parabola was passed through these points and crack length calculated at four regular intervals over the range of the set. The growth rate was computed by a standard least-squares formula which approximates the derivative at the center of five evenly spaced points. The set was then advanced one point and the process repeated until all the data was exhausted. Slightly different least-squares formulas were used for da/dn near the ends of the range of data.

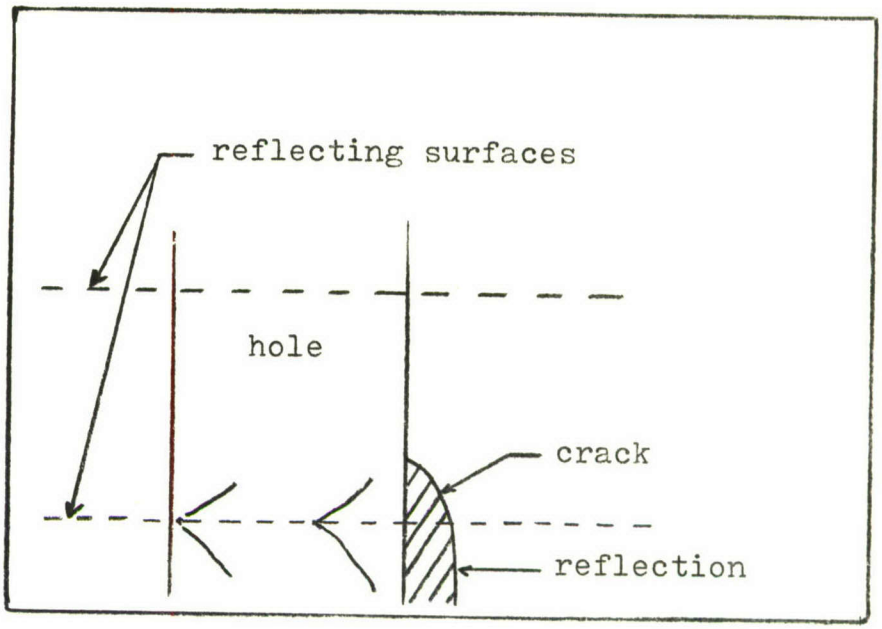

Fig. 3. Photo of a Corner Flaw, Test 9 (14,000 cycles)

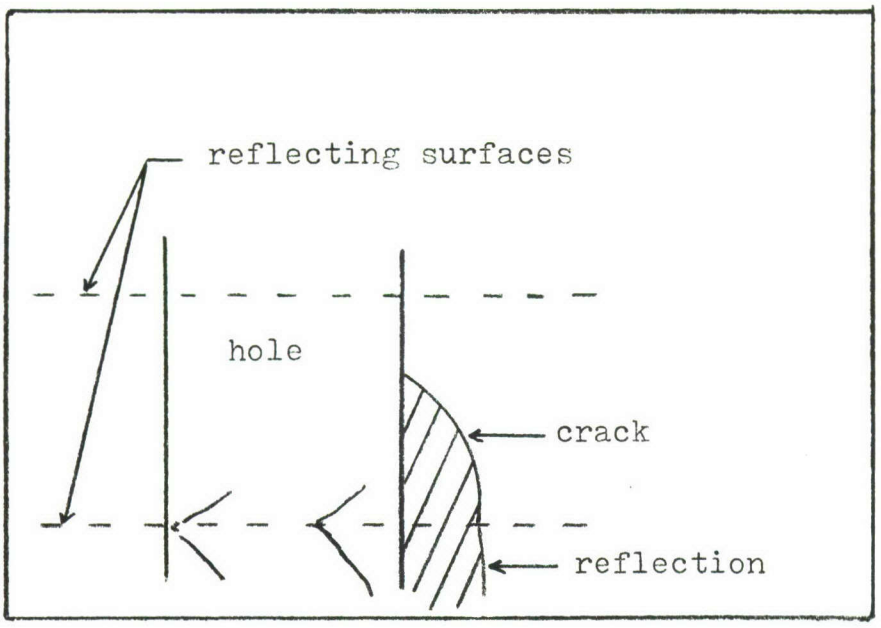

Fig. 4. Photo of a Corner Flaw, Test 9 (27,000 cycles)

IV. Experimental Results

Frequency Effect

The fatigue crack in both tests initiated slightly off the centerline of the thickness and then grew until the crack front was completely thru the thickness. Then the crack assumed a stable, almost symmetrical shape as shown in Figures 5 and 6. An average crack length was computed using the average of a_t, a_m, and a_b. The crack length at one of the plate's surfaces is a_t; a_m is the longest crack length (usually at mid-thickness); and a_b is the crack length at the other surface. For the 1 cps test, a_t was not used in the average because photograph quality did not permit accurate measurement of a_t.

Using Bowie's solution (Ref 3) for a thru-crack emanating from a hole, stress intensity factors for the various crack lengths were calculated. The log of crack growth rate was then plotted versus log ΔK, and the results are shown in Figures 7 thru 11. The least-squares straight line which best fits each set of data is also drawn, and the plots clearly show the linear relation of log da/dn versus log ΔK described by Eq 2. Plots of the separate tests' data are shown in Figures 7 and 8, and a plot of the combined 1 and 2 cps data and its corresponding Paris equation is shown in Fig. 9. Both the 1 and 2 cps data appear to follow the same Paris equation fairly well, but perhaps more examination is needed before any conclusions about frequency effect can be made. In Fig. 10 the least-squares line which best fits the 1 cps data is compared to the

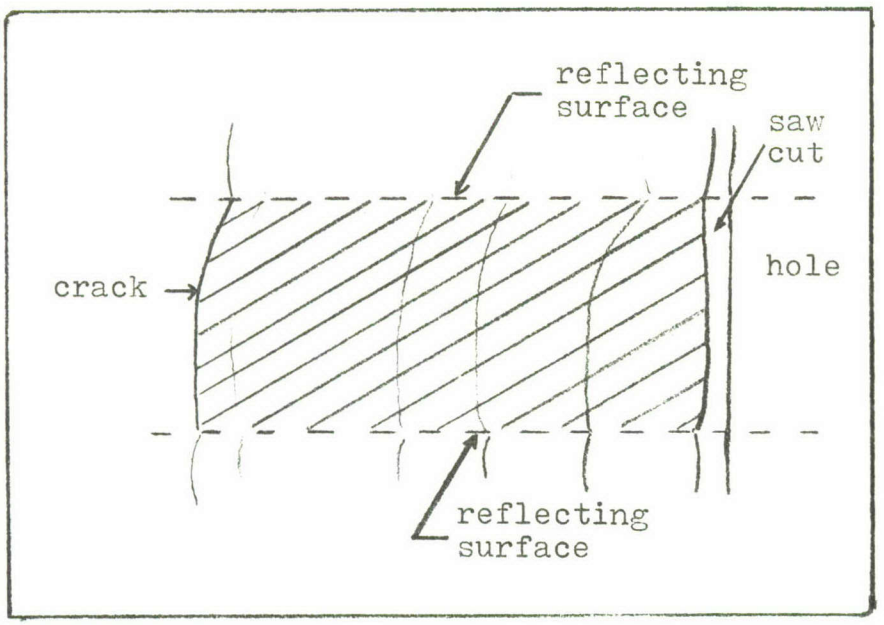

Fig. 5. Photo of Bowie Crack, Test 4 (55,000 cycles)

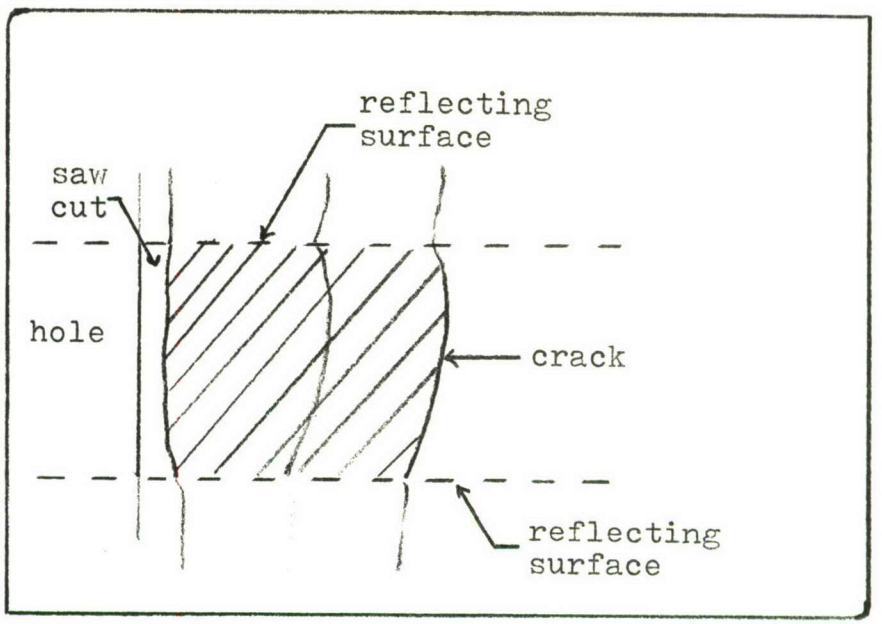

Fig. 6. Photo of Bowie Crack, Test 7 (23,000 cycles)

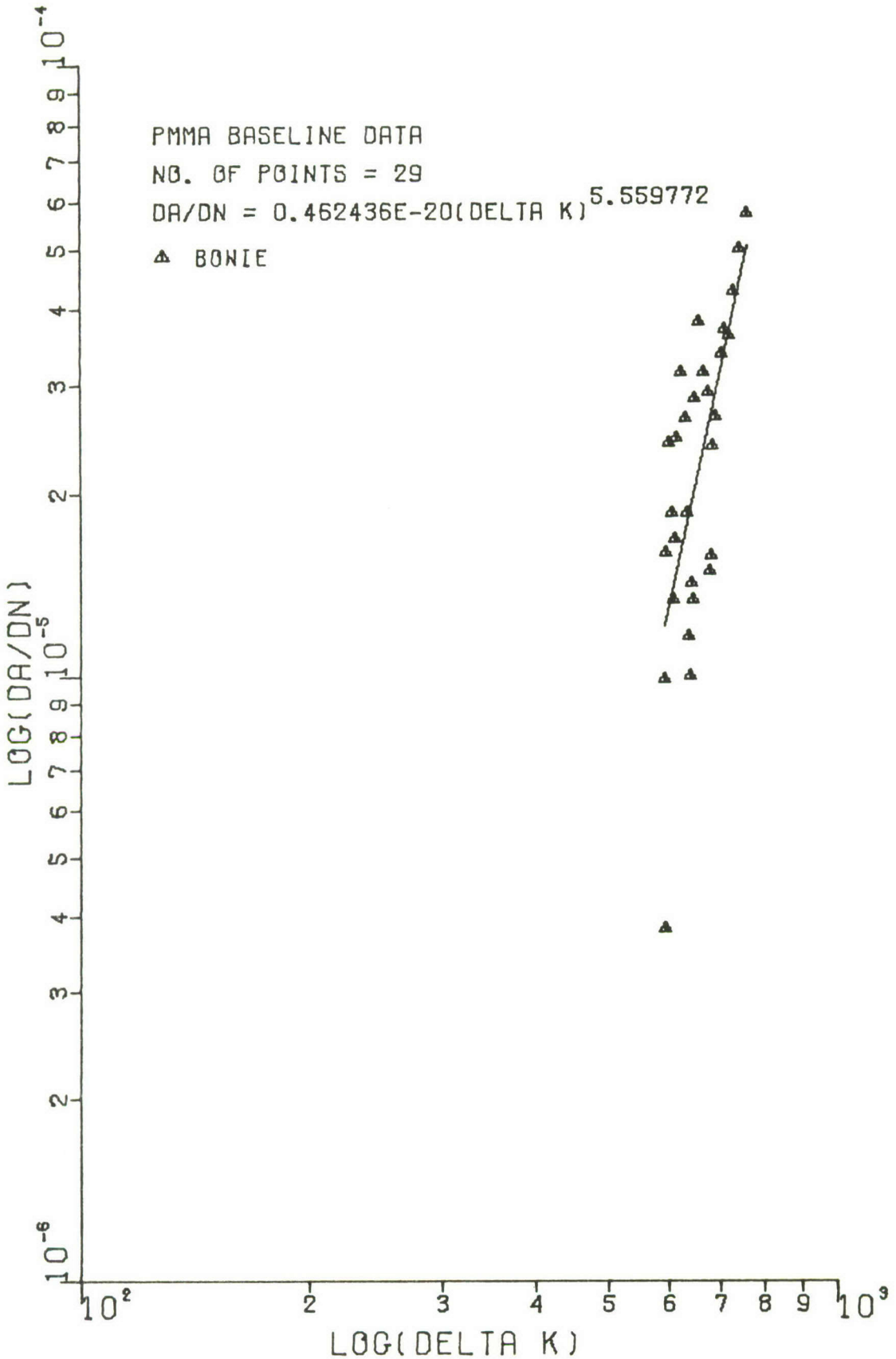

Fig. 7. Baseline Data, Test 4 (1 cps)

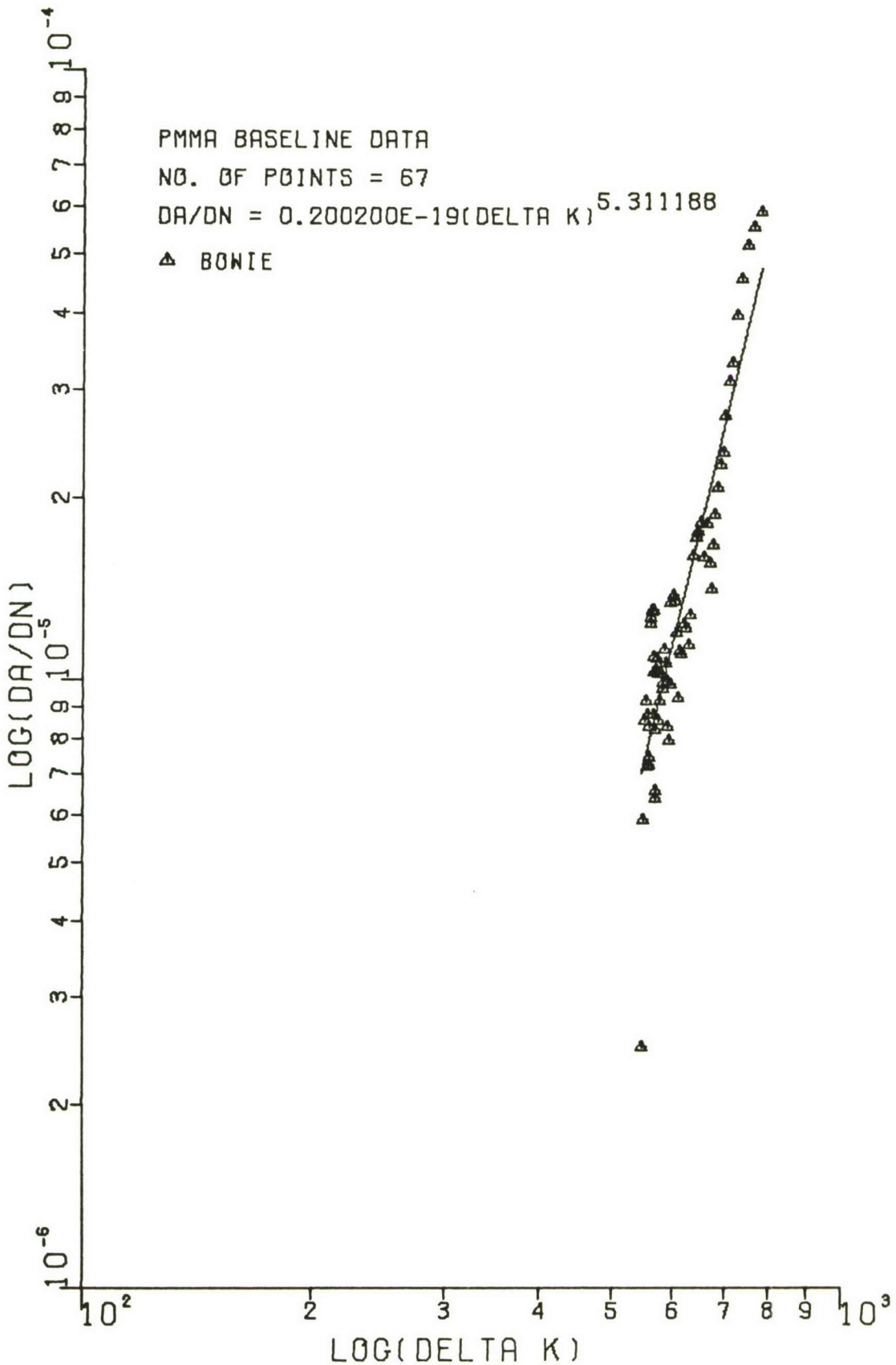

Fig. 8. Baseline Data, Test 7 (2 cps)

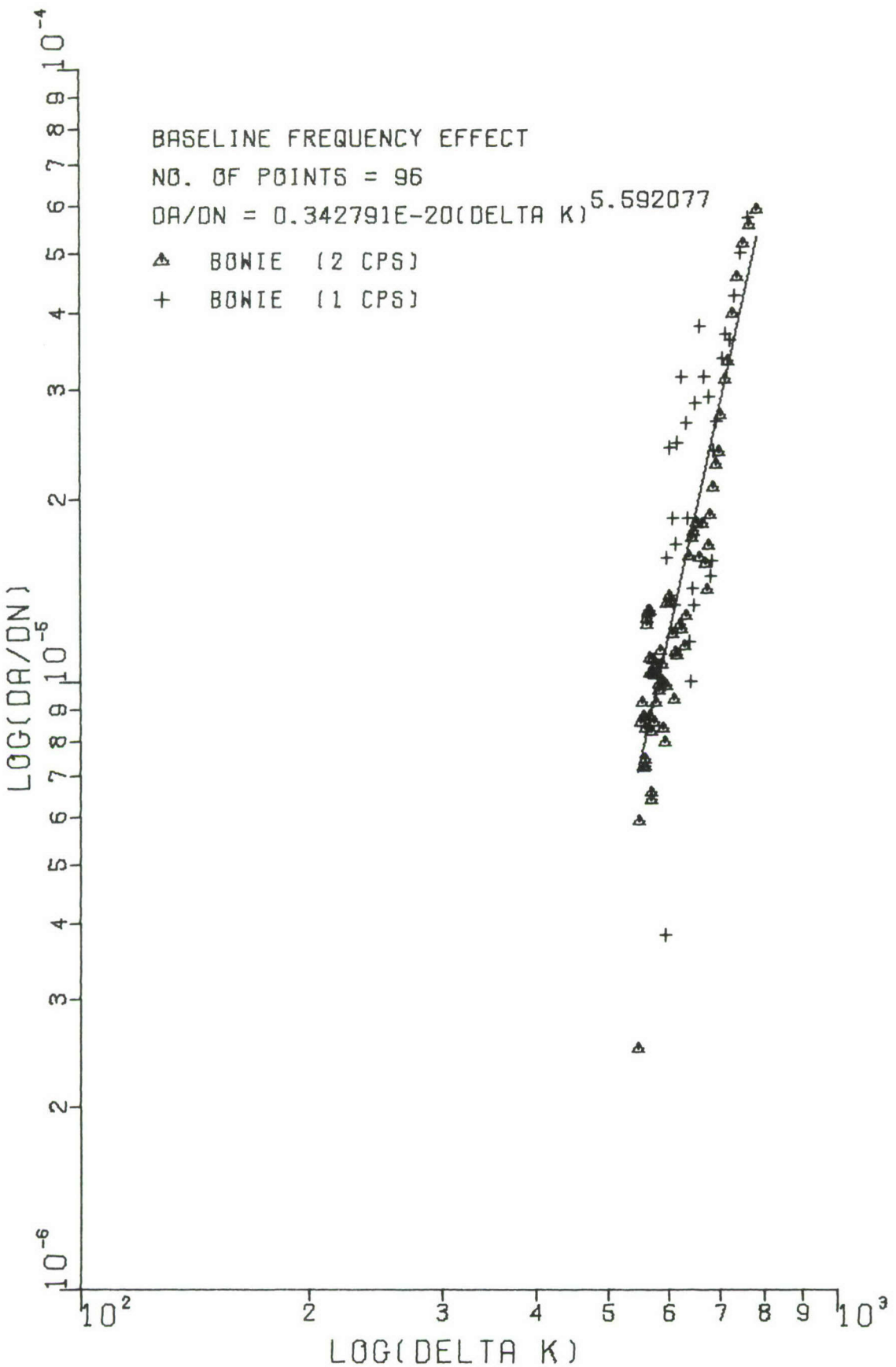

Fig. 9. Baseline Data, Tests 4 and 7 (96 points)

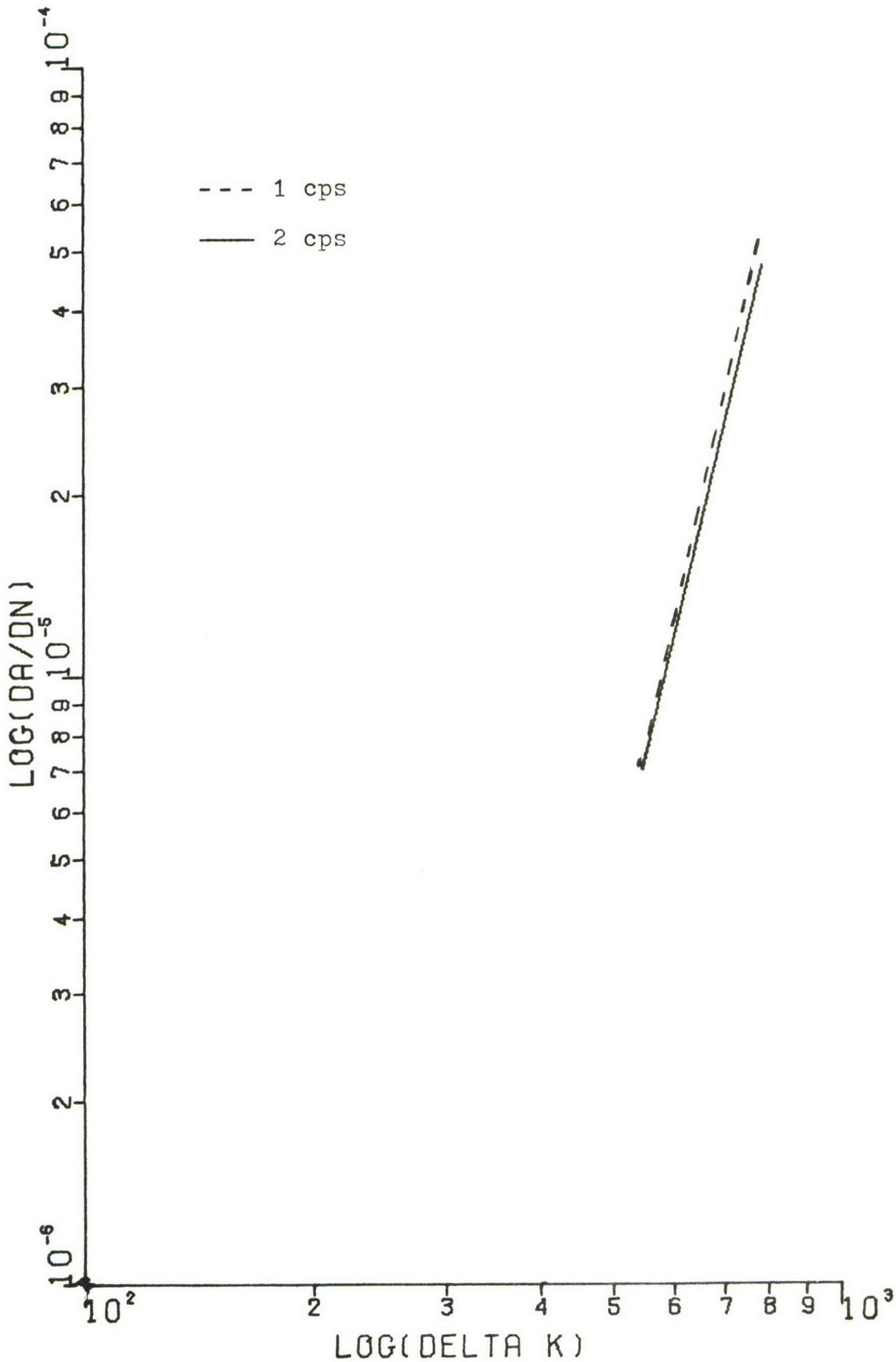

Fig. 10. Comparison of Paris Relations, 1 vs. 2 cps data

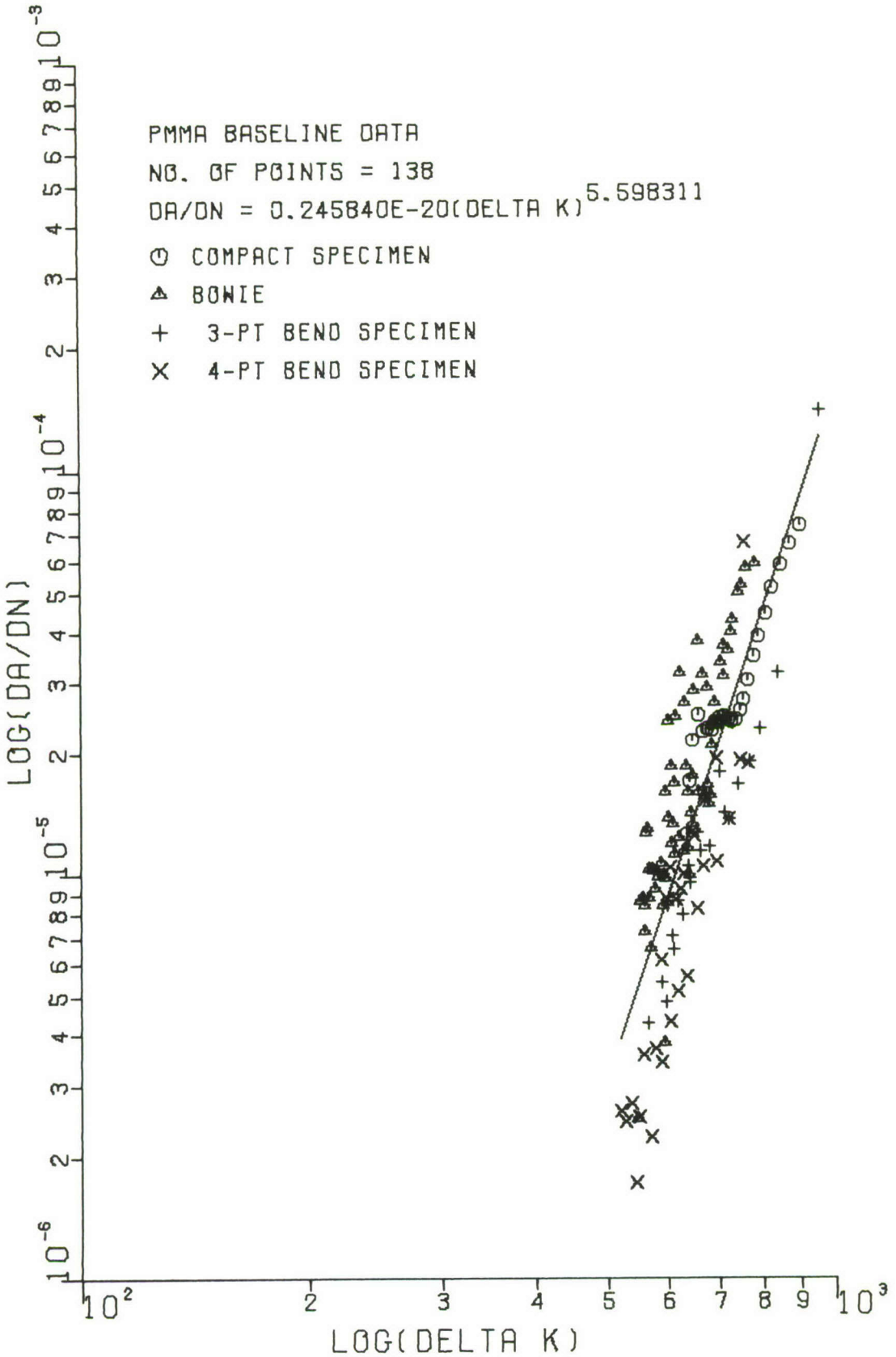

Fig. 11. Baseline Data, (138 points)

least-squares best fit of the 2 cps data. The very small effect of testing at the two frequencies is now more evident. When using baseline data one usually must set limits to define the range over which the data will give good results. The limits that were selected for this study were those used by Grandt and Hinnerichs in Ref. 6; specifically, if da/dn were less than $0.15(10)^{-5}$ inch/cycle or greater than $0.3(10)^{-3}$ inch/cycle, stress intensity factor and magnification factor were set equal to zero. These limits were substituted into the Paris equations of the separate 1 and 2 cps sets of data, the equations of which are given in Fig. 10, and stress intensity factors were calculated. At the upper limit the difference between the two values was less than 5%, and at the lower limit the difference was less than 1%. This was considered a very small difference for stress intensities in the range 400-1100 psi-$\sqrt{\text{in}}$, and it was thus concluded that tests could be run at 1 or 2 cps with no significant loss of accuracy. For evaluating present data, the 96 Bowie baseline data points were combined with the 226 baseline data points of Ref. 6 to produce a baseline data base of 322 points. The constants yielded from the 322 points were $C = 0.22138(10)^{-20}$ and $m = 5.591$. Since a plot of the 322 points tends to make individual data points indistinguishable, 138 points were selected from the full data base and are shown in Fig. 11.

Corner Flaw

Seven tests were conducted on the corner flaw geometry. Test numbers 1 and 2 were conducted at 1 cps, and Tests 3, 5,

6, 8, and 9 were done at 2 cps. Plots of crack length vs. cycles, crack shape (a/c) vs. a/T, magnification factor vs. a/T, and stress intensity factor vs. c are given for each test in Figures 24 thru 51 in the appendix. (See Fig. 1 for a visual explanation of the quantities a, c, and T.) Crack lengths at the surface, c, and along the hole, a, are plotted along with their associated stress intensity factors, KC and KA. Also, dimensionless magnification factors for both a and c crack lengths are plotted, with magnification factor at the hole, MFA, being given by

$$MFA = (KA)/(\sigma \sqrt{\pi a}) \qquad (3)$$

Magnification factor at the surface, MFC, is given by

$$MFC = (KC)/(\sigma \sqrt{\pi c}) \qquad (4)$$

The ratio a/T is a dimensionless quantity, T being thickness in inches. (Note for Test 2: The odd portion of the crack growth curve was caused by the lack of photographs for that portion of the growth.)

Specimen dimensions are generally a width of 8 inches, thickness of 0.72 inch, and a hole diameter of 0.75 inch. Actual specimen dimensions for each test specimen are given in Table II in the appendix. Tests covered periods of time ranging from hours to four days. It was found by Grandt (Ref 7) that interruptions had no apparent effect on test results.

Crack growth was characterized in early stages by growth to the natural crack shape. The term natural refers to the tendency of a starter crack in constant geometry specimens to assume about the same a/c ratio when subjected to the same loading. The a/c ratio in all cases was greater than one. Early growth to the natural shape can be seen in the first portion of the a/c curve for Tests 6 and 8, Figures 41 and 45. Some of the oscillation in early crack length measurements was probably caused by the combination of poor lighting and reflection, which produced a poor quality picture. In general, the quality of pictures increased as the crack grew, resulting in better illumination.

It was also observed in both baseline and corner flaw tests that the fatigue crack front at the surface (point C in Fig. 1) lagged behind the crack front within the thickness. This is probably direct observation of the transition from a plane strain to a plane stress condition as predicted for a thick specimen. Some specimens were cycled to fracture, and the fracture surfaces showed no shear lips, indicating that plane stress zones were very small and that plane strain fracture had definitely occurred.

V. Discussion of Results

The works of McGowan and Smith (Ref 15) and Hall and Finger (Ref 9) both noted a decrease in stress intensity factor at the hole, KA, and an increase in stress intensity factor at the surface, KC, as a/T reached higher values. McGowan and Smith conjectured that this result might be due to the fact that, when the crack is deep, a substantial part of the load is transferred to the side of the hole opposite the crack due to its greater stiffness. Thus, the remaining ligament between the "a" crack front and back surface of the plate carries a reduced load. Another point could also be considered. As the crack approaches the back surface of the plate, the ligament may become part of the plastic zone at the crack front, causing load redistribution.

The decrease in KA and increase in KC was, in general, not in evidence in present test data. This is probably because plasticity effects were kept to a small scale by using small loads in the fatigue test. Pitoniak (Ref 18) found several values for PMMA yield strength and fracture toughness, averages of which are 7000 psi and 1000 psi-$\sqrt{\text{in}}$, respectively. The present tests used a maximum stress of about 600 psi, less than 0.1 of the yield strength. This stress yielded maximum stress intensities near the crack front on the order of 100 psi-$\sqrt{\text{in}}$, again 0.1 of K_{Ic}. Therefore, it can be concluded that plasticity was on a small scale, and load redistribution did not occur at the higher a/T values. In general, it can be supposed that observation of the KA and KC changes are material and load dependent.

Figures 14 thru 23 in the appendix are plots of dimensionless magnification factor versus normalized a/T. There are five sets of "a" and "c" magnification factors for five ranges of a/c. The data points come from all seven tests on the corner flaw geometry and encompass 86% of the total number of test points. Results compare favorably with the preliminary tests of Grandt and Hinnerichs. Comparisons are given in Figures 12 and 13 of part of the data with the estimates of Gran, et.al., Hsu and Liu, and Hall and Finger (Refs 5,11,9). A discussion of the three estimates and how they compare with present data now follows. The present data points shown in the comparison plots are magnification factors for the 1.35-1.45 a/c range. Accordingly, points used to plot the estimates were calculated using nominal values of a/c of 1.4, thickness of 8 inches, and a hole radius of 0.37 inch. Further comparison between the estimates and present data is given in Table I. Present data given in the table are from Test 1 where pertinent parameters agreed quite closely with the nominal values used in the estimates' calculations.

Gran, et al.

The basic solution for an embedded elliptical flaw was modified to account for hole and free surface effects and also included a correction factor for out of shape ellipses. The final expression for stress intensity factor at the hole (KA) is

$$KA = \frac{1.12(3\sigma)\sqrt{\pi a}}{\Phi}\left(\frac{2T}{\pi a}\tan\frac{\pi a}{2T}\right)^{\frac{1}{2}} \qquad (5)$$

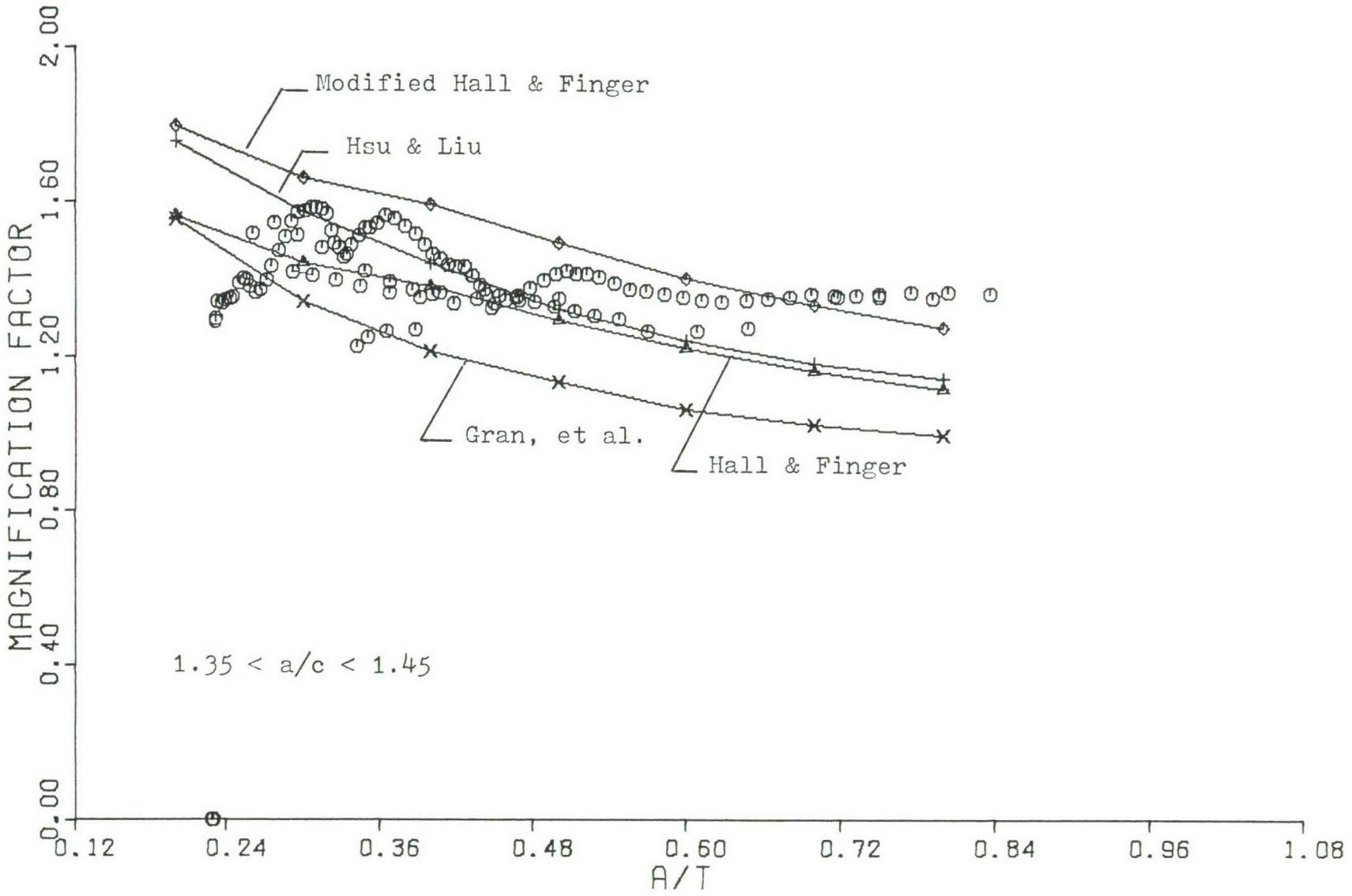

Fig. 12. Comparison of Estimates of the Magnification Factor at the Surface for an $a/c_{avg} = 1.4$

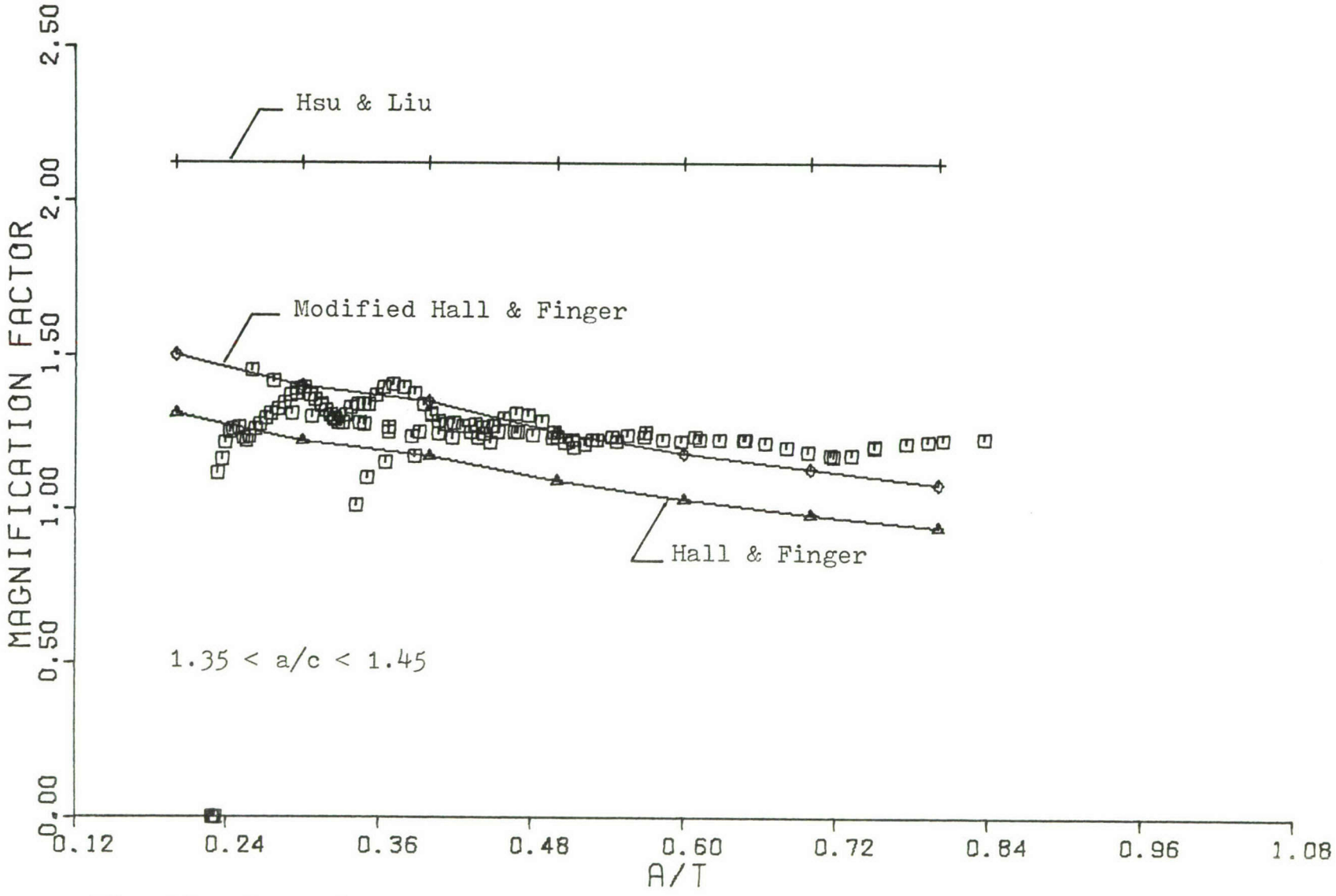

Fig. 13. Comparison of Estimates of the Magnification Factor at the Hole for an $a/c_{avg} = 1.4$

Table I

Comparison Table

a/T	Present Data	Gran	Hsu/ Liu	Hall/ Finger	Modified Hall/Finger
Comparison of Hole Magnification Factor Estimates:					
.3	1.39	2.60	2.12	1.22	1.40
.4	1.31	2.69	2.12	1.17	1.35
.5	1.25	2.82	2.12	1.09	1.25
.6	1.22	3.01	2.12	1.03	1.18
.7	1.19	3.33	2.12	.98	1.13
.8	1.23	3.90	2.12	.94	1.08
% Difference of MFA Estimates from Present Data:					
.3	--	+87	+53	-12	+1
.4	--	+105	+62	-11	+3
.5	--	+126	+70	-13	0
.6	--	+147	+74	-16	-3
.7	--	+180	+78	-18	-5
.8	--	+217	+72	-24	-12
Comparison of Surface Magnification Factor Estimates:					
a/T	Present Data	Gran	Hsu/ Liu	Hall/ Finger	Modified Hall/Finger
.3	1.58	1.34	1.57	1.44	1.66
.4	1.46	1.21	1.44	1.38	1.59
.5	1.41	1.13	1.32	1.29	1.49
.6	1.35	1.06	1.24	1.22	1.40
.7	1.36	1.02	1.18	1.16	1.33
.8	1.36	.99	1.14	1.11	1.27
% Difference of MFC Estimates from Present Data:					
.3	--	-15	-1	-9	+5
.4	--	-17	-1	-5	+9
.5	--	-20	-6	-9	+6
.6	--	-21	-8	-10	+4
.7	--	-25	-13	-15	-2
.8	--	-27	-16	-18	-7

Here Φ is the complete elliptical integral of the second kind. A plot of Φ values versus a/c is given in Ref 11. This yields a magnification factor at the hole (MFA) of

$$MFA = \frac{3.36}{\Phi} \left(\frac{2T}{\pi a} \tan \frac{\pi a}{2T} \right)^{\frac{1}{2}} \qquad (6)$$

For the stress intensity factor at the surface (KC),

$$KC = \frac{1.12\sigma \sqrt{\pi b}}{\Phi} \left(1 + \frac{1}{2}\left(\frac{r}{r+c}\right)^2 + \frac{3}{2}\left(\frac{r}{r+c}\right)^4 \right) \qquad (7)$$

and magnification factor at the surface (MFC) is given by

$$MFC = \frac{1.12}{\Phi} \left(1 + \frac{1}{2}\left(\frac{r}{r+c}\right)^2 + \frac{3}{2}\left(\frac{r}{r+c}\right)^4 \right) \qquad (8)$$

where b was set equal to c.

It can be seen from Table I that the estimate for magnification factor at the hole is considerably larger than present data at a/T = 0.3 and diverges with increasing a/T; therefore, this estimate is not included in the plot of Fig. 13. The estimate for the surface magnification factor is much closer to present data, ranging from 15% to 27% less, with an average of 21% less.

Hsu and Liu

Stress intensity expressions for truncated elliptical cracks at the corner of a quarter-infinite solid were derived. These were modified to account for the influence of the hole

and the front free surface to yield the following expression for magnification factor

$$MF = B \frac{M_1'}{\Phi} \tag{9}$$

B is Bowie's factor (Ref 3) which accounts for the influence of the hole on a full-thru crack, and M_1'/Φ is a factor that accounts for the front surface influence and also flaw shape. Plots of M_1'/Φ are given in Ref. 11. For MFA, B = 3.36 and M_1'/Φ is also constant, equaling 0.63. Then,

$$MFA = (3.36)\ (0.63) = 2.12 \tag{10}$$

for all values of a/T. For MFC, M_1'/Φ is constant and equals 0.86; but B varies with distance from the hole. Therefore,

$$MFC = 0.86\ B(c/r) \tag{11}$$

Table I shows that the MFA estimate ranges from 53% to 78% greater than present data, with an average of 68% greater. However, the MFC estimate ranges from 1% to 16% less than present data, with an average of 7.5% less.

Hall and Finger

Fracture measurements of flawed holes were used to empirically relate flaw size and fracture strength, K_{Ic}. Their failure criterion assumed the form

$$K_{Ic} = C\sigma \sqrt{\pi c_e}\ F(c_e/r) \qquad (12)$$

where c_e is an effective crack length corresponding to a thru-the-thickness, Bowie crack. They found that a value for C of 0.87 correlated well with their data.

For present estimates the form of Eq 12 was used to estimate K. Also it was necessary to interpolate the curves for c_e since Hall and Finger's data incorporated a maximum a/c of one. Using C = 0.87, the magnification factor expression becomes

$$MF = 0.87 \sqrt{c_e/b}\ F(c_e/r) \qquad (13)$$

Table I shows good agreement with present data. MFA estimates range from 11% to 24% below present data, with an average of 16% below. MFC estimates range from 5% to 18% below present data, with an average of 11% below.

It was noted that a higher value of C might give better agreement. One justification for a change could be a significant difference in plastic zone sizes of the testing materials. Hall and Finger used two test materials, 2219-T87 aluminum and 5Al-2.5Sn(ELI) titanium, that have similar plastic zone sizes, 0.060 and 0.050 inch. The plastic zone size of PMMA is much smaller, about 0.003 (Ref 18:33). Accordingly, a C value of 1.0 was used to yield modified Hall and Finger estimates.

Table I shows very good agreement with present data. MFA estimates range from 3% above to 12% below present data, with

an average of 2.7% below. Excellent agreement is shown for all values of a/T except the higher ones. MFC estimates range from 2% below to 9% above present data, with an average of 2.5% above.

VI. Conclusions and Recommendations

Conclusions

1. Fatigue crack growth rate, da/dn, as a function of stress intensity factor, K, for PMMA under constant amplitude, cyclic loading can be characterized by

$$da/dn = 0.22138(10)^{-20}K^{5.591} \qquad (14)$$

R-ratio (min/ max) should be near or equal to zero. For this study it was 0.029.

2. Testing at 1 or 2 cps has a negligible effect (<5%) on results in the range of crack growth from $0.15(10)^{-5}$ to $0.30(10)^{-3}$ inch/cycle.

3. Present estimates of stress intensity factors for corner flaws emanating from holes tend to overestimate K at the hole and underestimate K at the surface for flaw shapes in the range of 1.4. A modified Hall and Finger empirical relation shows good agreement with present data, especially for K at the hole.

4. The scatter of test data, particularly at early growth stages, is probably a result of the quality of photographs being very sensitive to illumination of the crack. Scatter in the magnification factor plots at early a/T values could possibly be a result of the crack not reaching its natural shape by that range in a/T. A better method of crack initiation would probably yield better quality pictures and more efficient examination of

early growth.

5. The fatigue crack growth test is a useful experimental technique for obtaining stress intensity factor calibrations, especially for complex, three-dimensional geometries.

Recommendations

1. The modified Hall and Finger relation suggests the possibility of using the fatigue crack growth test to find an empirical relation for complex flaw geometries. Further crack growth rate tests should include a study to find a relation between stress intensity factor and crack length that fits the experimental data well and yields conservative estimates of stress intensities that can be used either for approximation or to identify trends.

2. Fatigue crack growth tests should be conducted with various specimen thicknesses and hole diameters which would yield various crack shapes. Thus the effect of crack shape, a/c, could be determined.

3. Tests of other flaw geometries are of importance and should be studied. Geometries such as the completely embedded flaw at a hole, two corner flaws at a hole, or flaws at a hole with partial load transfer should receive primary consideration.

Bibliography

1. Arad,L., J.C. Radon and L.E. Culver. "Fatigue Crack Propagation in Polymethylmethacrylate; the Effect of the Mean Value of Stress Intensity Factor." Journal Mechanical Engineering Science, 13:75-81 (1971).

2. Besuner, P.M. "Residual Life Estimates for Structures with Partial Thickness Cracks," submitted for publication. Author is Research Engineer for United Aircraft Corporation, Pratt & Whitney Aircraft Division, East Hartford, Connecticut, 1974.

3. Bowie, O.L. "Analysis of an Infinite Plate Containing Radial Cracks Originating from the Boundary of an Internal Circular Hole," Journal of Mathematics and Physics, Vol. 35, pp. 60-71, 1956.

4. Cruse, T.A. and P.M. Besuner. "Residual Life Prediction for Surface Cracks in Complex Structural Details," submitted for publication. Authors are engineers for United Aircraft Corporation, Pratt & Whitney Aircraft Division, East Hartford, Connecticut, 1974.

5. Gran, R.J., F.D. Orazio, P.C. Paris, G.R.Irwin, and R. Hertzberg. "Investigation and Analysis Development of Early Life Aircraft Structural Failures," Technical Report AFFDL-TR-70-149, Wright-Patterson Air Force Base, Ohio, March 1971.

6. Grandt, A.F. and T.D. Hinnerichs. "Stress Intensity Factor Measurements for Flawed Fastener Holes," presented at the Army Symposium on Solid Mechanics, South Yarmouth, Cape Cod, Massachusetts, 10-12 September 1974.

7. Grandt, A.F. and G.M. Sinclair. "Stress Intensity Factors for Surface Cracks in Bending," Stress Analysis and Growth of Cracks, Proceedings of the 1971 National Symposium on Fracture Mechanics, Part I, ASTM STP 513,1972, pp. 37-58.

8. Hall, L.R., W.L. Engstrom, and R.C. Shah. "Fracture and Fatigue Crack Growth Behavior of Surface Flaws and Flaws Originating at Fastener Holes," Technical Report AFFDL-TR-74-47, Air Force Flight Dynamics Laboratory, Wright Patterson Air Force Base, Ohio, March 1974.

9. Hall, L.R. and R.W. Finger. "Fracture and Fatigue Growth of Partially Embedded Flaws," Proc. of Air Force Conference on Fatigue and Fracture of Aircraft Structures and Material, AFFDL-TR-70-144, Air Force Flight Dynamics Laboratory, Wright-Patterson Air Force Base, Ohio, 235-262, September 1970.

10. Hertzberg, R.W., H. Nordberg, and J.A. Manson. "Fatigue Crack Propagation in Polymeric Materials." Journal of Materials Science, 5:521-526 (1970).

11. Hsu, T.M. and A.F. Liu. "Stress Intensity Factors for Truncated Elliptical Cracks," presented at the Seventh National Symposium on Fracture Mechanics, College Park, Maryland, August 27-29, 1973.

12. Kobayashi, A.S. "Stress Intensity Factor of a Corner Crack," Interim Technical Report No. 3, sponsored by Army Research Office, Durham, August 1974.

13. Liu, A.F. "Stress Intensity Factor for a Corner Flaw," Journal of Engineering Fracture Mechanics, Vol. 4, March 1972.

14. McEvily, A.J., R.C. Boettner, and R.L. Johnston. "On the Formation and Growth of Fatigue Cracks in Polymers," Fatigue - An Interdisciplinary Approach, Proceedings of the 10th Sagamore Army Materials Research Conference, Syracuse University Press, 1964, pp. 95-103.

15. McGowan, J.J. and C.W. Smith. "Stress Intensity Factors for Deep Cracks Emanating from the Corner Formed by a Hole Intersecting a Plate Surface," presented at the 8th National Symposium on Fracture Mechanics, Brown University, August 26-28, 1974.

16. Mukherjee, B., L.E. Culver, and K.J. Burns. "Growth of Part-through and Through-thickness Fatigue Cracks in Sheet Glassy Plastics," Experimental Mechanics, 90-96 (February 1969).

17. Paris, P.C. and F. Erdogan. "A Critical Analysis of Crack Propagation Laws," Journal of Basic Engineering, Transactions of the ASME, Vol. 85, Series D, No. 4, December 1963, pp. 528-533.

18. Pitoniak, F.J. "Experimental Study of Fatigue Crack Propagation and Retardation Using Polymethylmethacrylate," Technical Report AFFDL-TR-72-235, Air Force Flight Dynamics Laboratory, Wright-Patterson Air Force Base, Ohio, November 1972.

19. Plane Strain Fracture of Metallic Materials, ASTM STP 410 ASTM (1965).

20. Smith, H.R. and D.E. Piper. "Stress-Corrosion Testing with Precracked Specimens," D6-24872, The Boeing Company, Seattle, Washington, June 1970.

Appendix

Test Data and Plots

Table II

Actual Specimen Dimensions

Test Number	Type of Test	Width,W (inches)	Thickness,T (inch)	Hole Diam,2r (inch)
4	Baseline	7.95	0.078	0.742
7	Baseline	7.98	0.717	0.740
1	Corner flaw	7.98	0.729	0.747
2	Corner flaw	7.97	0.690	0.753
3	Corner flaw	7.98	0.730	0.750
5	Corner flaw	7.95	0.720	0.742
6	Corner flaw	7.95	0.698	0.739
8	Corner flaw	7.98	0.704	0.743
9	Corner flaw	7.97	0.704	0.743

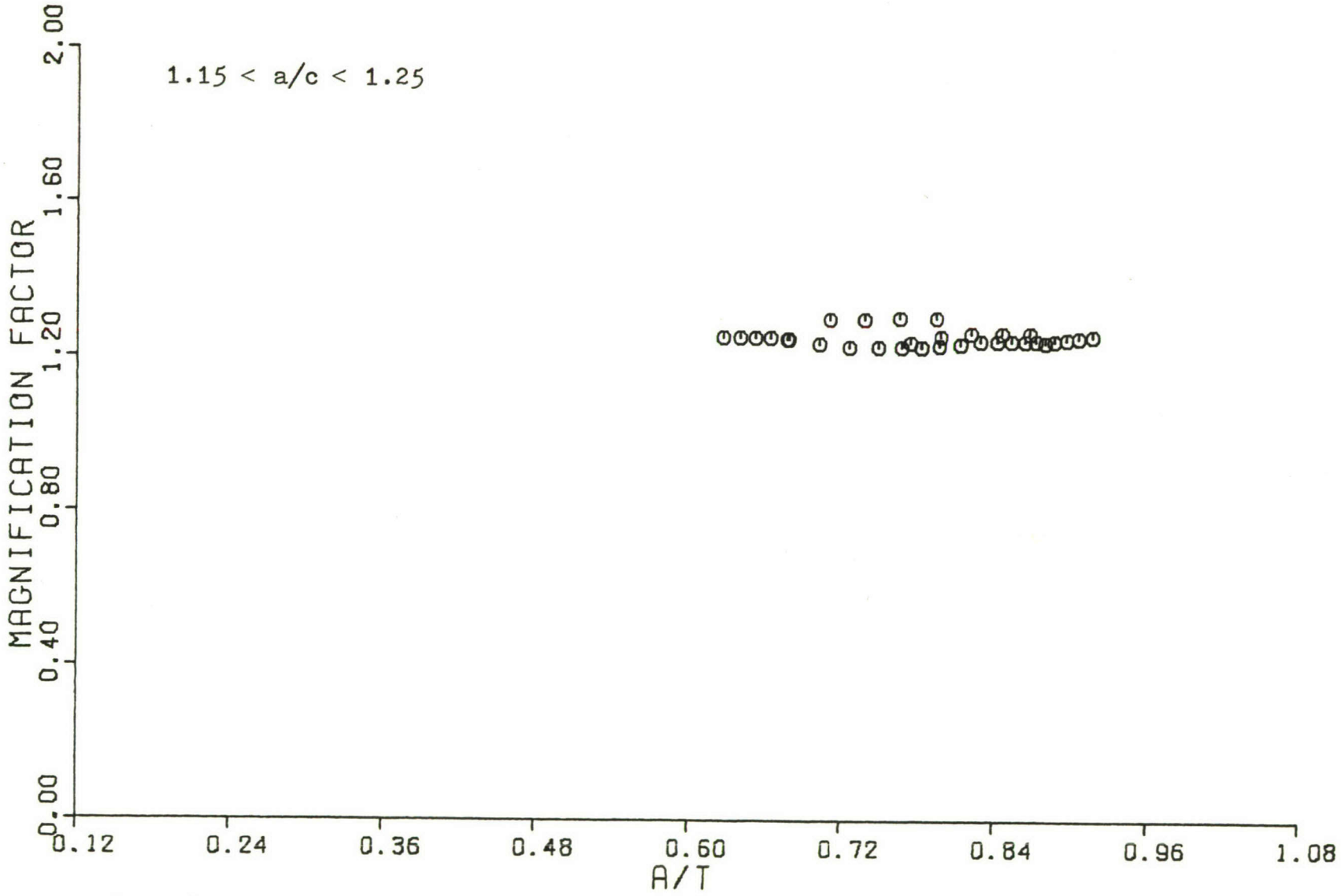

Fig. 14. Magnification Factor at the Surface for $a/c_{avg} = 1.2$

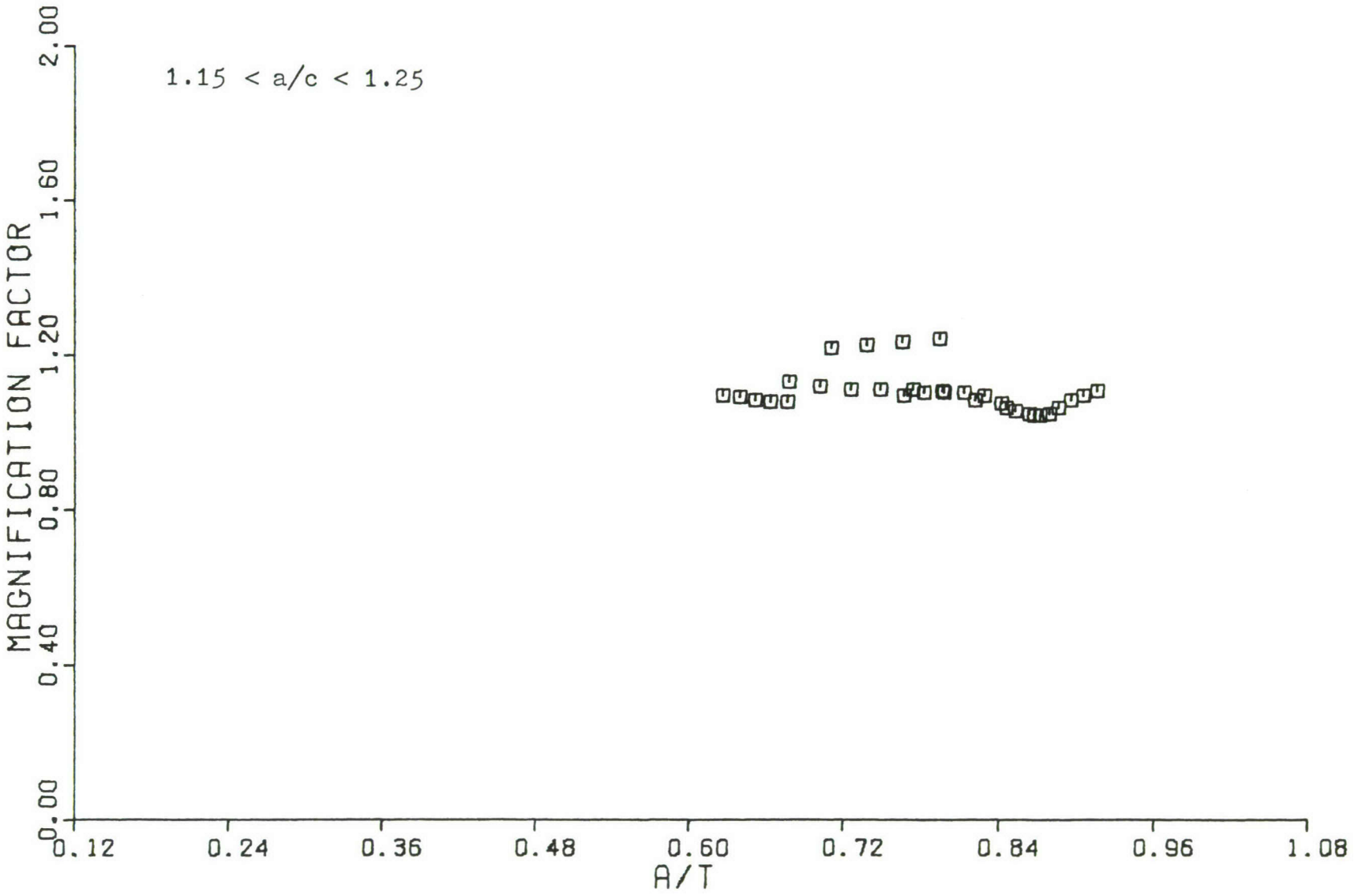

Fig. 15. Magnification Factor at the Hole for $a/c_{avg} = 1.2$

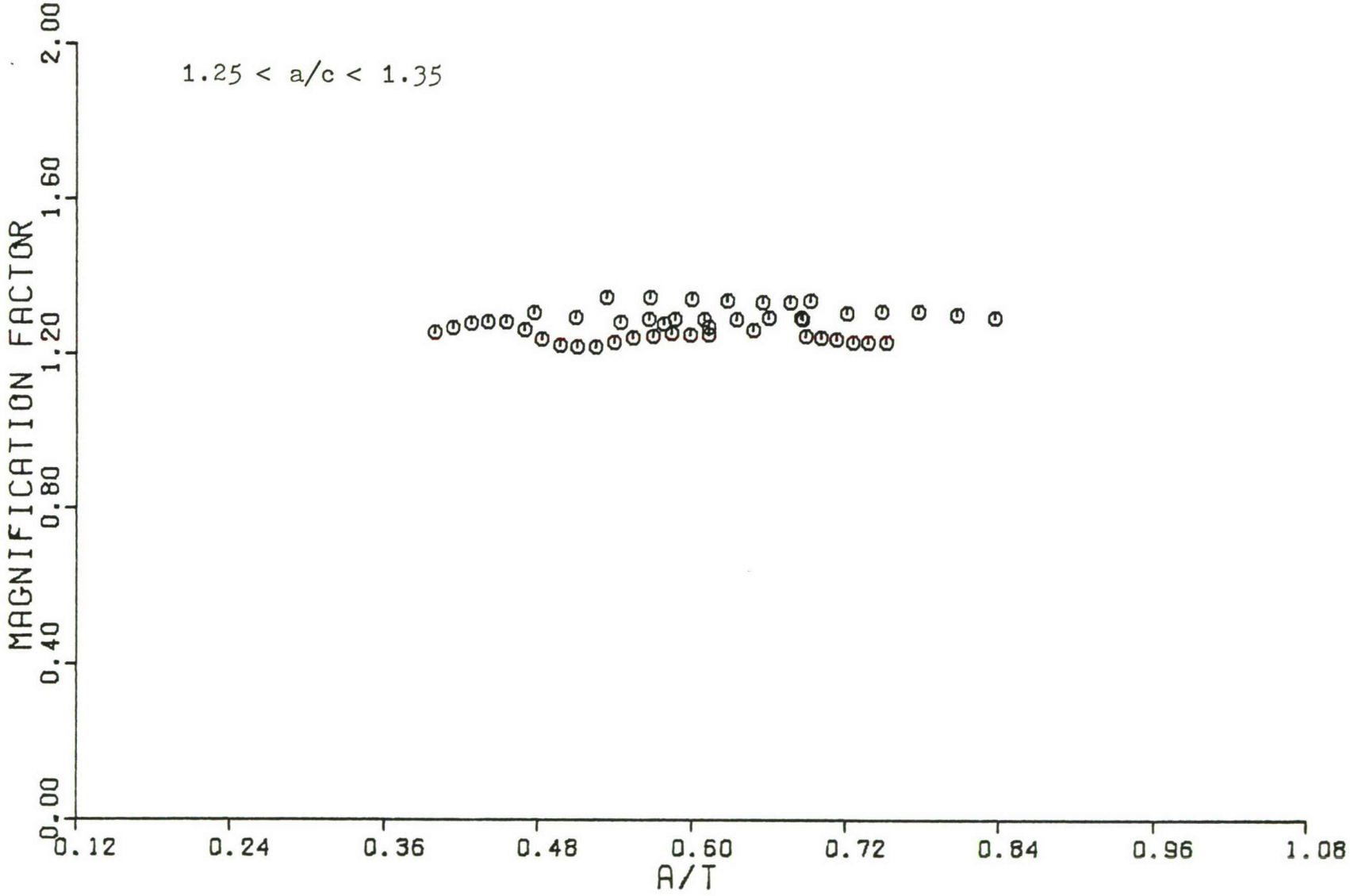

Fig. 16. Magnification Factor at the Surface for a/c_{avg} = 1.3

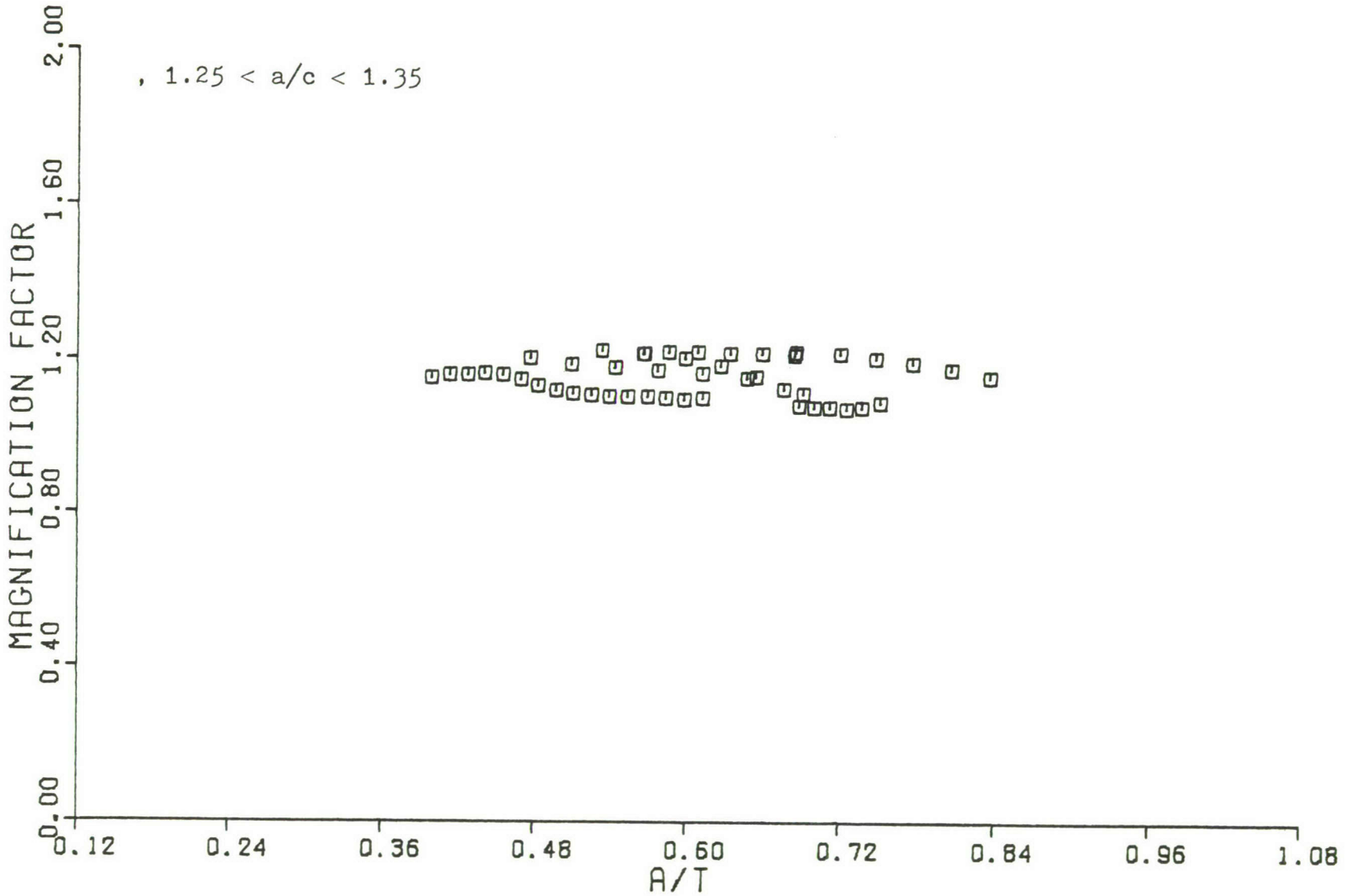

Fig. 17. Magnification Factor at the Hole for a/c_{avg} = 1.3

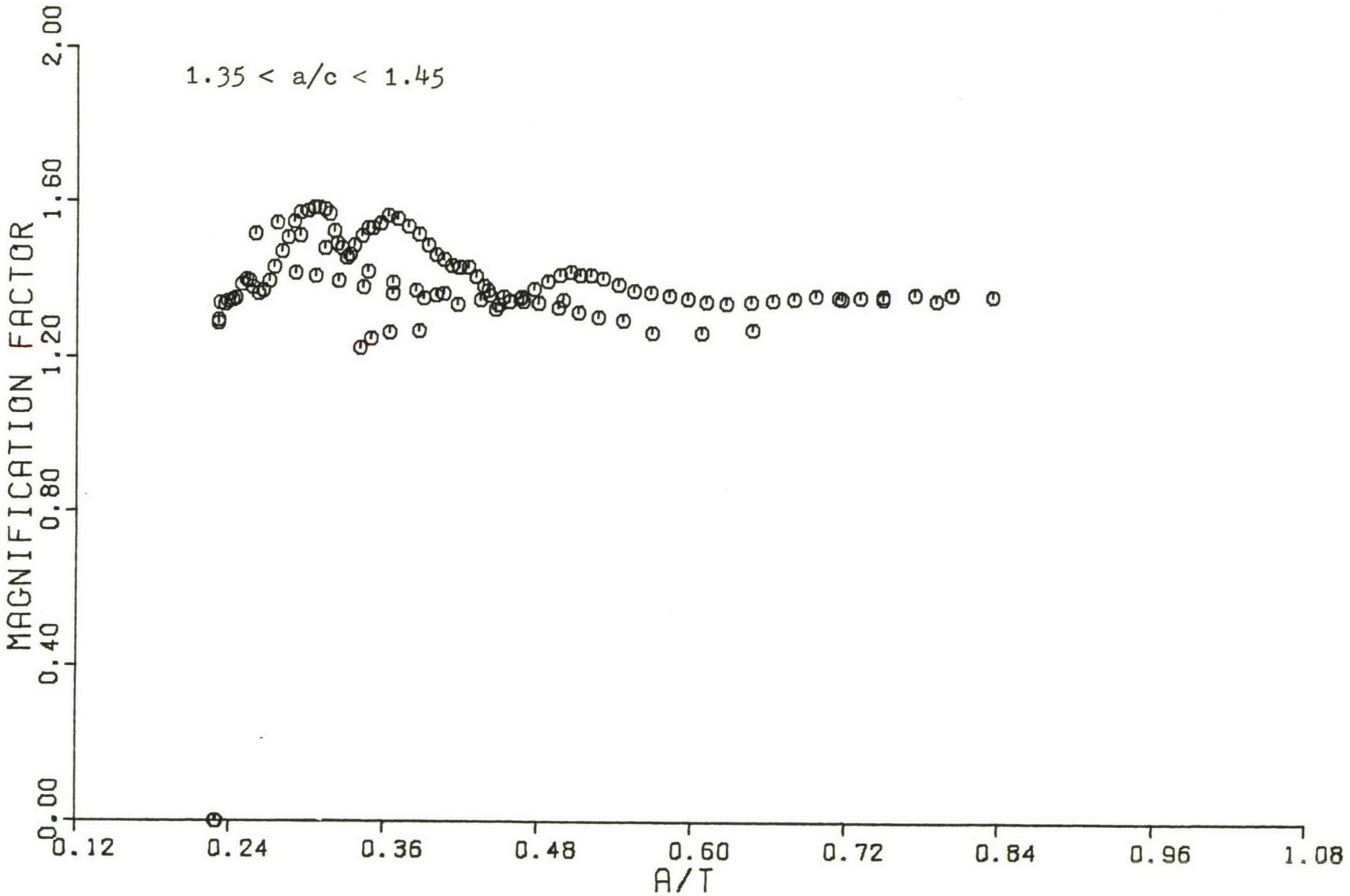

Fig. 18. Magnification Factor at the Surface for $a/c_{avg} = 1.4$

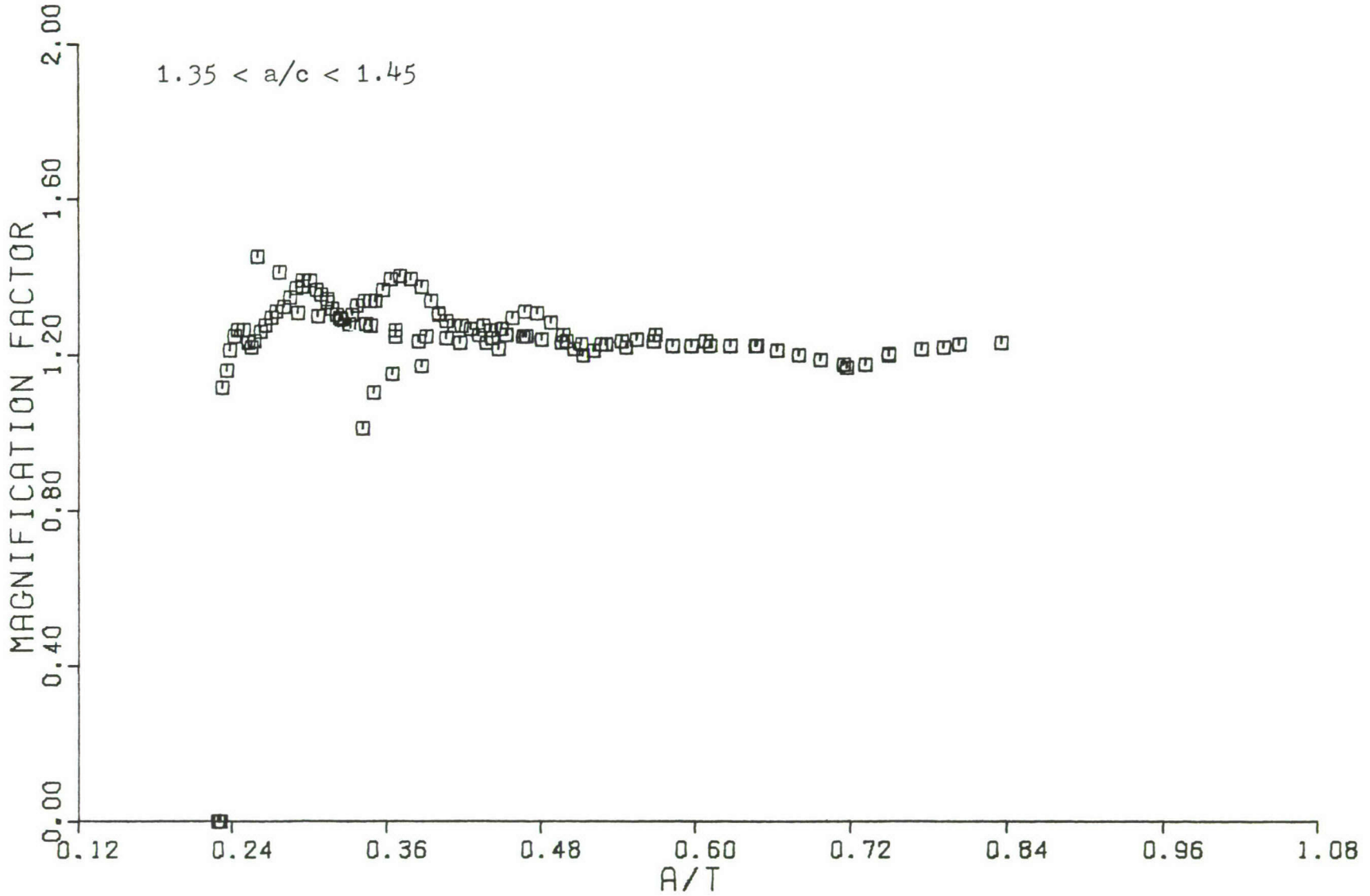

Fig. 19. Magnification Factor at the Hole for a/c_{avg} = 1.4

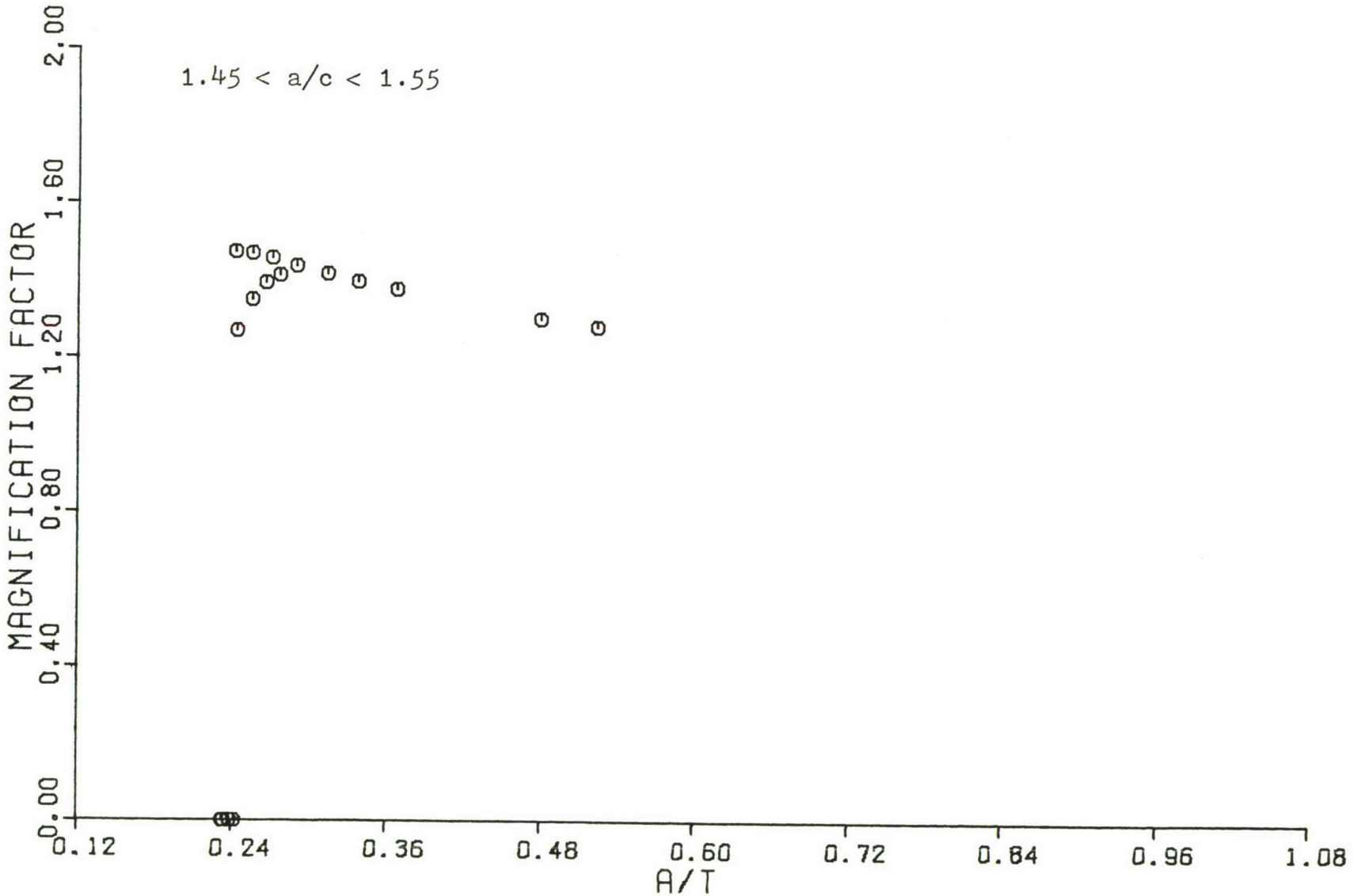

Fig. 20. Magnification Factor at the Surface for $a/c_{avg} = 1.5$

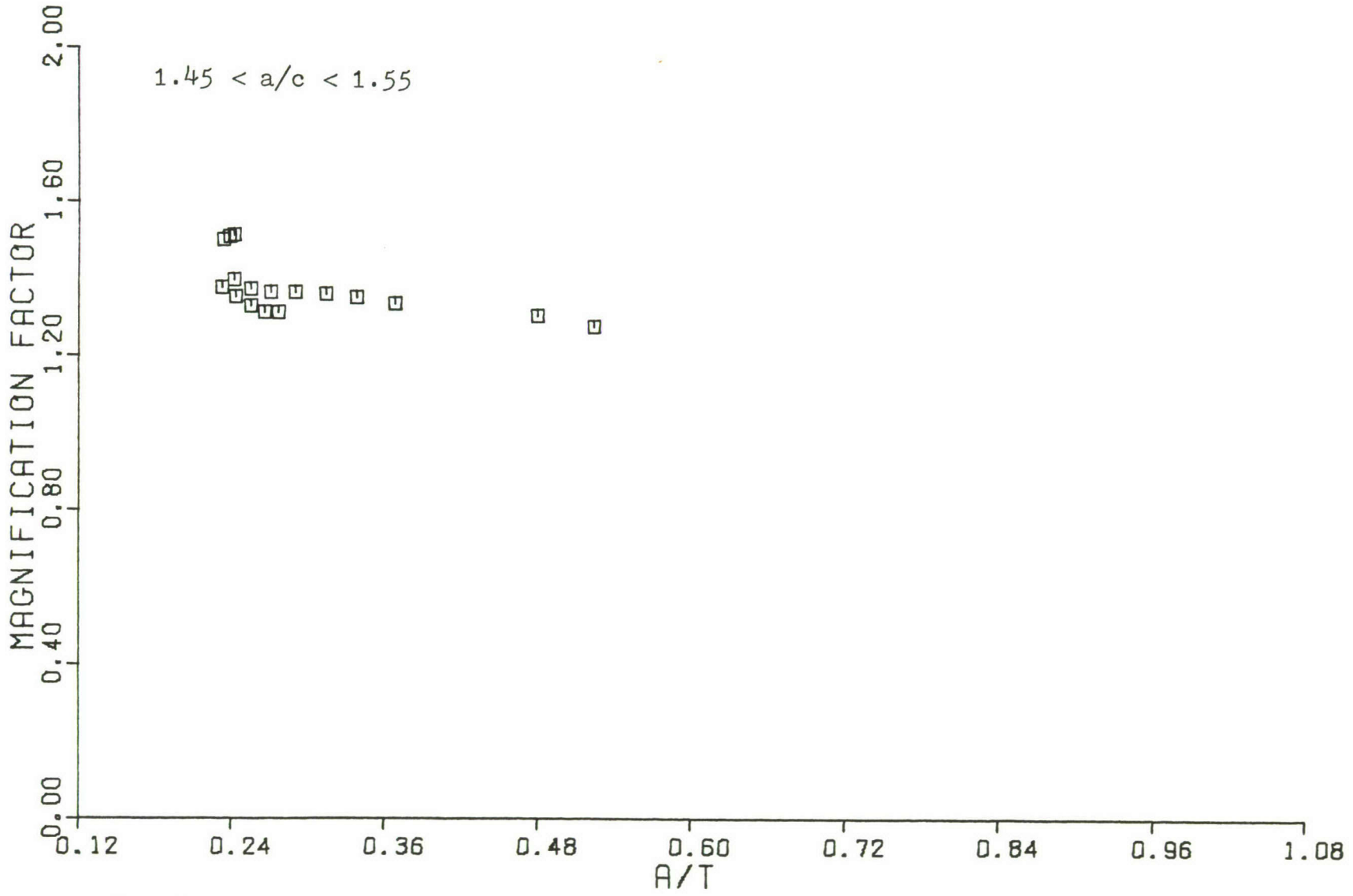

Fig. 21. Magnification Factor at the Hole for $a/c_{avg} = 1.5$

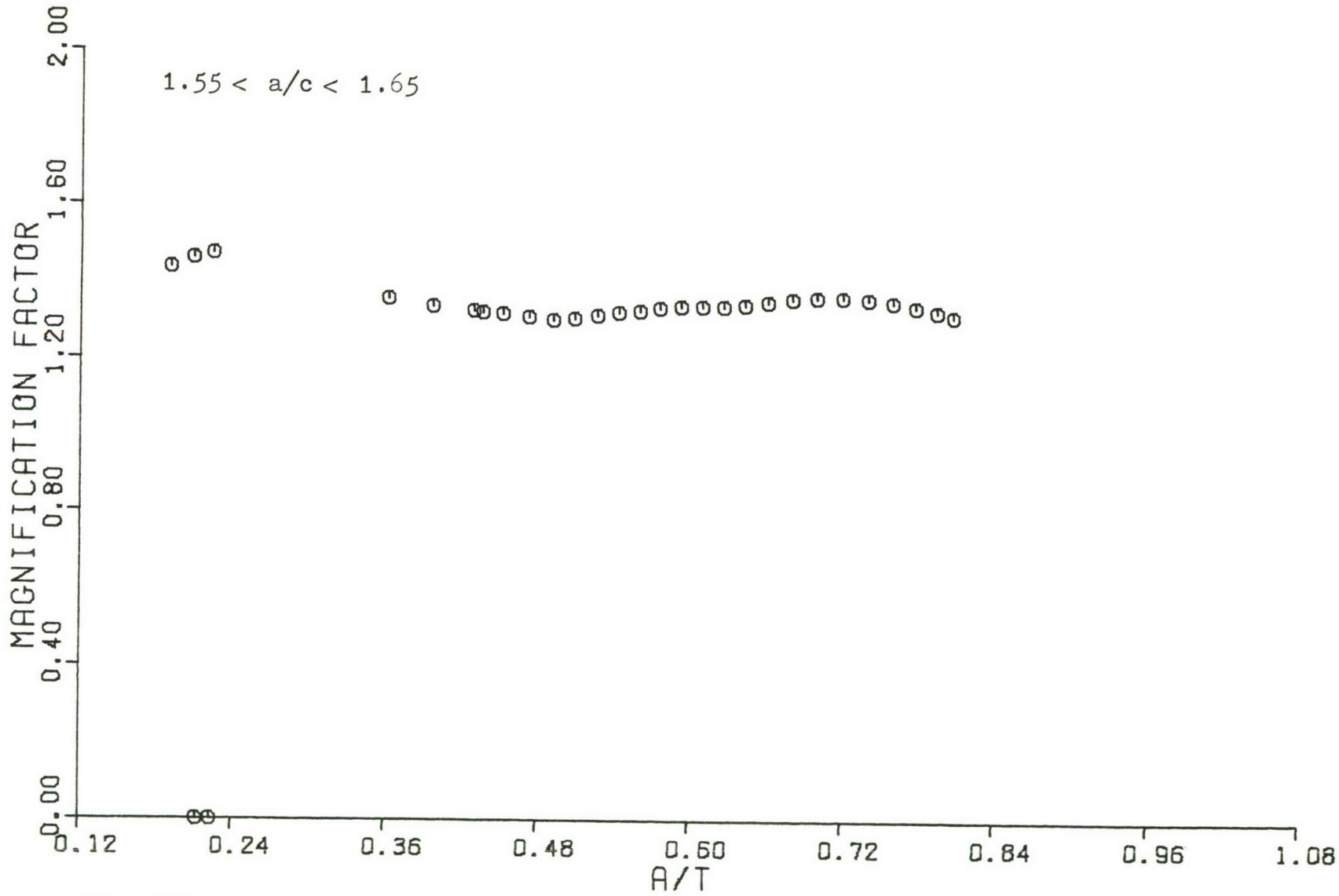

Fig. 22. Magnification Factor at the Surface for $a/c_{avg} = 1.6$

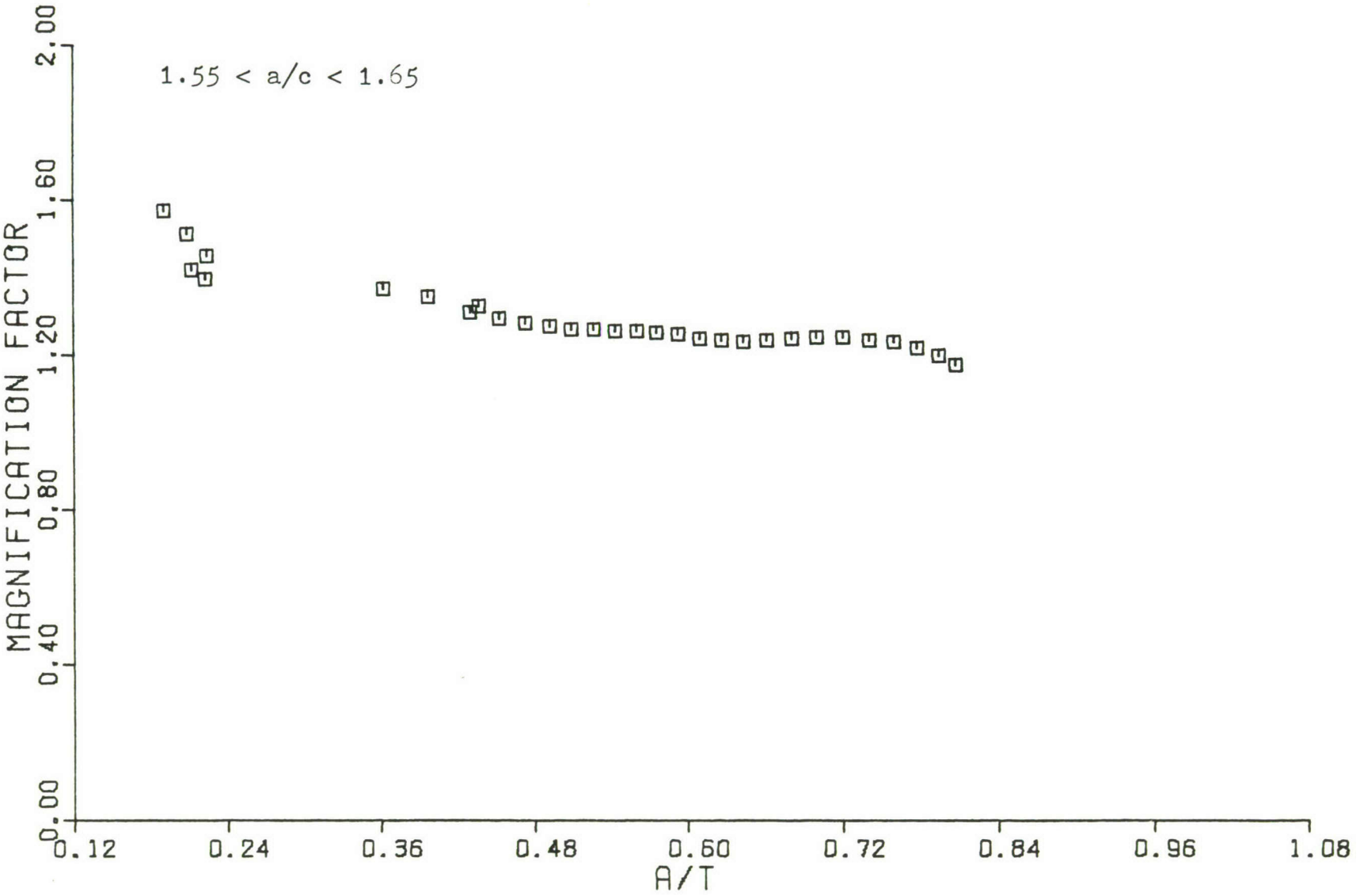

Fig. 23. Magnification Factor at the Hole for a/c_{avg}= 1.6

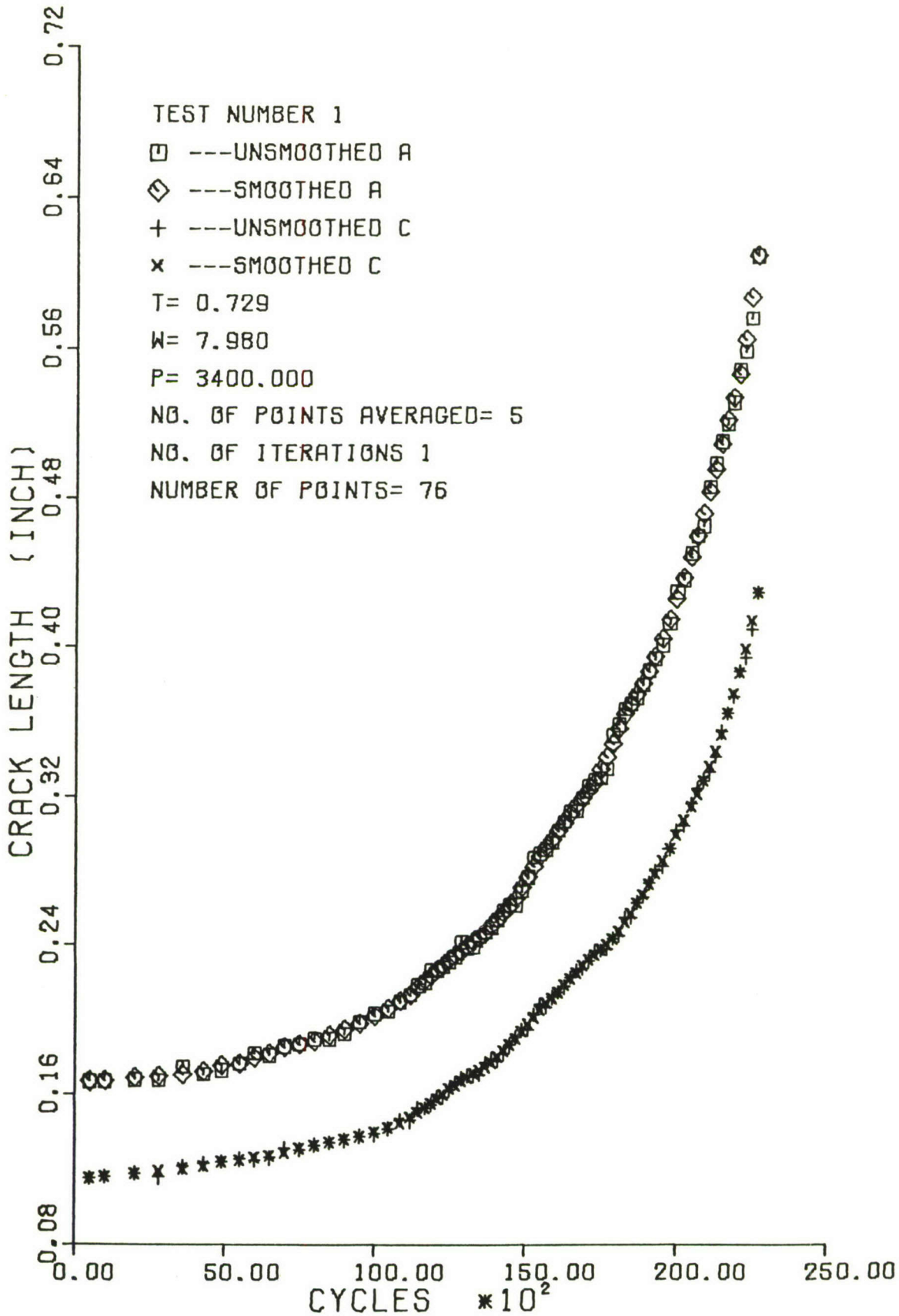

Fig. 24. Crack Length vs. Cycles, Test 1

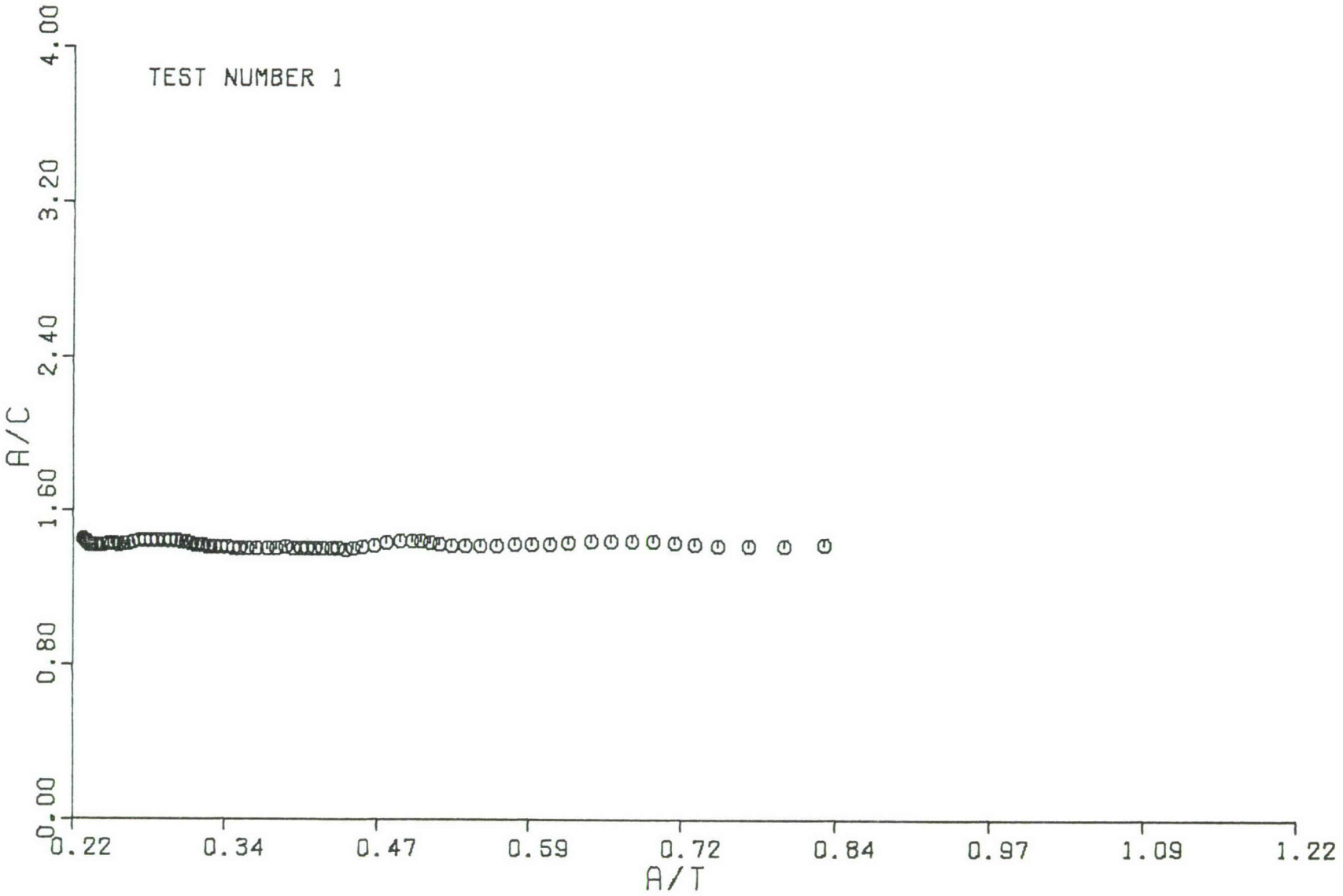

Fig. 25. Crack Shape vs. a/T, Test 1

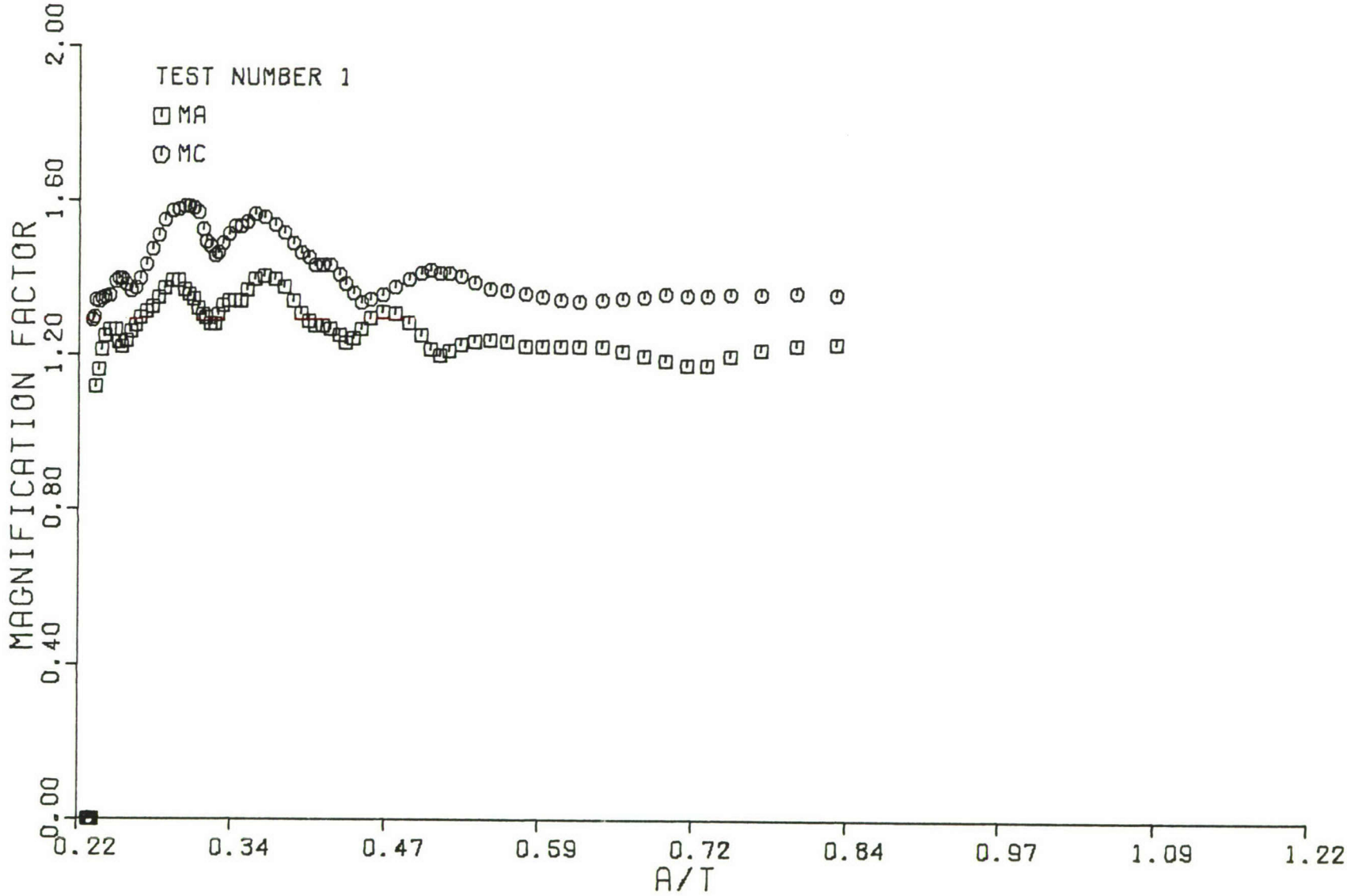

Fig. 26. Magnification Factor vs. a/T, Test 1

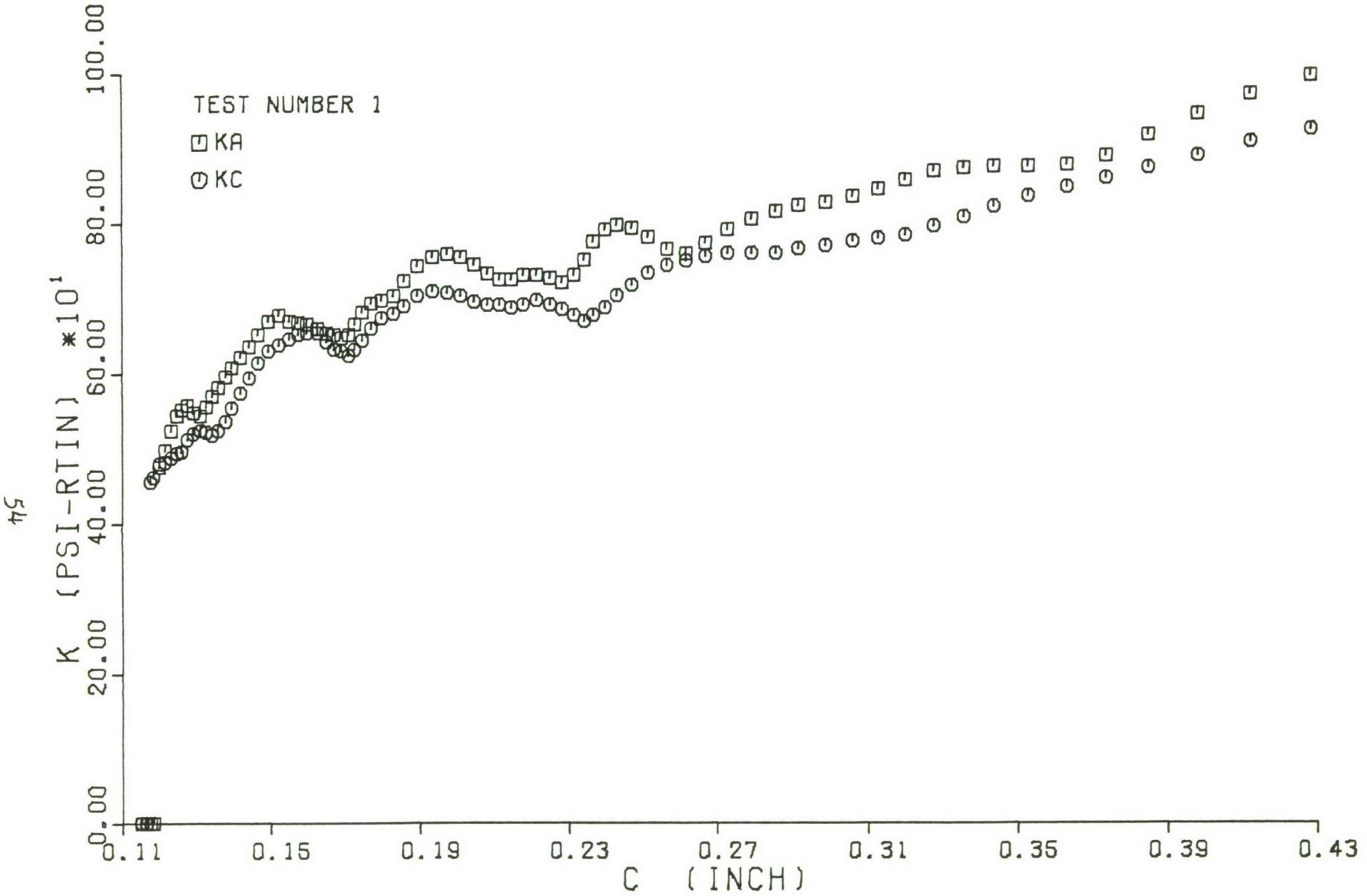

Fig. 27. Stress Intensity Factor vs. c Crack Length, Test 1

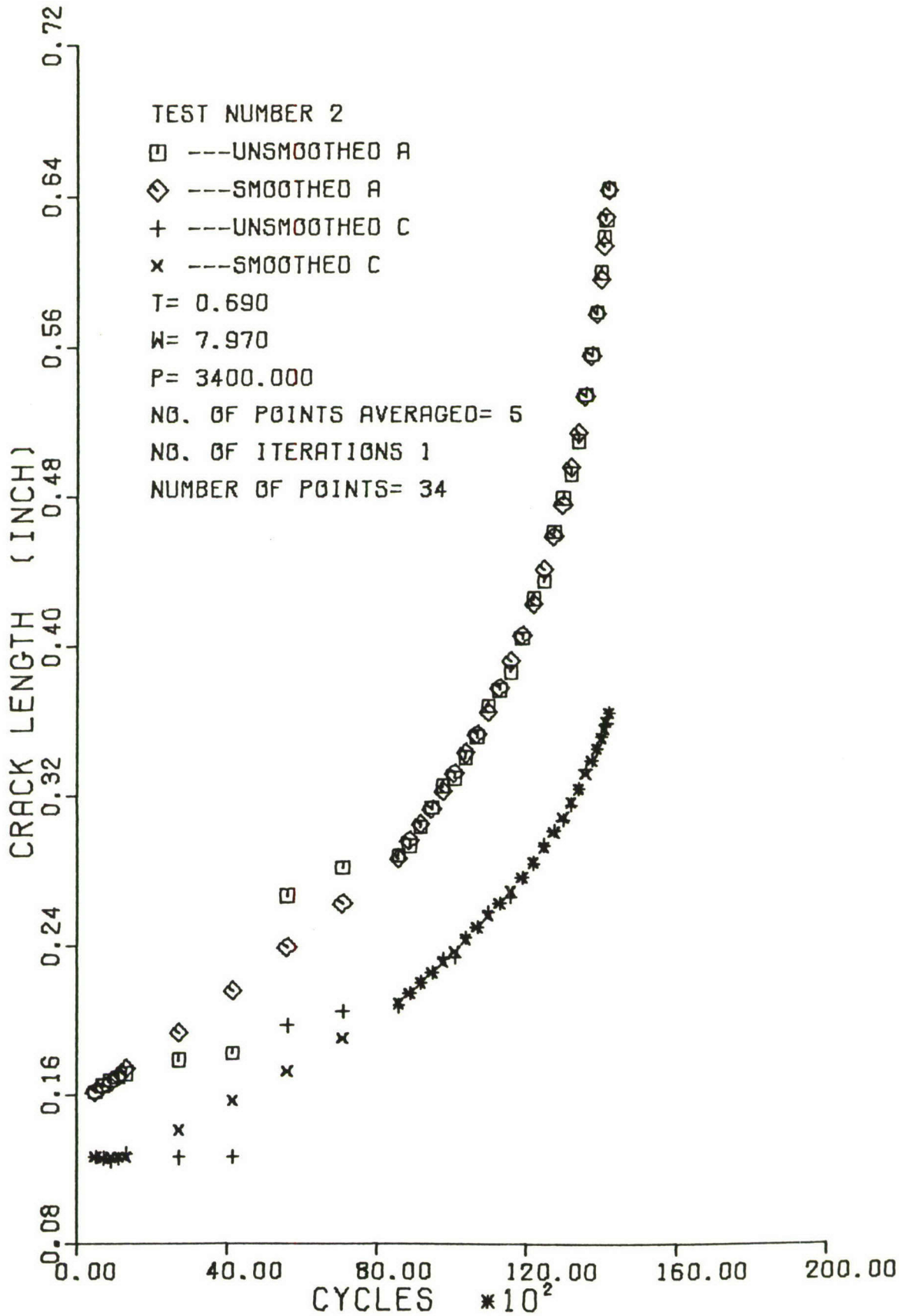

Fig. 28. Crack Length vs. Cycles, Test 2

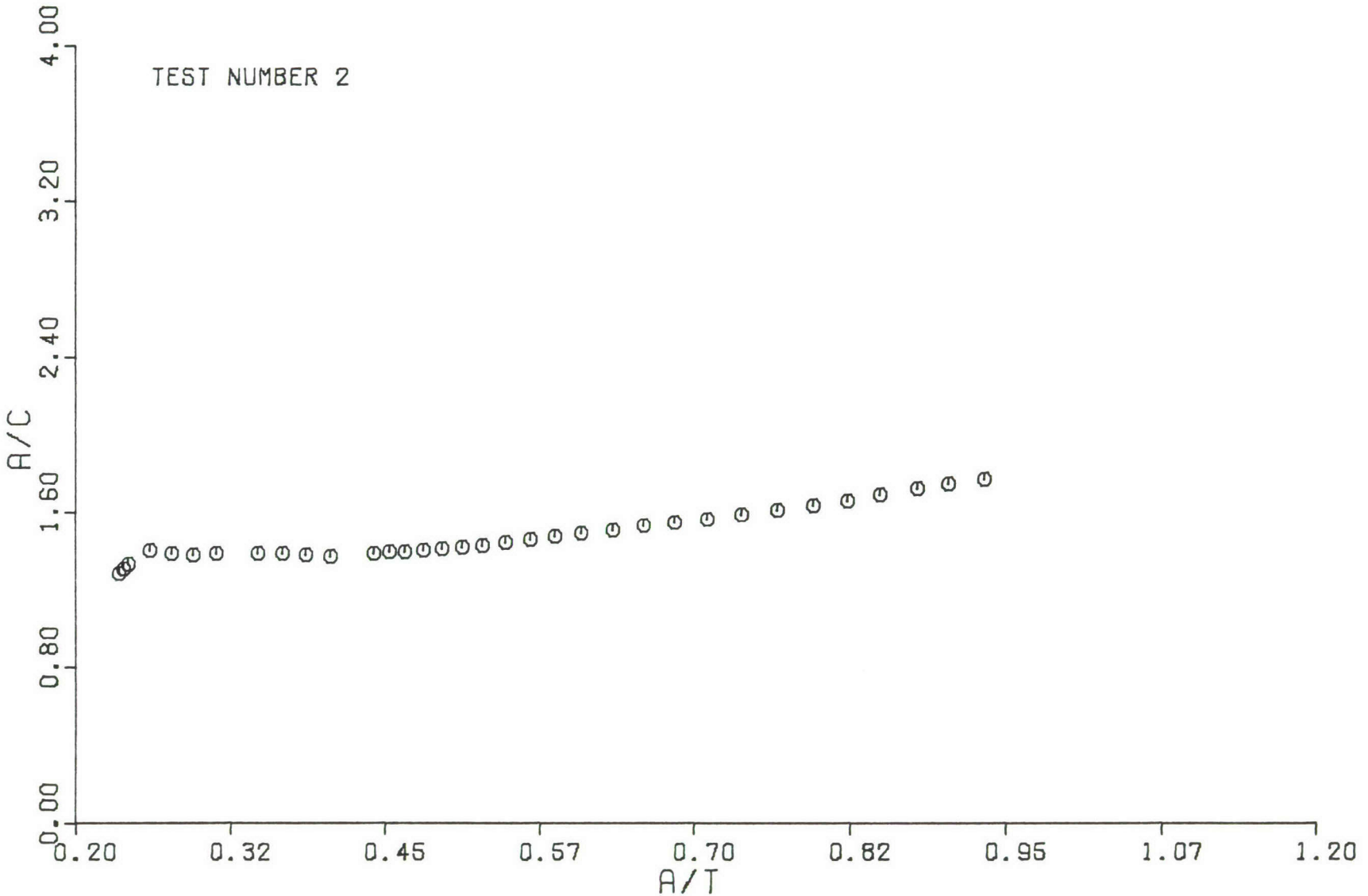

Fig. 29 . Crack Shape vs. a/T, Test 2

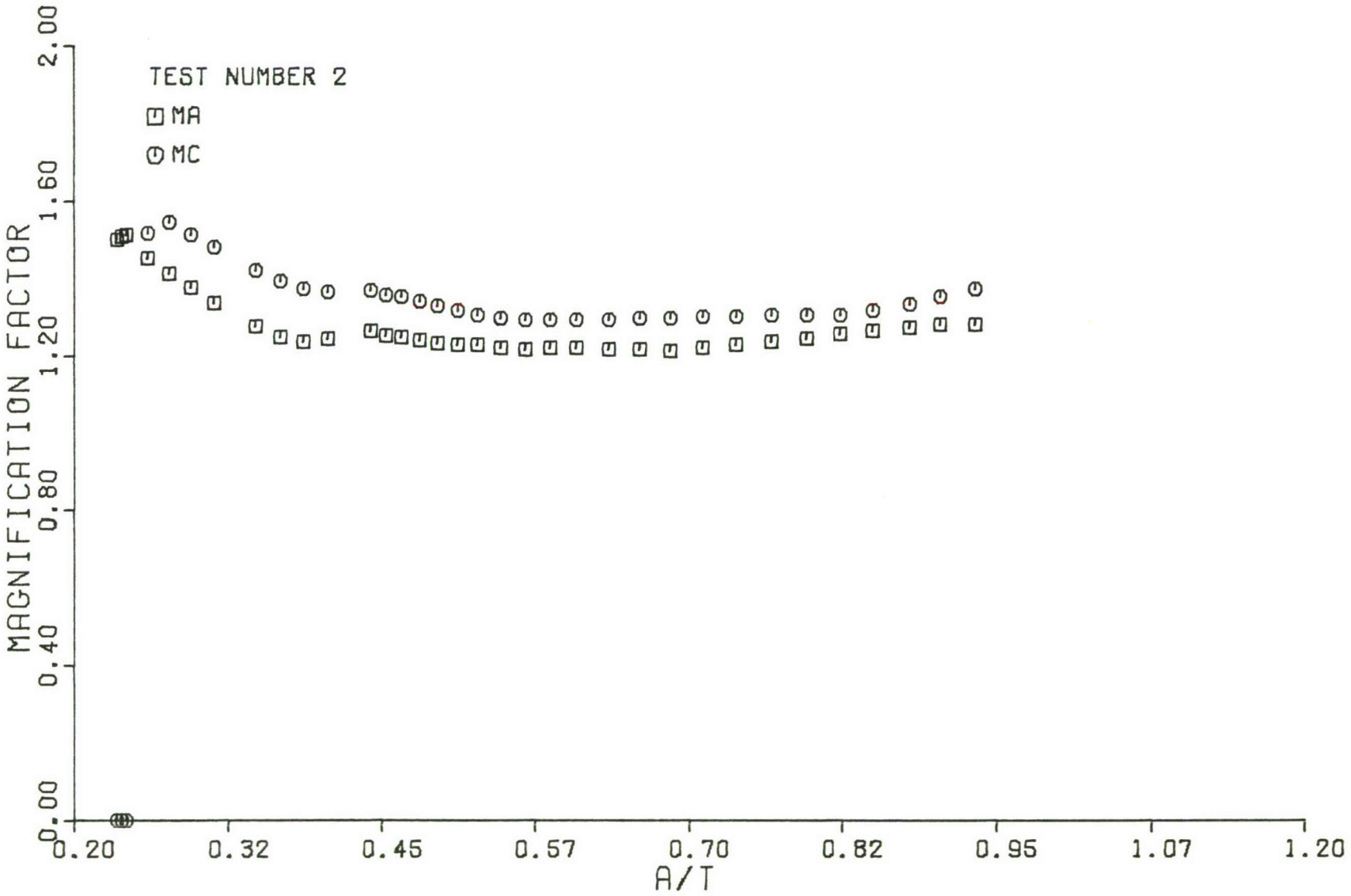

Fig. 30. Magnification Factor vs. a/T, Test 2

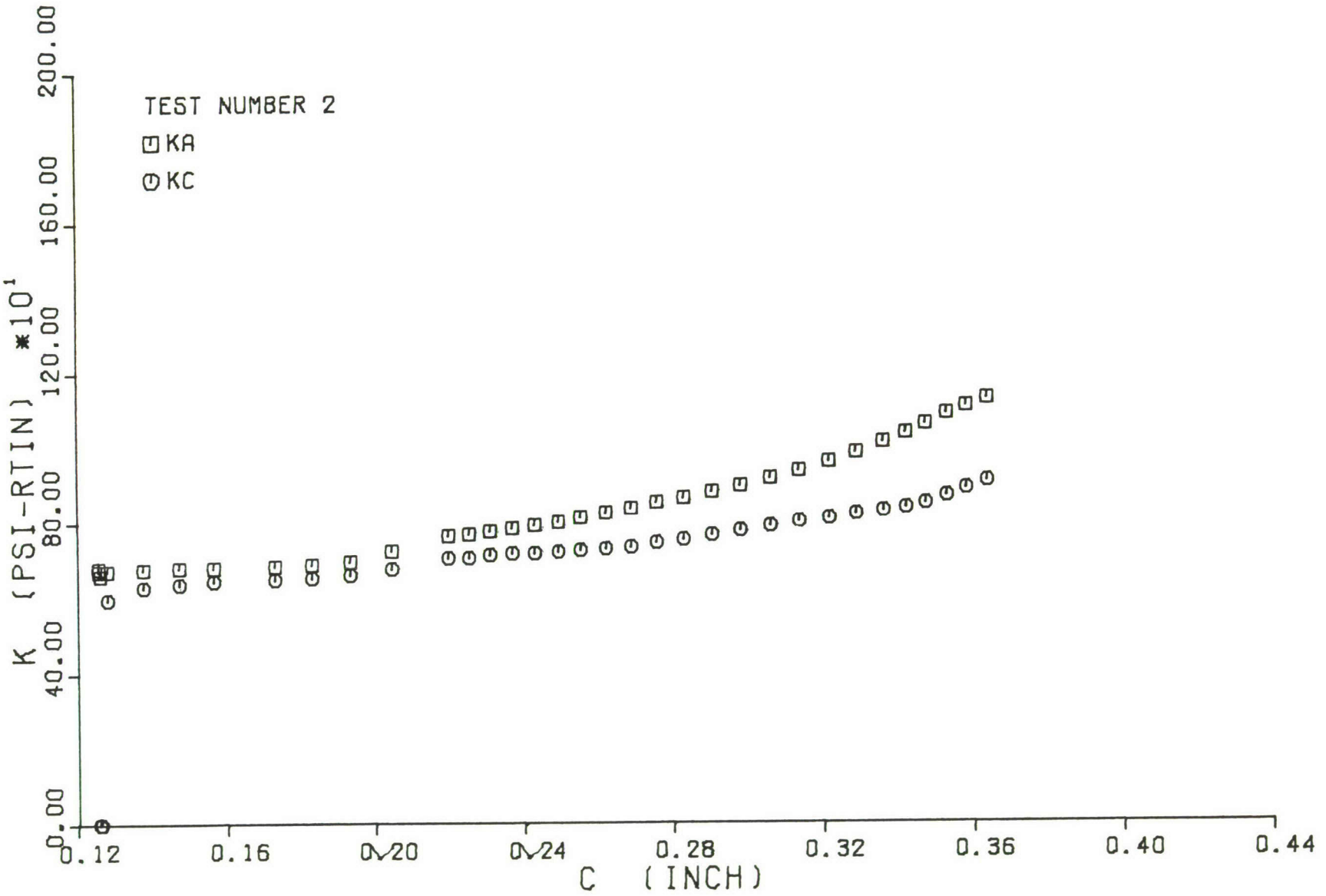

Fig. 31. Stress Intensity Factor vs. c Crack Length, Test 2

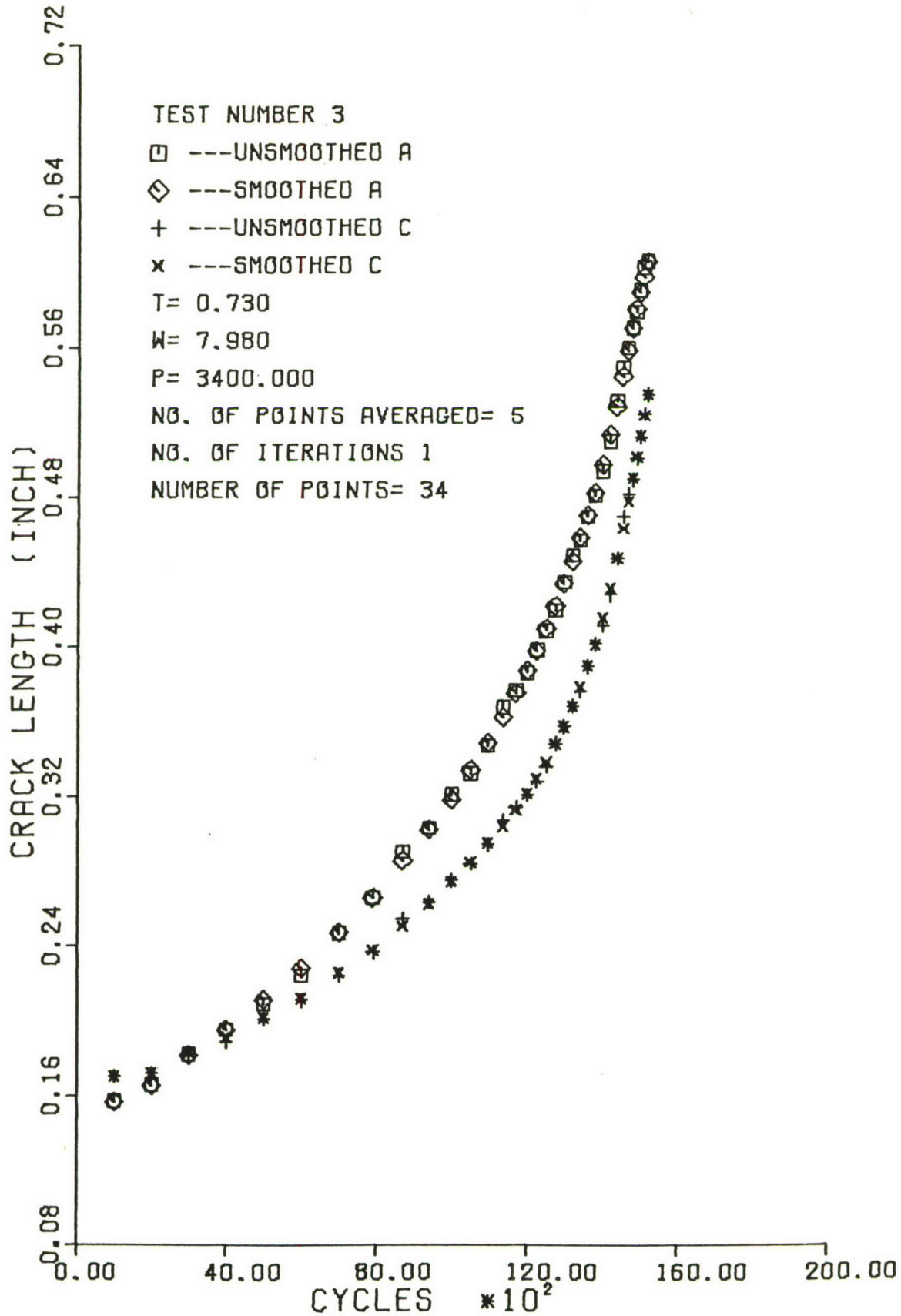

Fig. 32. Crack Length vs. Cycles, Test 3

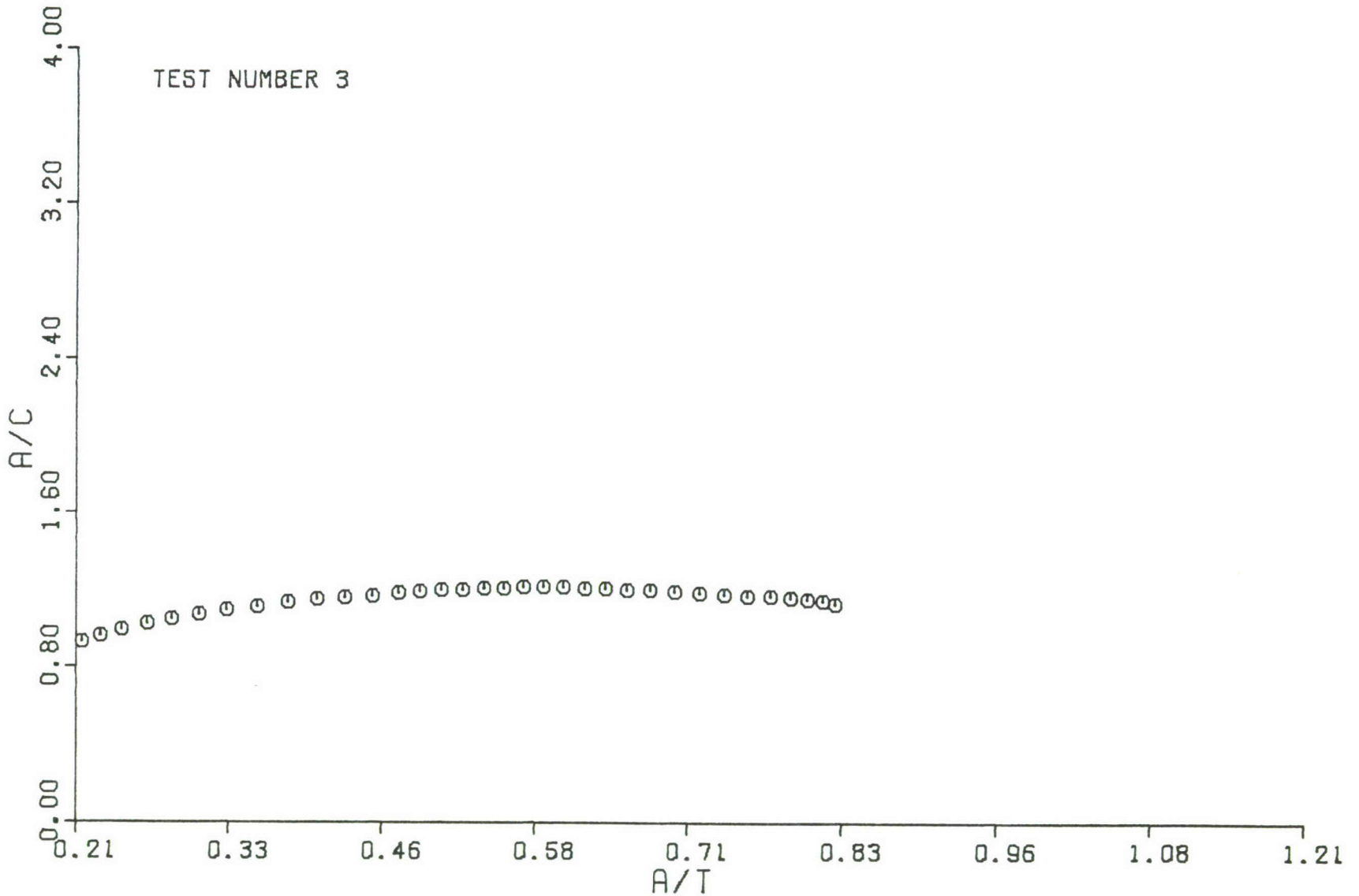

Fig. 33. Crack Shape vs. a/T, Test 3

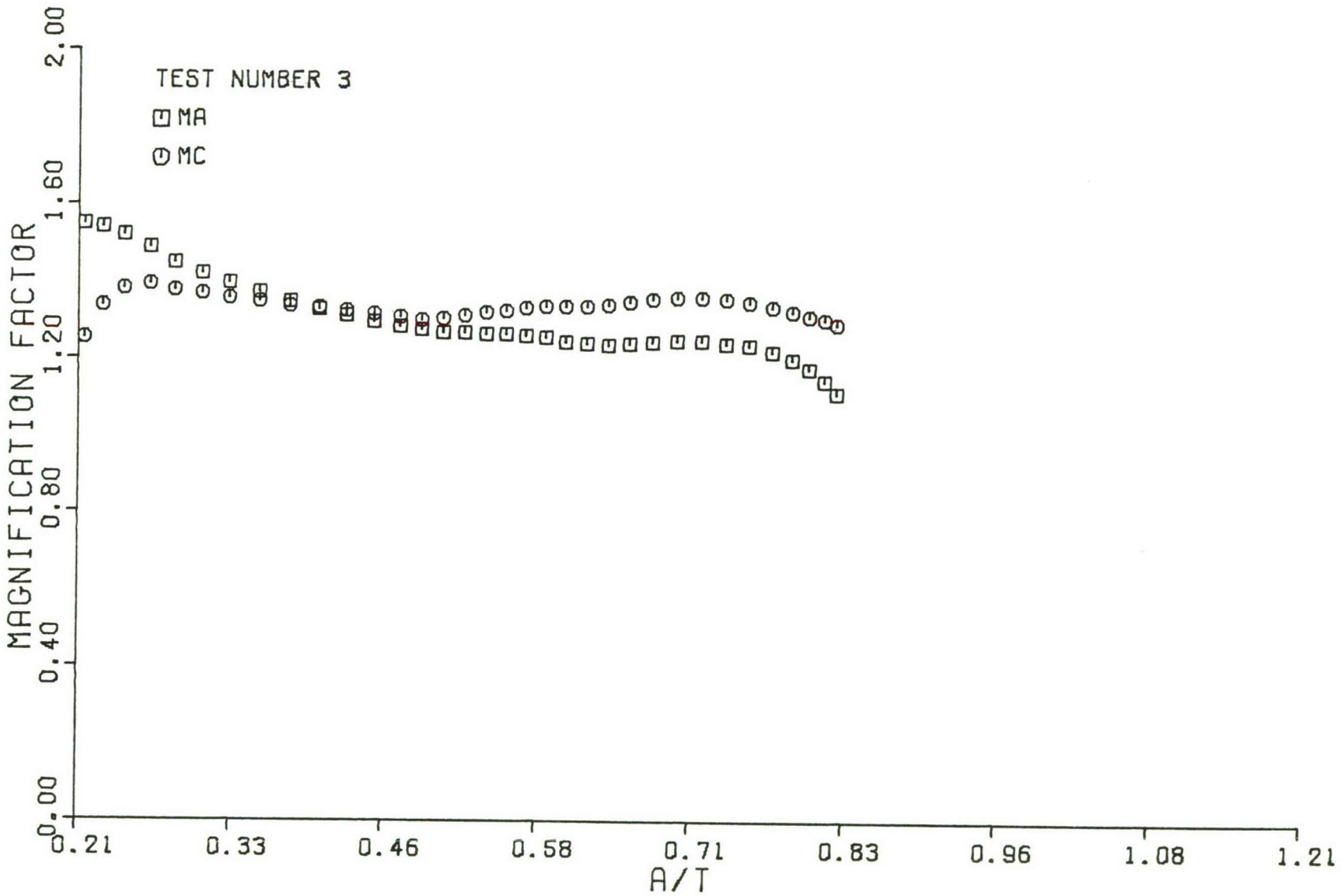

Fig. 34. Magnification Factor vs. a/T, Test 3

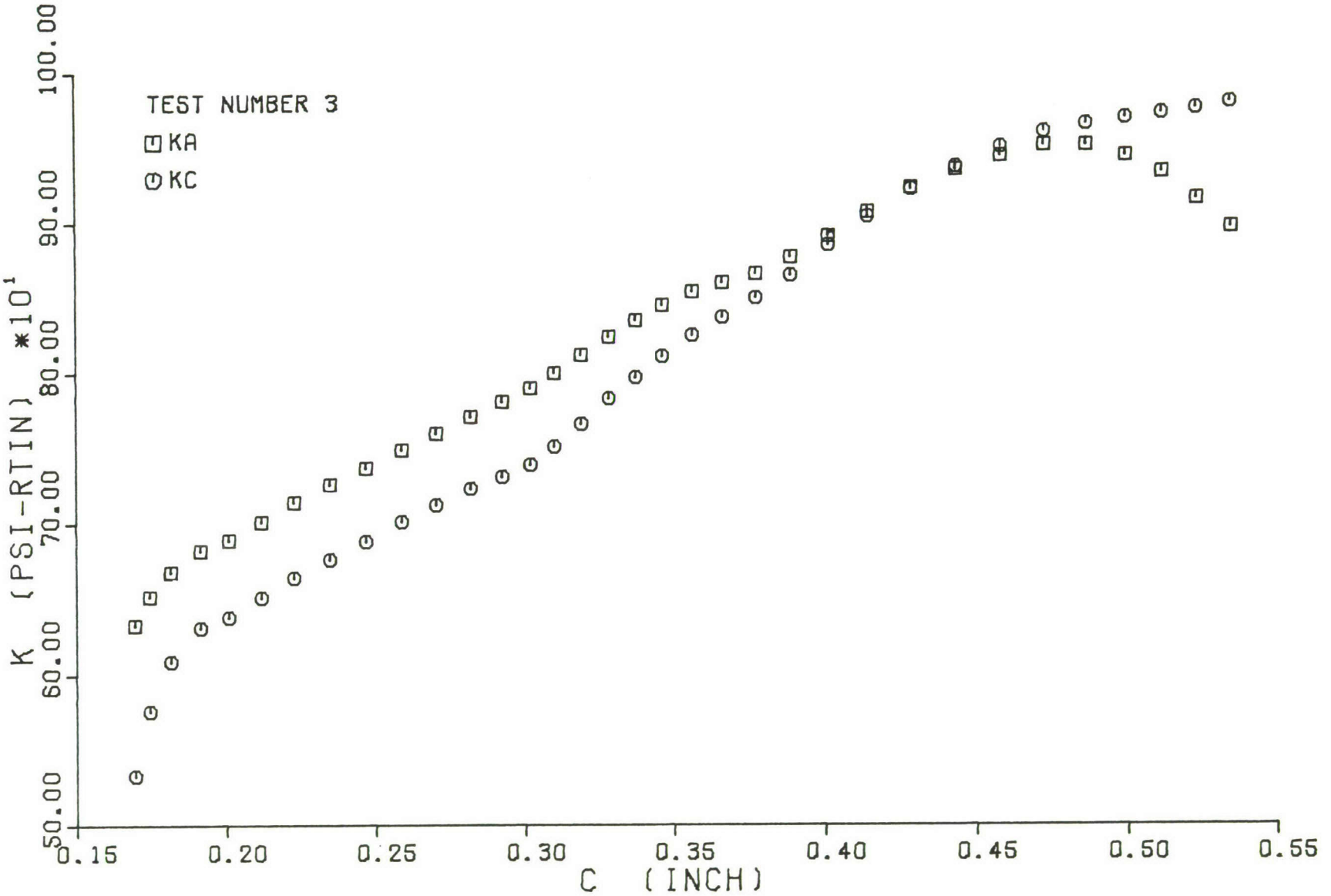

Fig. 35. Stress Intensity Factor vs. c Crack Length, Test 3

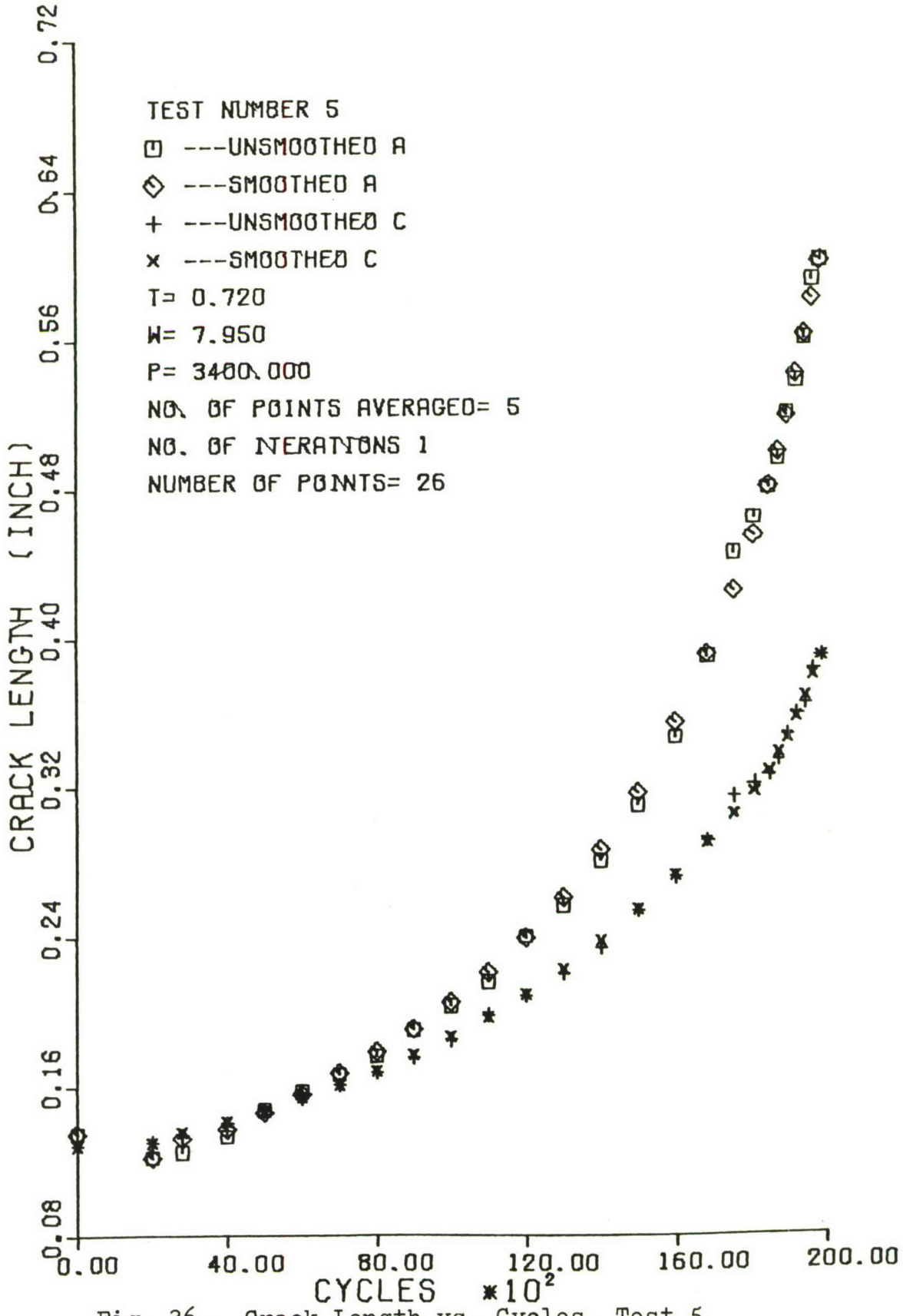

Fig. 36. Crack Length vs. Cycles, Test 5

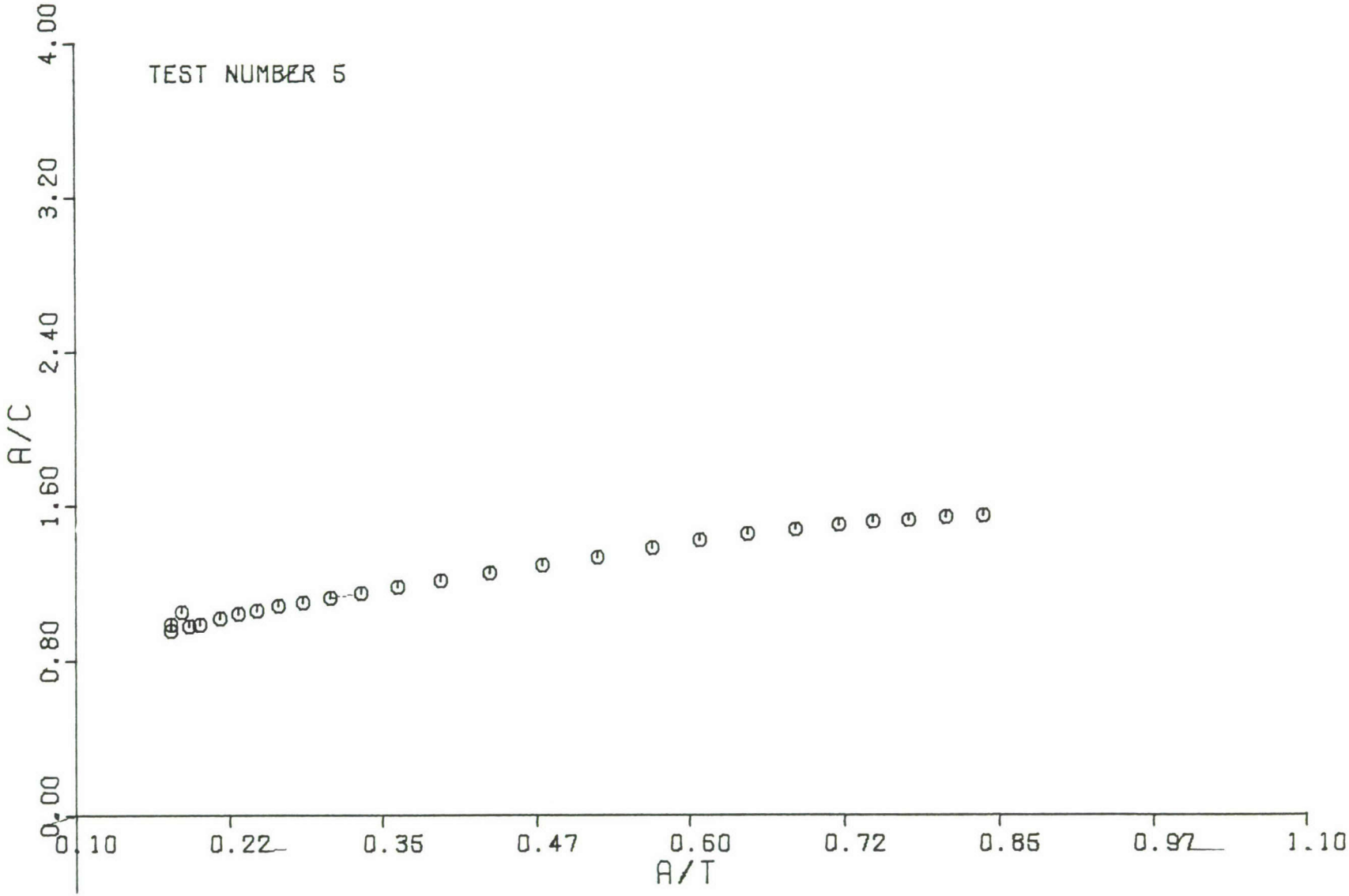

Fig. 37. Crack Shape vs. a/T, Test 5

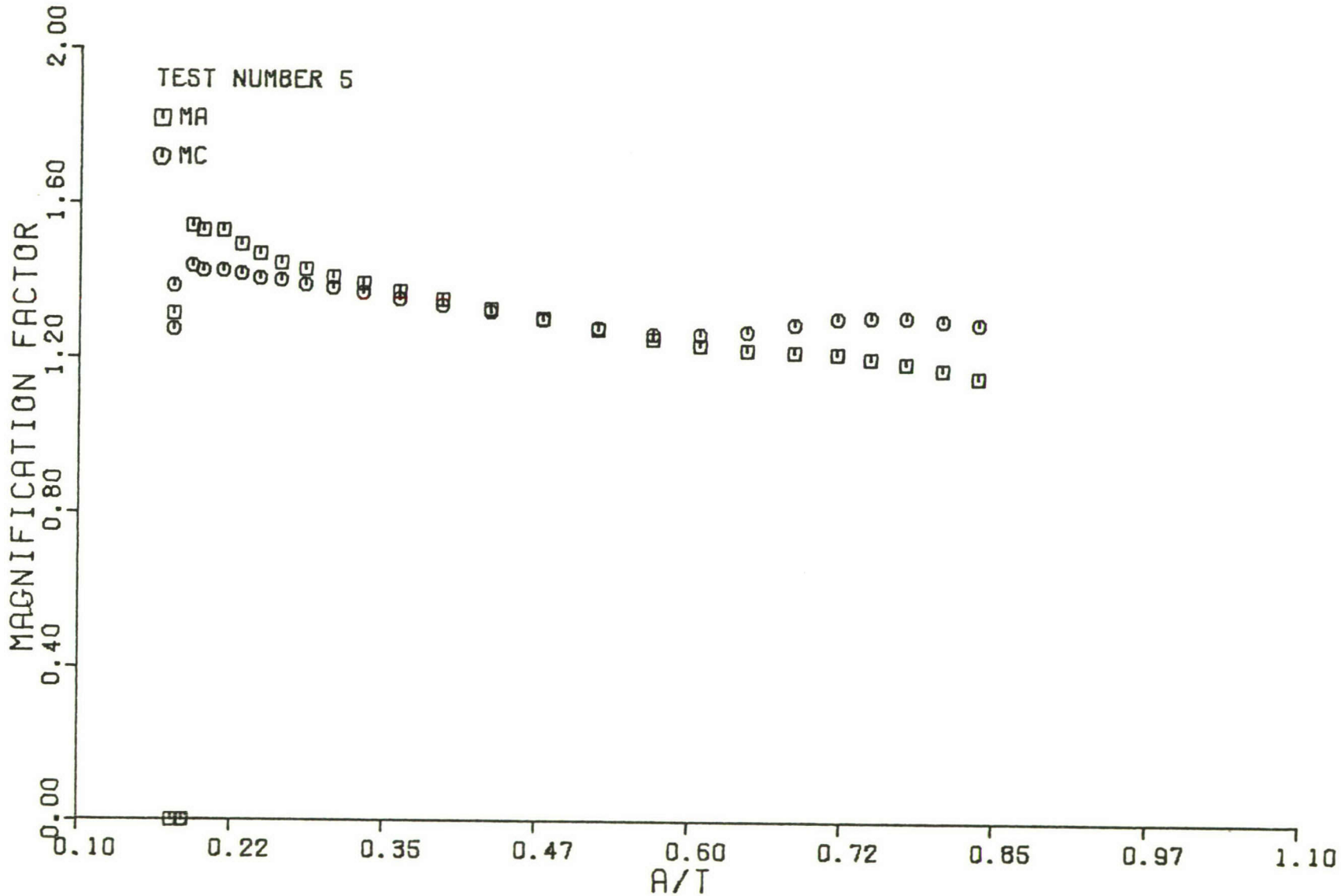

Fig. 38. Magnification Factor vs. a/T, Test 5

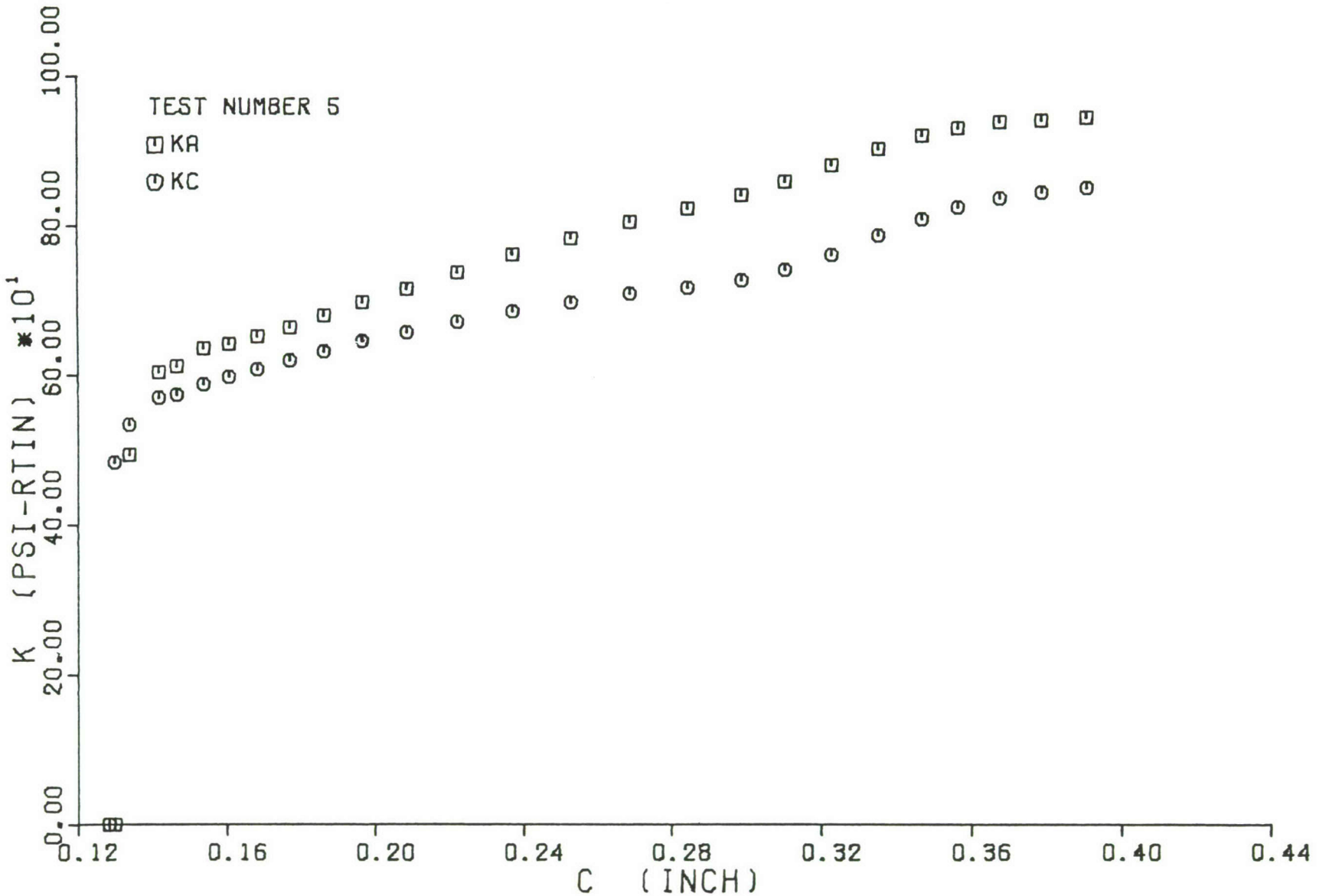

Fig. 39. Stress Intensity Factor vs. c Crack Length, Test 5

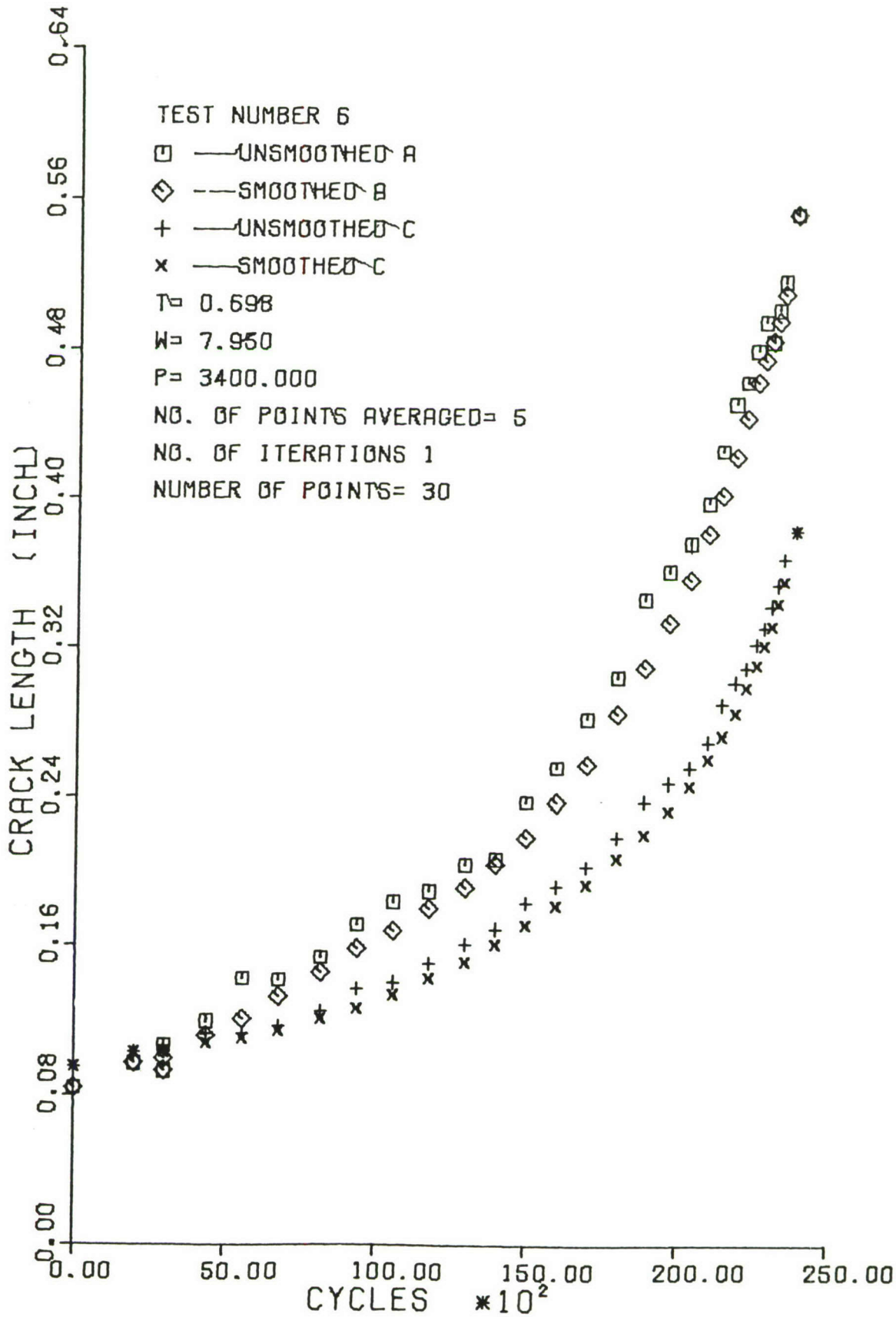

Fig. 40. Crack Length vs. Cycles, Test 6

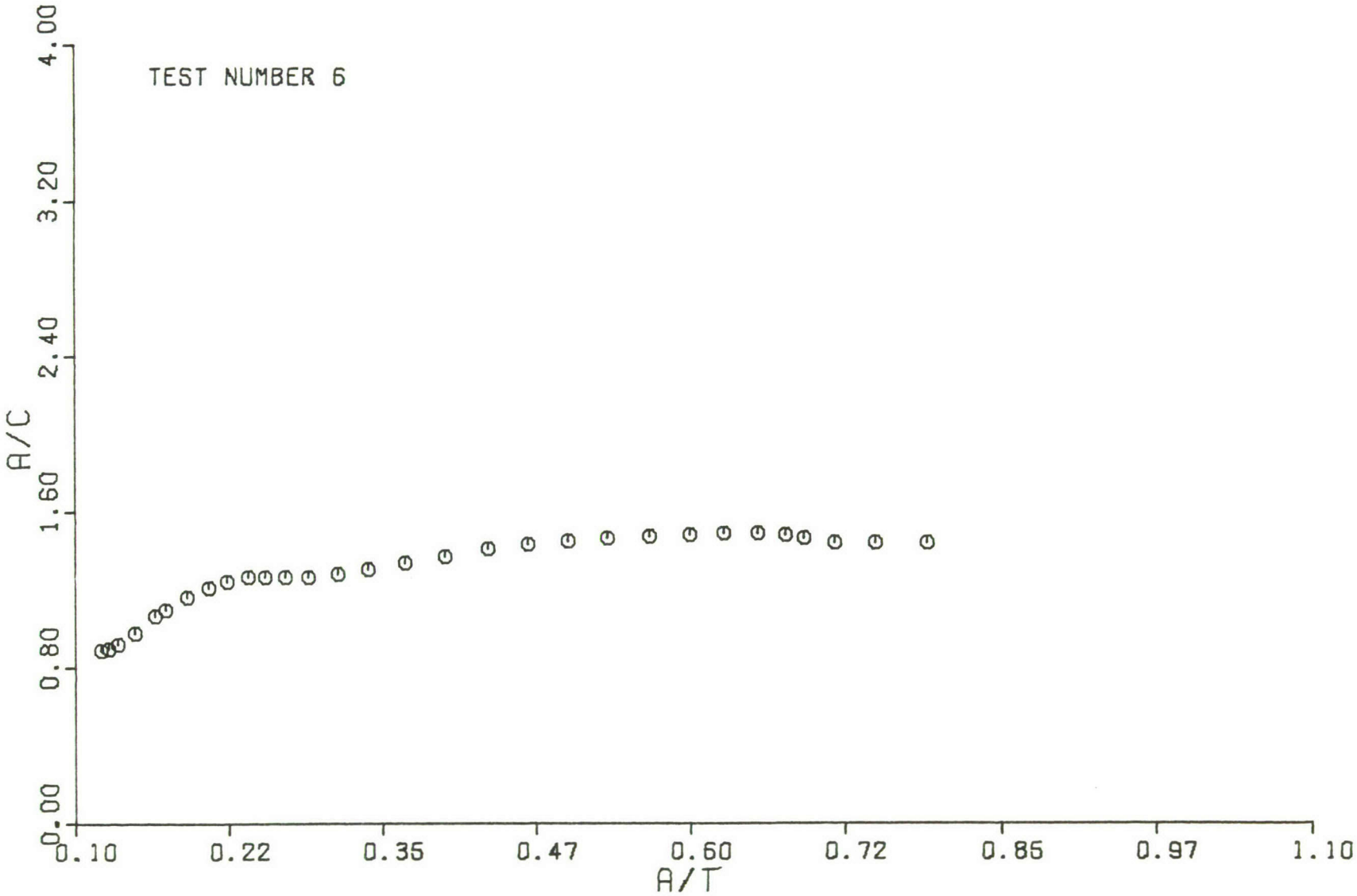

Fig. 41. Crack Shape vs. a/T, Test 6

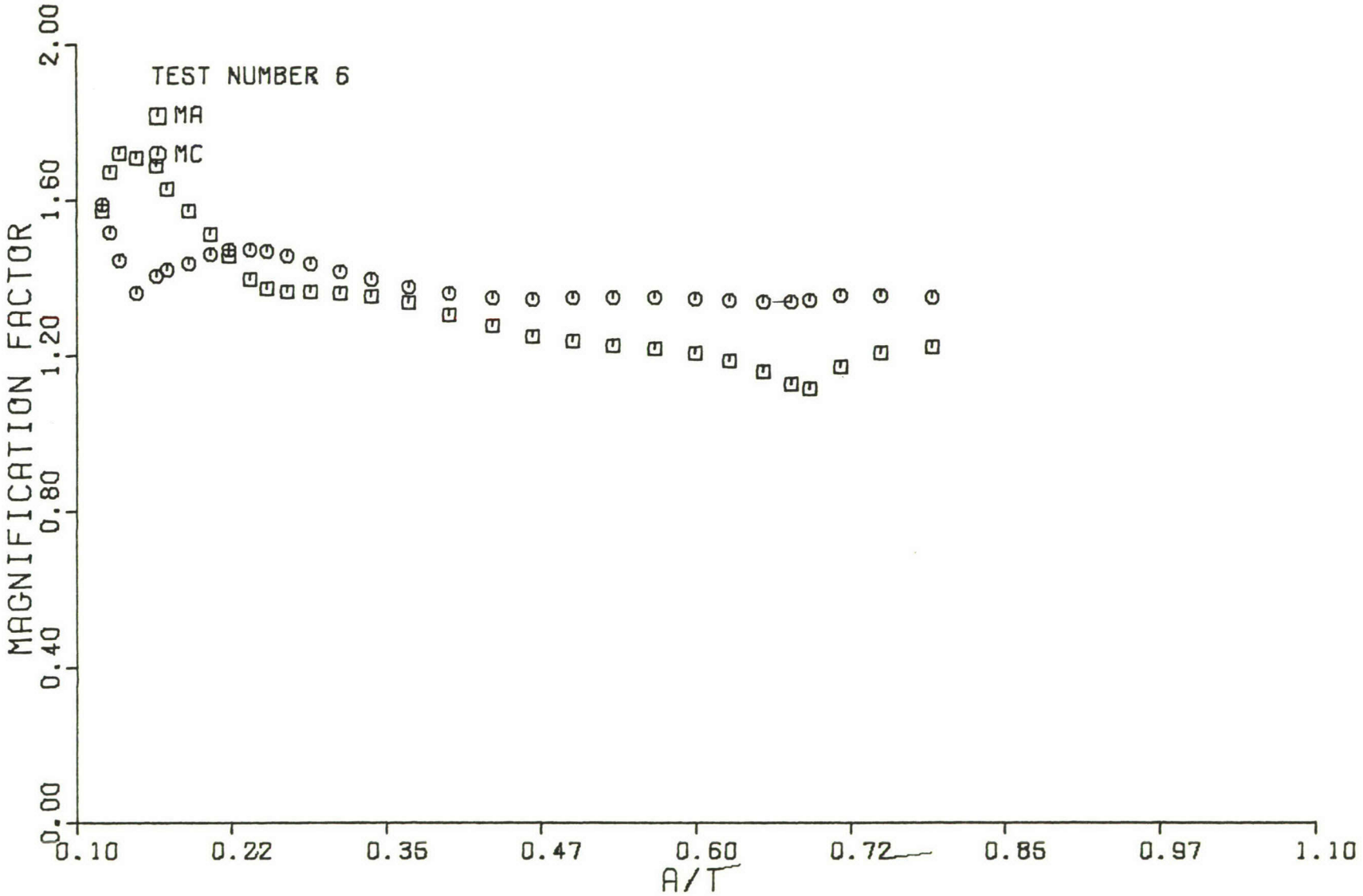

Fig. 42. Magnification Factor vs. a/T, Test 6

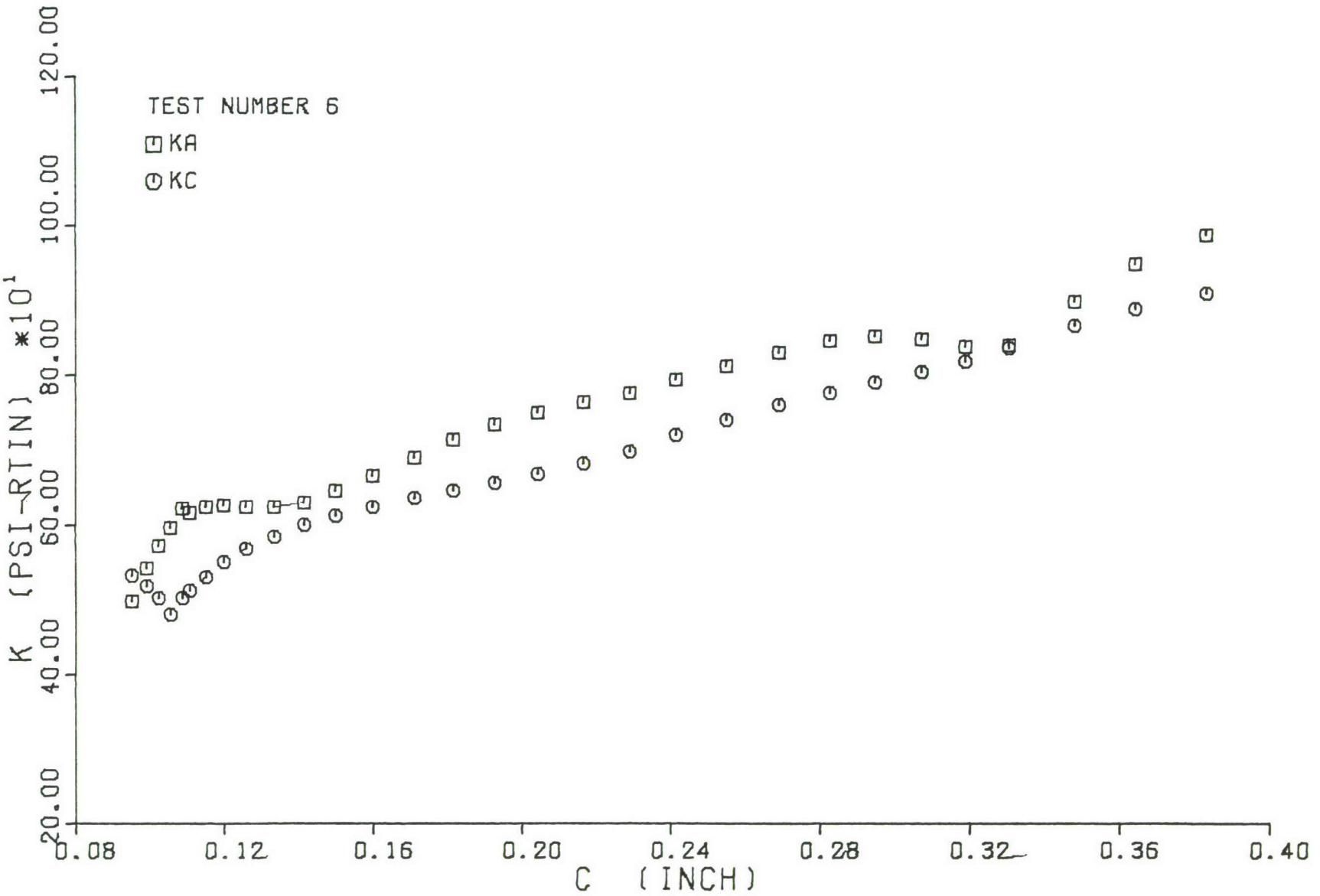

Fig. 43. Stress Intensity Factor vs. c Crack Length, Test 6

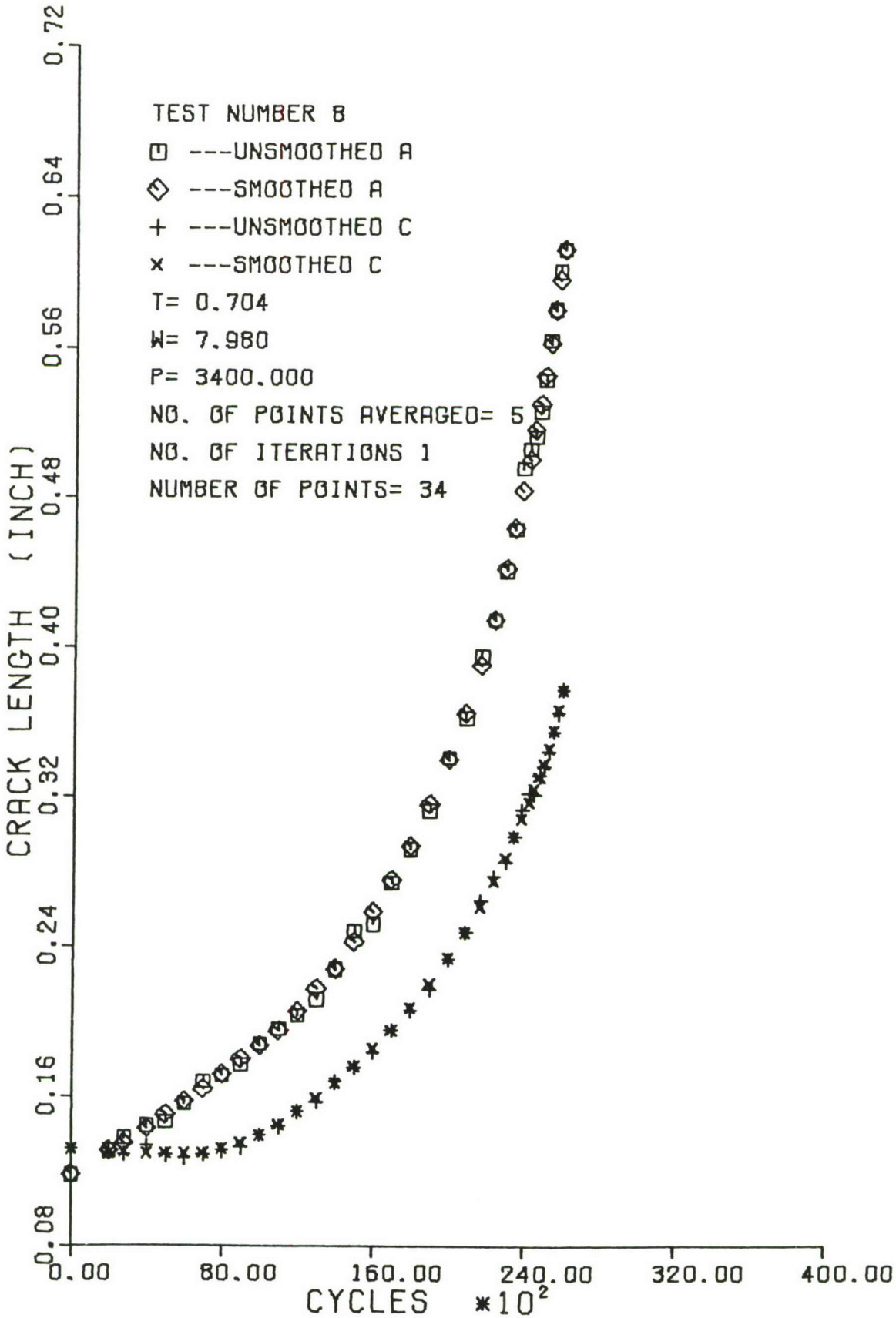

Fig. 44. Crack Length vs. Cycles, Test 8

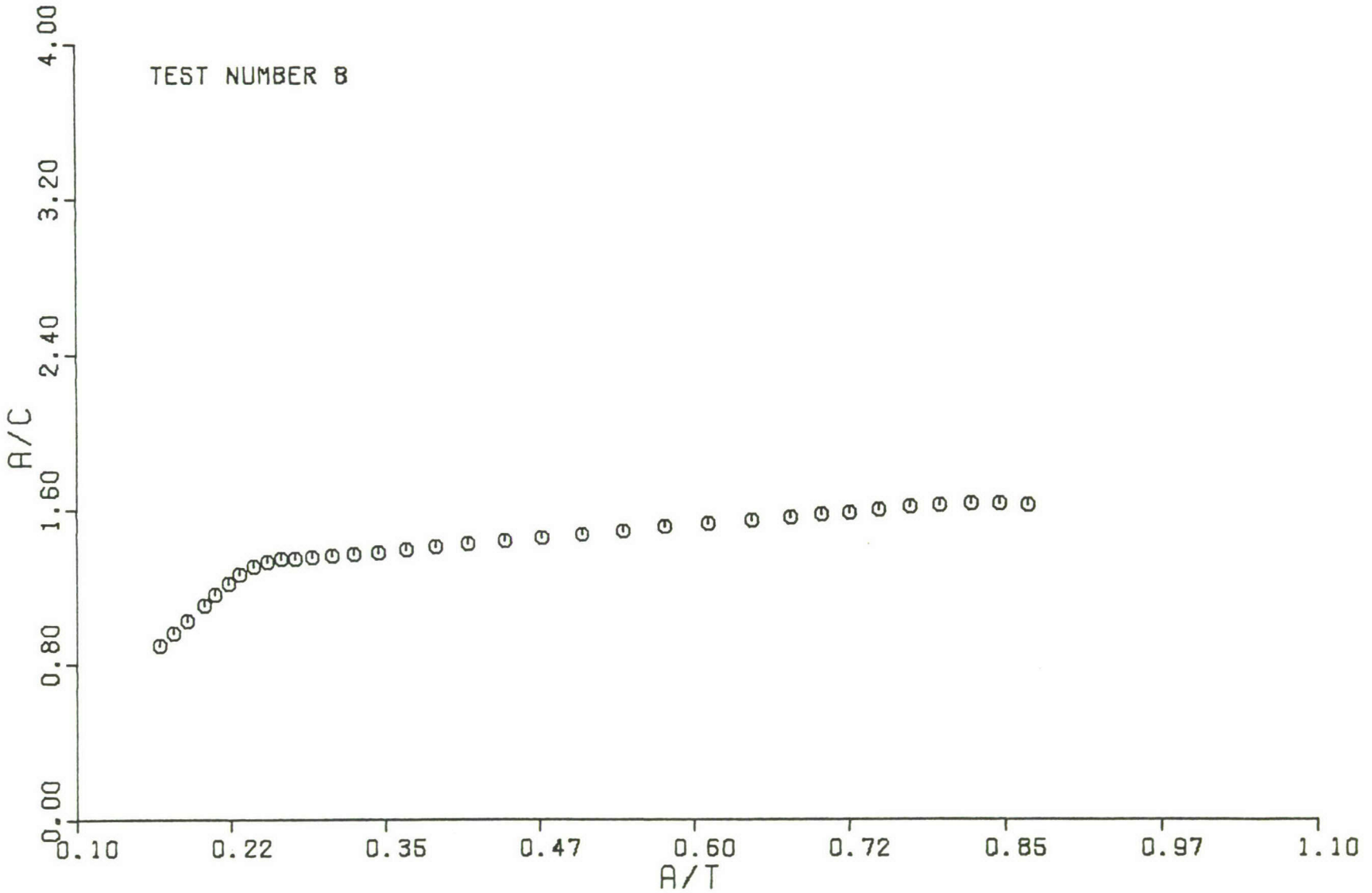

Fig. 45. Crack Shape vs. a/T, Test 8

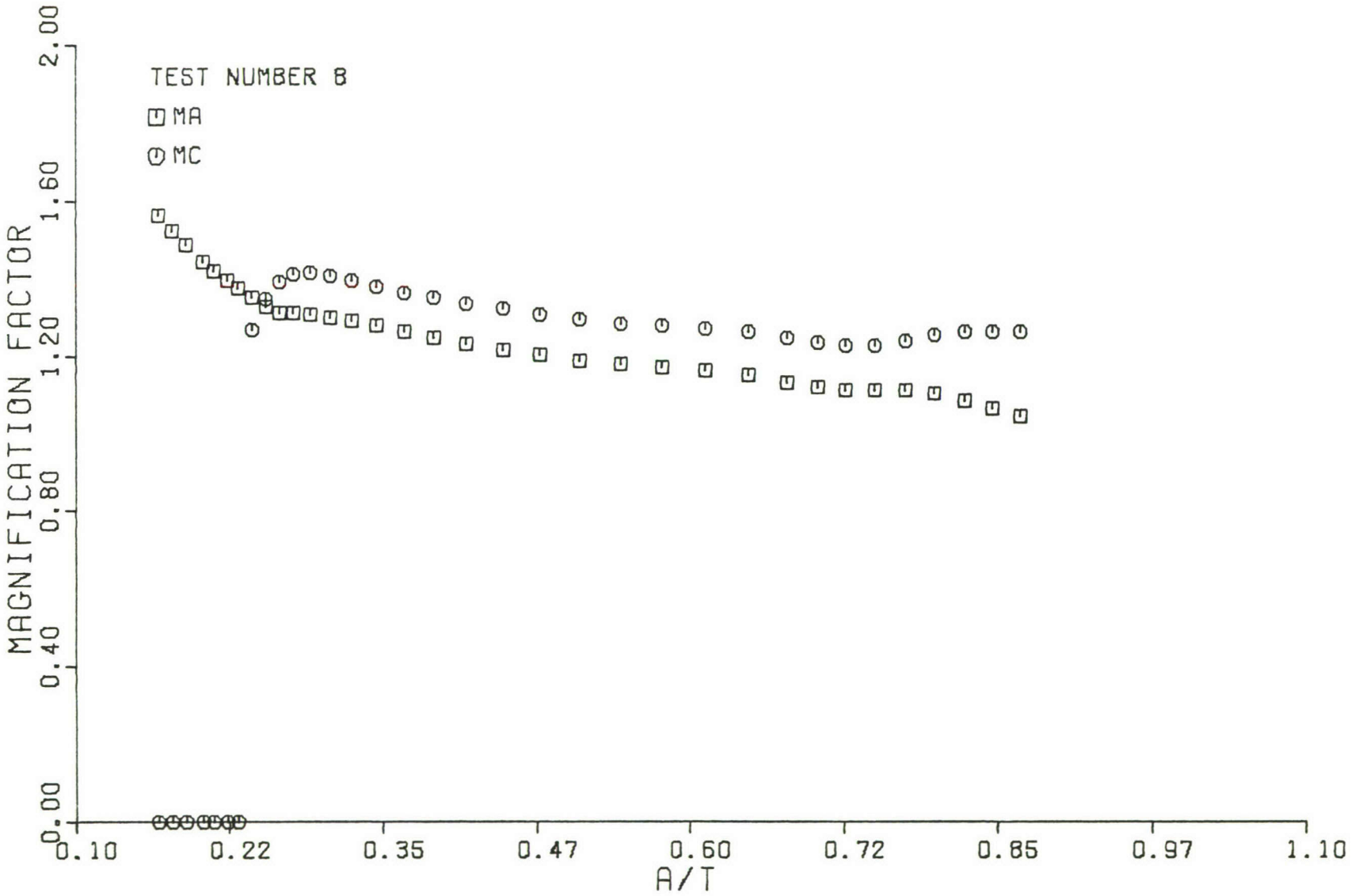

Fig. 46. Magnification Factor vs. a/T, Test 8

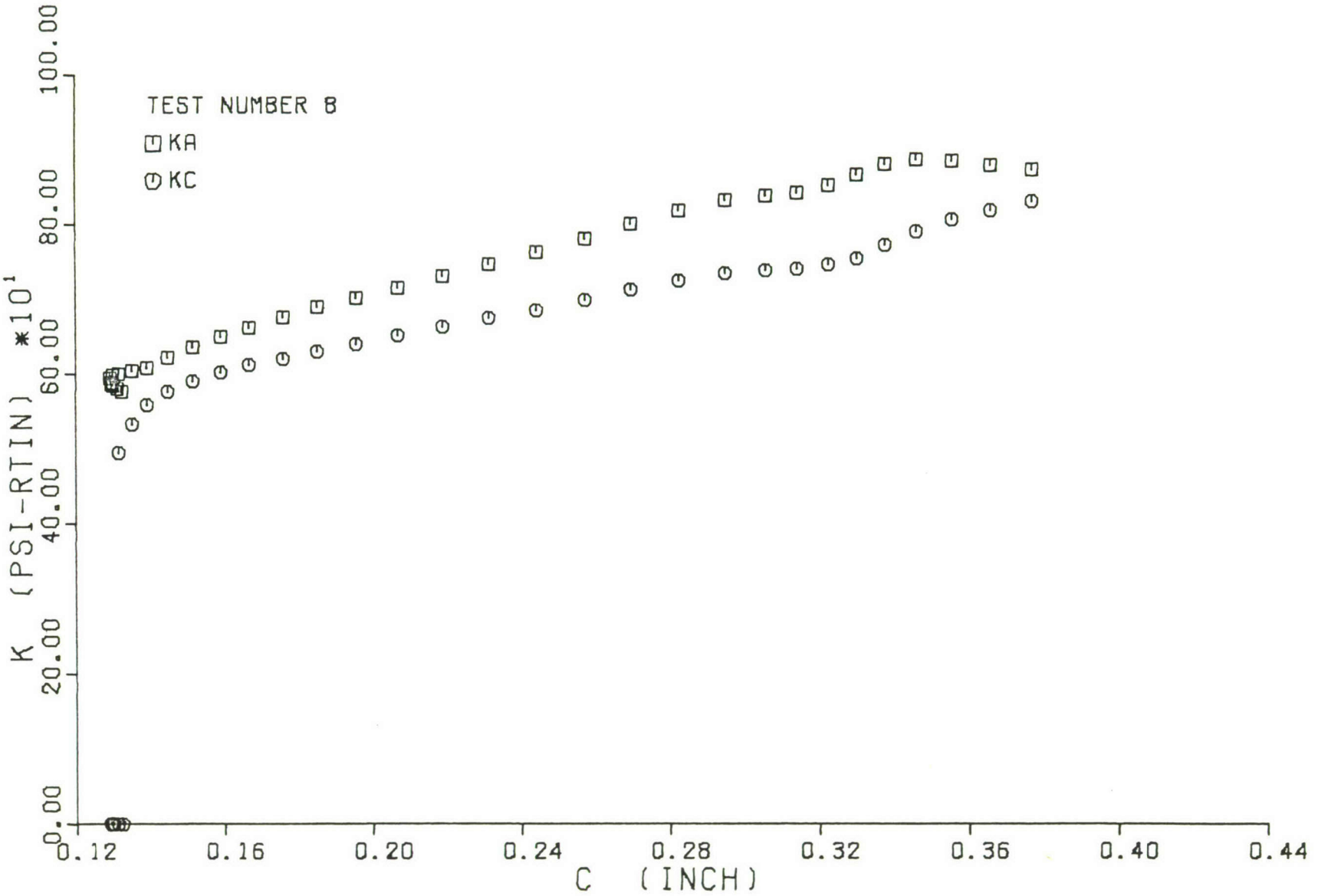

Fig. 47. Stress Intensity Factor vs. c Crack Length, Test 8

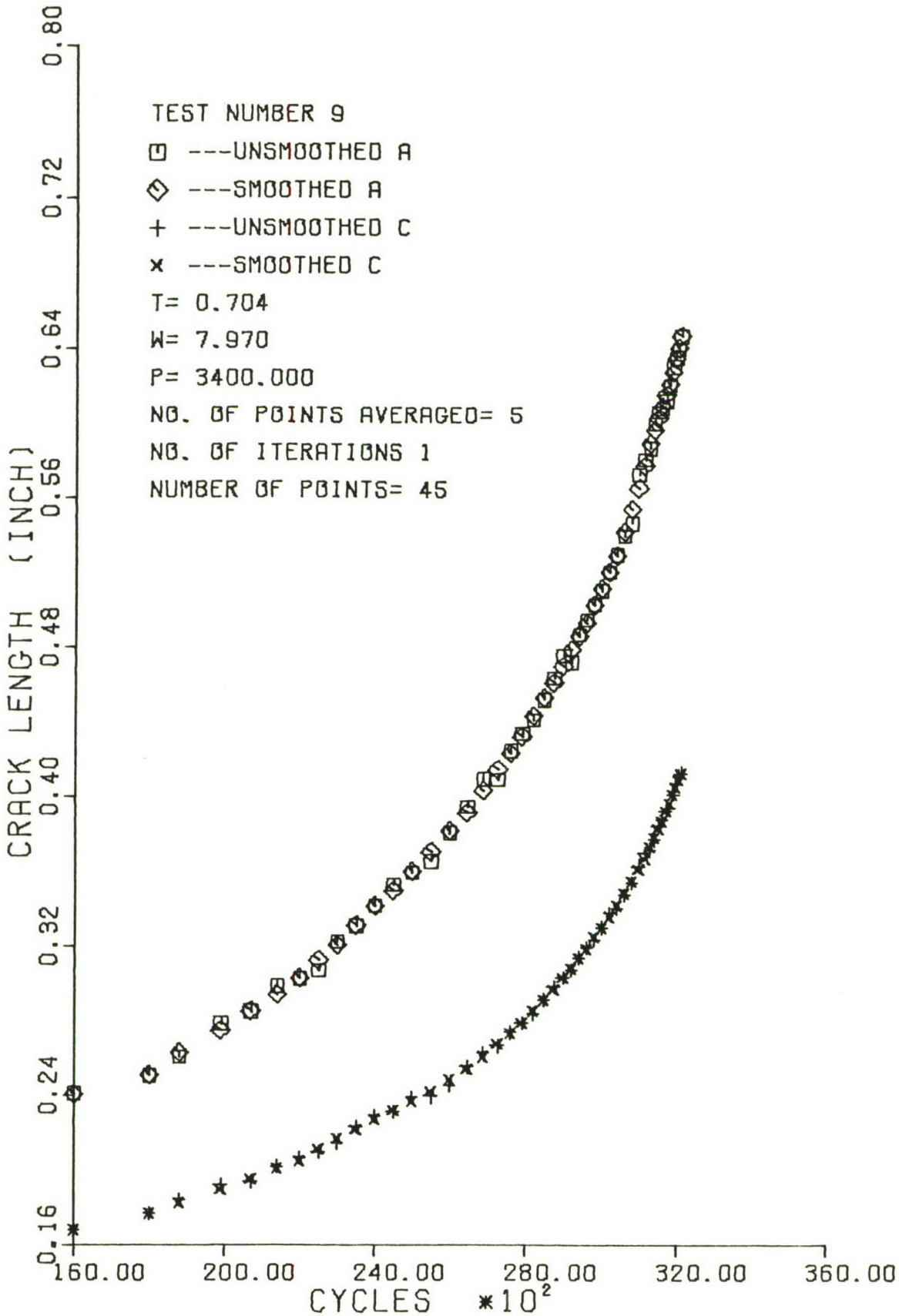

Fig. 48. Crack Length vs. Cycles, Test 9

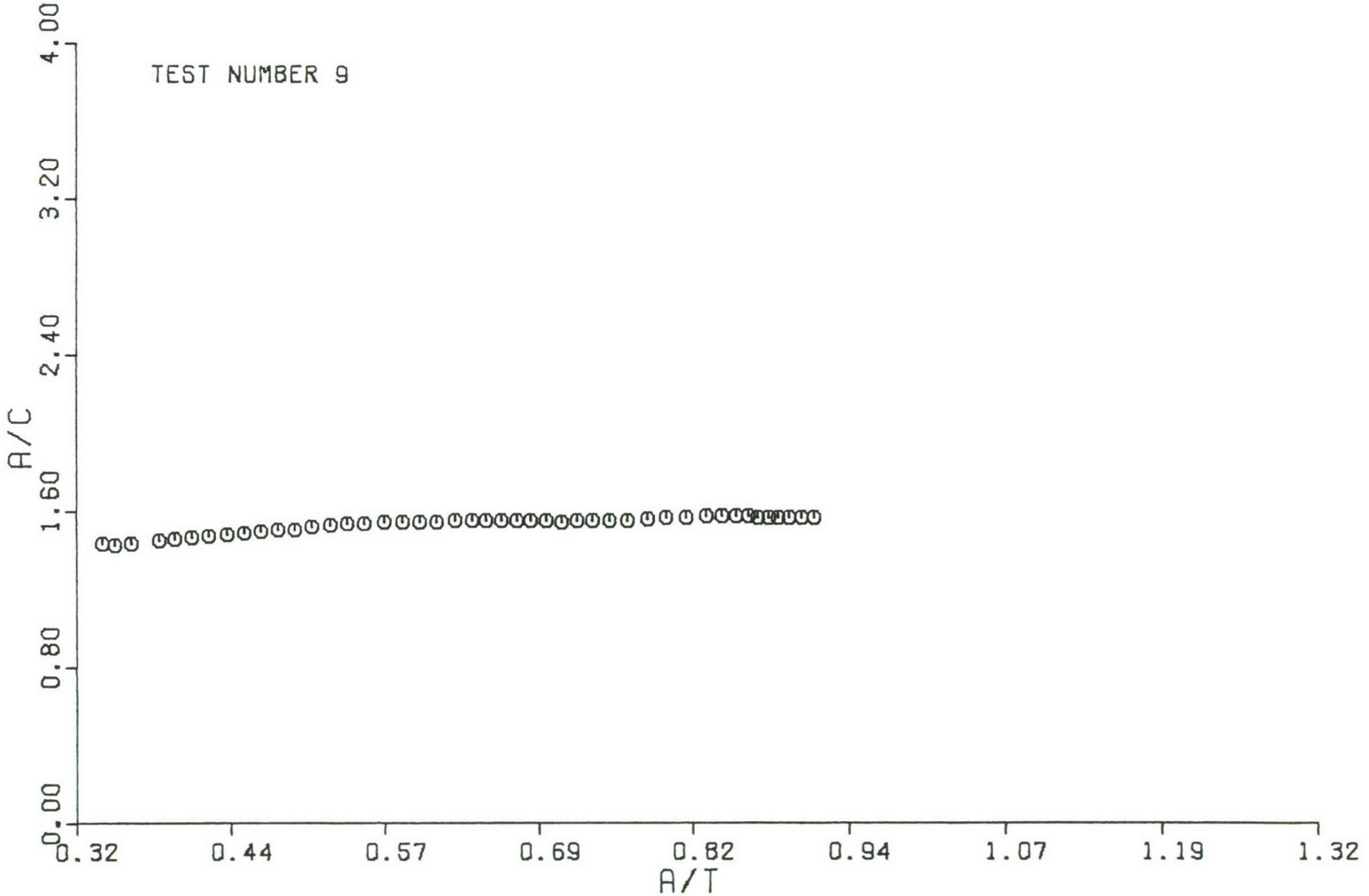

Fig. 49. Crack Shape vs. a/T, Test 9

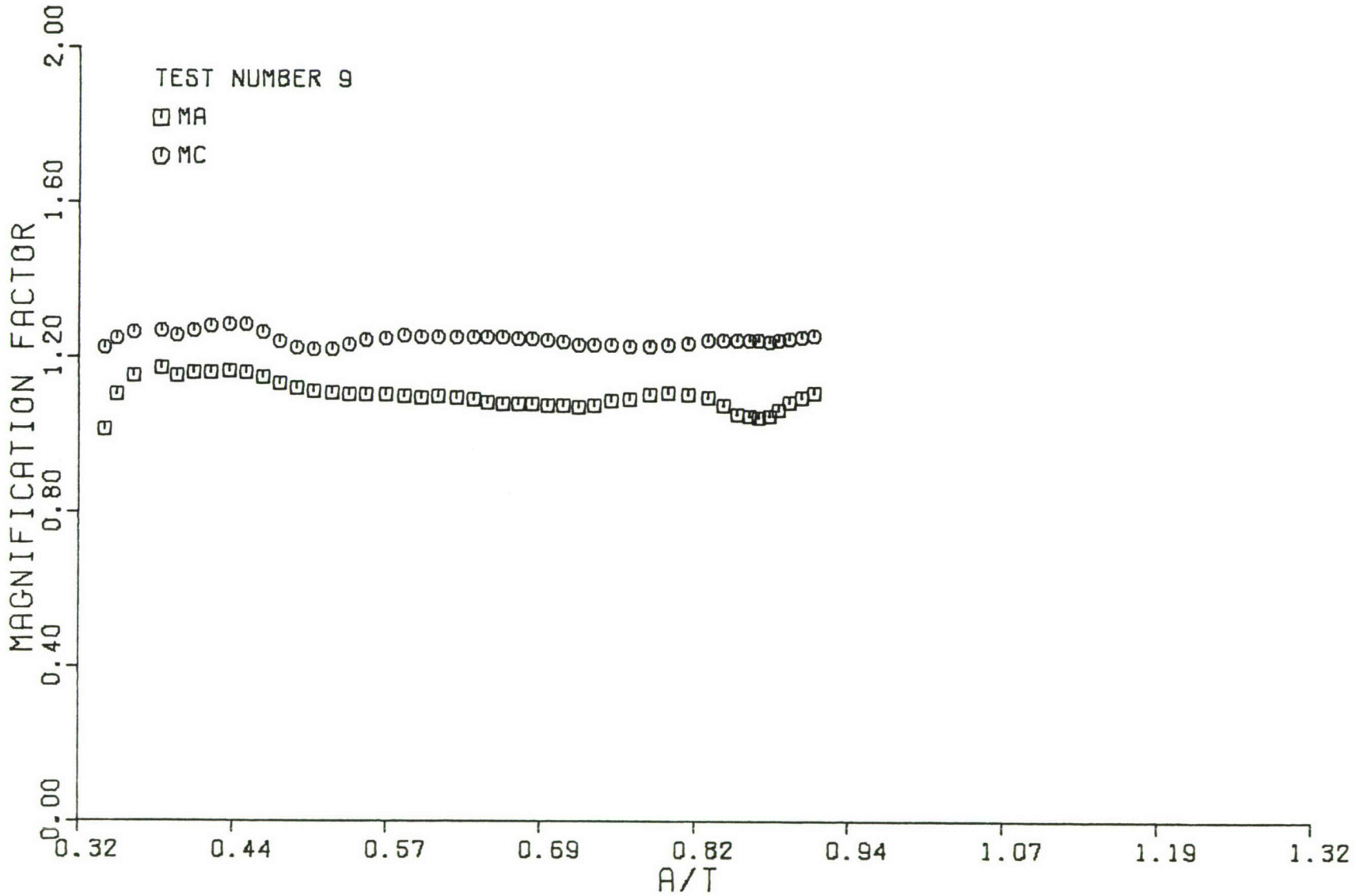

Fig. 50. Magnification Factor vs. a/T, Test 9

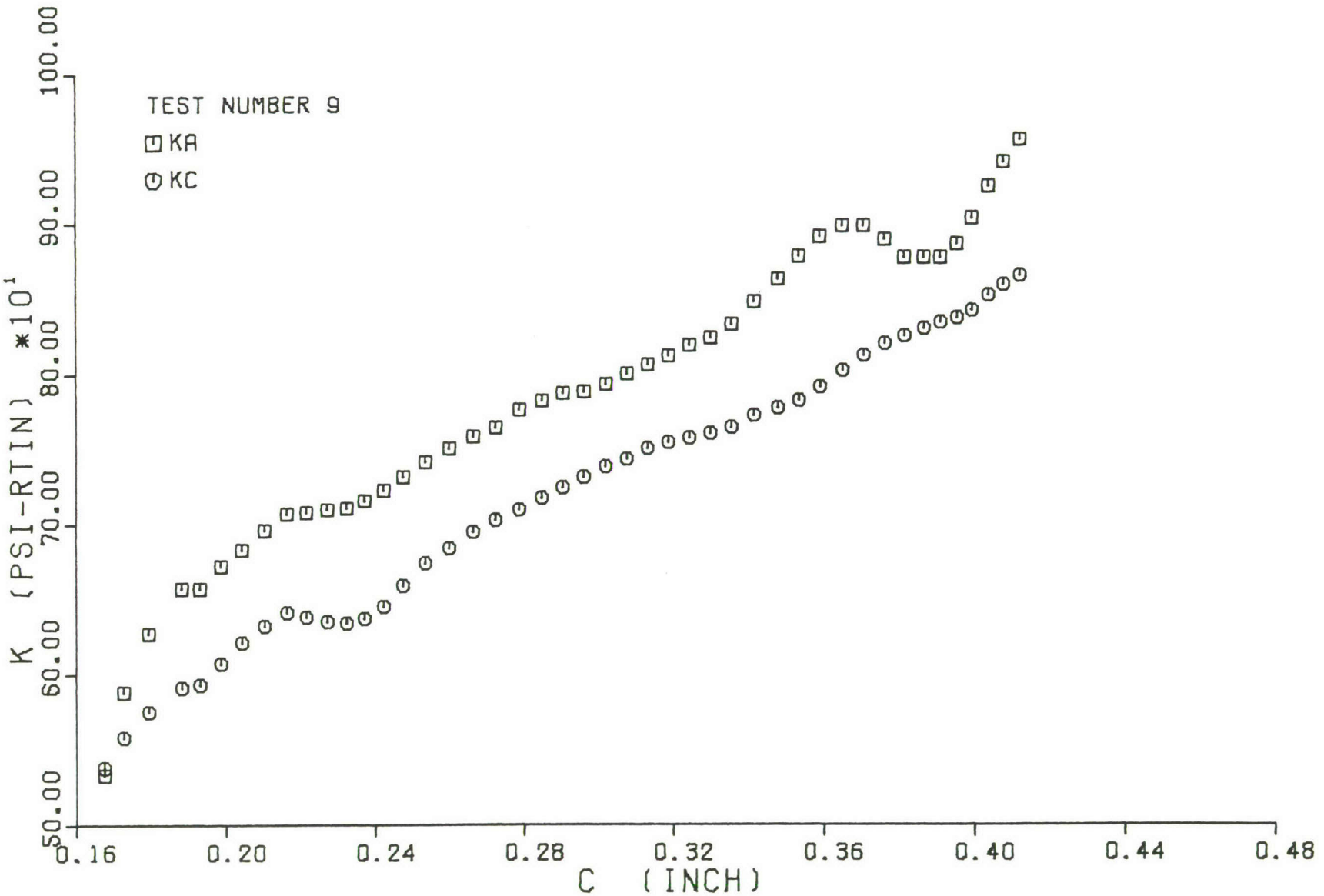

Fig. 51. Stress Intensity Factor vs. c Crack Length, Test 9

TEST 1 NUMBER OF DATA POINTS 76

CYCLES	A(INCH)	C(INCH)
500	.167	.115
1000	.167	.116
2000	.168	.118
3000	.167	.116
3500	.175	.121
4500	.170	.123
5000	.172	.124
5500	.176	.125
6000	.182	.125
6500	.180	.126
7000	.185	.131
7500	.186	.131
8000	.189	.133
8500	.189	.135
9000	.192	.136
9500	.199	.138
10000	.203	.139
10500	.204	.142
11000	.209	.146
11250	.213	.146
11500	.218	.153
11700	.219	.153
11900	.227	.155
12100	.226	.159
12300	.228	.158
12500	.231	.162
12700	.233	.166
12900	.241	.169
13100	.238	.170
13300	.238	.169
13500	.244	.170
13700	.246	.177
13900	.249	.179
14100	.253	.178
14300	.258	.182
14500	.261	.186
14700	.261	.190
14900	.269	.194
15100	.276	.194

CYCLES	A(INCH)	C(INCH)
15300	.287	.203
15500	.289	.208
15700	.291	.207
15900	.295	.212
16100	.301	.214
16300	.306	.217
16500	.312	.223
16700	.312	.226
16900	.319	.227
17100	.325	.231
17300	.329	.236
17500	.330	.237
17700	.335	.238
17900	.352	.243
18100	.358	.245
18300	.366	.254
18500	.369	.254
18700	.372	.263
18900	.379	.266
19100	.387	.273
19300	.393	.280
19500	.401	.282
19700	.412	.292
20100	.429	.301
20300	.436	.304
20500	.450	.316
20700	.459	.324
20900	.464	.328
21100	.486	.333
21300	.498	.341
21500	.510	.354
21700	.519	.364
21900	.531	.373
22100	.549	.386
22300	.559	.394
22500	.576	.409
22700	.609	.429

TEST 2 NUMBER OF DATA POINTS 34

CYCLES	A(INCH)	C(INCH)
500	.162	.126
700	.165	.126
925	.168	.124
1100	.170	.126
1300	.172	.128
1500	.179	.126
1700	.182	.127
8000	.267	.197
8300	.282	.205
8600	.288	.208
8900	.293	.214
9200	.303	.220
9500	.314	.225
9800	.325	.233
10100	.329	.233
10400	.340	.244
10700	.351	.250
11000	.368	.258
11300	.377	.262
11600	.386	.266
11900	.404	.276
12200	.425	.283
12500	.434	.293
12800	.461	.301
13000	.479	.306
13200	.492	.315
13400	.509	.323
13600	.534	.334
13800	.556	.339
13900	.578	.345
14000	.600	.351
14100	.618	.357
14150	.627	.358
14200	.644	.364

TEST 3 NUMBER OF DATA POINTS 34

CYCLES	A(INCH)	C(INCH)
1000	.157	.170
2000	.166	.172
3000	.182	.183
4000	.195	.189
5000	.209	.201
6000	.224	.211
7000	.247	.224
8000	.266	.236
9000	.290	.254
9500	.303	.263
10000	.321	.275
10500	.332	.284
11000	.347	.294
11500	.368	.307
11750	.377	.314
12000	.386	.321
12250	.398	.328
12500	.408	.336
12750	.419	.348
13000	.435	.357
13200	.449	.368
13400	.457	.376
13600	.470	.389
13800	.481	.401
14000	.494	.412
14200	.510	.428
14400	.532	.447
14600	.550	.470
14700	.560	.481
14800	.571	.489
14900	.579	.501
15000	.591	.512
15100	.603	.525
15200	.606	.535

TEST 4 NUMBER OF DATA POINTS 68

CYCLES	AT(INCH)	AM(INCH)	AB(INCH)	AAVG(INCH)
1	.283	.321	.166	.257
2000	.284	.330	.170	.261
3000	.285	.331	.179	.265
4000	.301	.342	.186	.276
5000	.309	.348	.201	.286
6000	.313	.357	.210	.294
6500	.316	.359	.218	.298
7000	.322	.366	.223	.303
8000	.320	.368	.232	.307
8250	.322	.371	.240	.311
8500	.326	.375	.242	.315
9000	.330	.380	.249	.319
9250	.332	.383	.254	.323
9500	.337	.388	.258	.328
9750	.337	.392	.262	.330
10000	.342	.392	.263	.332
10250	.346	.398	.267	.337
10500	.344	.396	.271	.337
10750	.349	.401	.274	.341
11250	.352	.403	.274	.343
11750	.353	.405	.281	.346
12750	.359	.411	.289	.353
13250	.371	.423	.298	.364
13750	.374	.428	.302	.368
14250	.377	.432	.305	.371
15000	.380	.438	.315	.378
15500	.386	.446	.319	.384
16000	.391	.449	.326	.388
16500	.394	.454	.338	.395
17500	.403	.463	.343	.403
18500	.410	.473	.356	.413
19500	.419	.485	.368	.424
20500	.434	.501	.387	.441
21500	.440	.501	.385	.442
22000	.447	.506	.391	.448
23000	.452	.512	.404	.456
24000	.463	.526	.415	.468
25000	.472	.533	.426	.477
26000	.502	.562	.451	.505

CYCLES	AT(INCH)	AM(INCH)	AB(INCH)	AAVG(INCH)
27000	.499	.564	.458	.507
28000	.515	.576	.469	.520
29000	.520	.585	.481	.529
31000	.542	.609	.499	.550
33000	.568	.632	.527	.576
35000	.587	.653	.546	.595
37000	.621	.687	.580	.629
38000	.622	.688	.585	.631
39000	.628	.696	.601	.642
41000	.665	.730	.634	.677
43000	.718	.777	.676	.724
44000	.714	.779	.683	.725
45000	.733	.802	.706	.747
46000	.758	.828	.734	.773
47000	.770	.832	.737	.780
48000	.791	.851	.757	.800
50000	.815	.881	.787	.827
51000	.833	.890	.800	.841
52000	.856	.918	.831	.869
53000	.883	.943	.854	.893
54000	.895	.954	.866	.905
55000	.923	.984	.900	.936
56000	.965	1.012	.921	.966
57000	.992	1.043	.960	.999
58000	1.022	1.075	.990	1.029
59000	1.058	1.119	1.034	1.070
60000	1.122	1.170	1.097	1.130
61000	1.168	1.220	1.142	1.177
62000	1.231	1.284	1.193	1.236

TEST 5 NUMBER OF DATA POINTS 26

CYCLES	A(INCH)	C(INCH)
1	.135	.128
2000	.122	.131
3000	.125	.134
4000	.134	.141
5000	.148	.148
6000	.157	.154
7000	.166	.161
8000	.176	.167
9000	.190	.175
10000	.203	.184
11000	.216	.198
12000	.240	.208
13000	.256	.220
14000	.280	.234
15000	.310	.253
16000	.346	.272
17000	.390	.291
18000	.446	.315
18250	.465	.322
18500	.481	.326
18750	.496	.335
19000	.521	.348
19250	.538	.359
19500	.561	.365
19750	.592	.383
19900	.603	.391

TEST 6 NUMBER OF DATA POINTS 30

CYCLES	A(INCH)	C(INCH)
1	.084	.095
2000	.097	.103
3000	.093	.103
4000	.107	.107
6000	.120	.112
7000	.142	.113
8000	.141	.117
9000	.154	.124
11000	.171	.137
12000	.184	.140
13000	.189	.150
14000	.204	.161
15000	.207	.169
16000	.237	.183
17000	.256	.192
18000	.282	.202
19000	.304	.218
20000	.346	.238
20500	.361	.248
21000	.376	.256
21500	.398	.270
22000	.427	.290
22300	.452	.302
22600	.463	.310
22900	.480	.322
23100	.496	.331
23300	.485	.343
23500	.502	.354
23700	.517	.368
23900	.553	.383

TEST 7 NUMBER OF DATA POINTS 29

CYCLES	AM(INCH)	AB(INCH)	AAVG(INCH)
1	.565	.432	.499
1000	.550	.428	.489
2000	.578	.452	.515
3000	.601	.481	.541
4000	.612	.493	.553
5000	.648	.533	.591
6000	.642	.523	.583
7000	.649	.536	.593
8000	.693	.579	.636
9000	.742	.631	.687
10000	.745	.641	.693
11000	.750	.644	.697
12000	.773	.674	.723
13000	.777	.682	.730
14000	.771	.682	.726
15000	.811	.721	.766
16000	.816	.728	.772
17000	.892	.806	.849
18000	.918	.832	.875
19000	.912	.832	.872
20000	.950	.862	.906
21000	.952	.864	.908
22000	.974	.898	.936
23000	1.014	.938	.976
24000	1.043	.966	1.005
26000	1.113	1.038	1.075
27000	1.163	1.092	1.127
28000	1.183	1.115	1.149
29000	1.262	1.191	1.227

TEST 8 NUMBER OF DATA POINTS 34

CYCLES	A(INCH)	C(INCH)
1	.118	.132
2000	.131	.130
3000	.138	.129
4000	.145	.133
5000	.146	.129
6000	.156	.127
7000	.168	.129
8000	.171	.131
9000	.177	.132
10000	.188	.139
11000	.196	.144
12000	.203	.152
13000	.212	.157
14000	.227	.168
15000	.248	.176
16000	.252	.183
17000	.274	.195
18000	.292	.206
19000	.312	.217
20000	.341	.233
21000	.362	.247
22000	.395	.264
22500	.414	.276
23000	.440	.285
23500	.462	.298
24000	.495	.313
24300	.505	.322
24500	.512	.321
24750	.526	.331
25000	.542	.336
25250	.564	.344
25500	.580	.354
25750	.600	.365
26000	.612	.377

TEST 9 NUMBER OF DATA POINTS 45

CYCLES	A(INCH)	C(INCH)
16000	.241	.168
18000	.251	.177
19000	.261	.184
20000	.279	.192
21000	.285	.194
21500	.299	.202
22000	.303	.206
22500	.307	.210
23000	.322	.214
23500	.331	.223
24000	.342	.229
24500	.353	.231
25000	.359	.239
25500	.365	.240
26000	.380	.246
26500	.394	.256
27000	.409	.263
27300	.409	.267
27600	.424	.274
27900	.434	.279
28200	.441	.284
28500	.452	.292
28800	.463	.299
29000	.475	.303
29200	.471	.307
29400	.486	.314
29600	.494	.319
29800	.502	.323
30000	.510	.330
30200	.520	.338
30400	.529	.340
30600	.539	.347
30800	.546	.354
31000	.572	.363
31200	.580	.369
31300	.586	.371
31400	.599	.376
31500	.606	.384
31600	.608	.387

CYCLES	A(INCH)	C(INCH)
31700	.612	.392
31800	.620	.394
31900	.630	.401
32000	.635	.406
32050	.639	.411
32100	.646	.412

☆ U. S. GOVERNMENT PRINTING OFFICE: 1975 — 657-630/58